MECHANISMS IN BIOMINING OF MAGNESITE AND ITS SCALE UP PRODUCTION

by

Gonca Altın Yılmazer

Submitted to Graduate School of Natural and Applied Sciences

in Partial Fulfillment of the Requirements

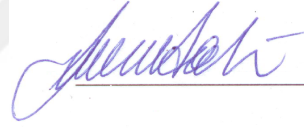for the Degree of Doctor of Philosophy in

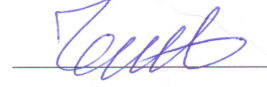Biotechnology

Yeditepe University

2016

MECHANISMS IN BIOMINING OF MAGNESITE AND ITS SCALE UP PRODUCTION

APPROVED BY:

Prof. Dr. Fikrettin Şahin
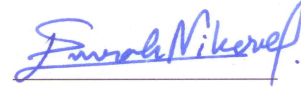(Thesis Supervisor)

Prof. Dr. Bülent Keskinler

Prof. Dr. Meral Birbir

Prof. Dr. Mustafa Özilgen

Assist. Prof. Emrah Nikerel

DATE OF APPROVAL: …./…./2016

ACKNOWLEGEMENTS

ABSTRACT

MECHANISMS IN BIOMINING OF MAGNESITE AND ITS SCALE UP PRODUCTION

Magnesite, that is called magnesium carbonate ($MgCO_3$) mineral, is one of the important ores of Turkey among countries rich in terms of ore resources. Since magnesium found in magnesite is a valuable raw material at the pure state or various compound states for present-day technology, developing new approaches on obtaining and enrichment of this material are very beneficial on account of national economics. In order to trade magnesite economically, SiO_2 and $CaCO_3$ rates of raw material needs to be less than 2 percent and 1 percent, respectively. A number of different enrichment methods have been developed to increase purity of magnesite. The aim of the present study is to develop a biomining process which will be used for enrichment of magnesite from different ores in Turkey by dissolving carbonate compounds, to scale up this process and to determine Ca dissolving factors. Previously and newly isolated and identified bacterial strains, *Enterococcus* spp., *Lactococcus* spp. *Staphylococcus* spp., and fungi isolate *Neurospora* spp. were used. Optimum working parameters were identified for all microorganisms. Results indicated that, microorganisms show effective dissolving capacity at 30ºC, pH between 3 and 7, in the presence of glucose as carbon source. The subcronic toxicology tests performed with Wistar rats, showed that *Enterococcus* spp., and *Lactococcus* spp. strains are not pathogenic and toxic for mammalian. *Lactococcus* spp. was used at scale up studies and 3 L and 30 L fermenter processes were performed successfully. Consequently, genomic, transcriptomic and proteomic analysis of *Enterococcus* spp. and *Lactococcus* spp. strains were performed to illustrate the molecular mechanisms of magnesite biomining. This is the first study to demonstrate *Enterococcus* spp. and *Lactococcus* spp. strains can be used for enrichment of magnesite in industrial scale. A further study needs to be done to identify other microorganisms from nature that have potential to be used in magnesite biomining and formulation of them for industrial scale.

ÖZET

MANYEZİT BİYOMADENCİLİĞİNİN MEKANİZMASI VE BÜYÜK ÖLÇEKTE ÜRETİMİ

Magnezyum karbonat minerali ($MgCO_3$) olarak da adlandırılan manyezit, maden kaynakları yönünden zengin ülkeler arasında yer alan Türkiye'nin önemli cevherlerinden birisidir. Manyezit içerisinde magnezyum bulunduğu için, gerek saf halde gerekse çeşitli bileşikler halinde günümüz teknolojisi için oldukça kıymetli bir hammaddedir, bu materyalin elde edilmesi ve zenginleştirilmesi yönünde yapılacak yeni çalışmalar ülke ekonomisi açısından oldukça önemlidir. Ekonomik anlamda manyezitin satılabilmesi için cevherin SiO_2 oranının %2'den ve $CaCO_3$ oranının da %1'den daha az olması gerekmektedir. Bugüne kadar, manyezitin saflığını artırma amacıyla birçok farklı cevher zenginleştirme yöntemi geliştirilmiştir. Çalışmamızın amacı; Türkiye'nin farklı maden yataklarındaki manyezitin zenginleştirilmesi amacıyla karbonat bileşenlerinin çözülerek bir biyo-madencilik yöntemi geliştirmek, bu yöntemi büyük ölçekte denemek ve kalsiyumu çözen etkenleri tespit etmektir. Önceden ve yeni izole edilmiş bakteri soyları, *Enterococcus* spp. ve *Lactococcus* spp., *Staphylococcus* spp., ve *Neurospora* spp. fungusu kullanılmıştır. Tüm mikroorganizmalar için optimum çalışma parametreleri belirlenmiştir. Deney sonuçlarına göre mikroorganizmalar 30ºC sıcaklıkta, pH3-7 aralığında, karbon kaynağı olarak glikoz varlığında etkili bir çözücülük göstermektedir. Wistar sıçanları ile yapılan subkronik toksisite çalışmalarına göre *Enterococcus* spp. ve *Lactococcus* spp. suşları memeliler için patojen değillerdir. *Lactococcus* spp. ölçek büyütme çalışmalarında kullanılmış ve 3 L ve 30 L fermentör denemeleri başarılı bir şekilde gerçekleştirilmiştir. Son olarak, manyezit biyomadenciliğinin moleküler mekanizmasını açıklamak için *Enterococcus* spp. ve *Lactococcus* spp. suşlarının genomik, transkriptomik ve proteomik analizleri yapılmıştır. Bu, *Enterococcus* spp. ve *Lactococcus* spp. suşlarının manyezit zenginleştirmede endüstriyel ölçekte kullanılabileceğini gösteren ilk çalışmadır. Gelecek çalışmalar için doğadan manyezit çözme potansiyeli olan başka mikroorganizmalar izole edilmesi ve bunların endüstriyel ölçekte formüle edilmesi gerekir.

TABLE OF CONTENTS

LIST OF FIGURES

LIST OF TABLES

LIST OF SYMBOLS/ABBREVIATIONS

o	Degree
P	Density of fluid
d	Diameter
$	Dollars
μ	Micro
%	Percent
n	Revolution per minute
η	Viscosity
VL	Volume
A1	*Lactococcus garviaea*
Al	Aluminium
ALT	Alanine Amino transferase
ATP	Adenosine Tri Phosphate
BC	Before Christ
bp	Basepair
C	Centigrad
Ca	Calcium
$CaCO_3$	Calcium Carbonate
$CaMg(CO_3)_2$	Dolomite
CaO	Calcium oxide
Cfu	Colony forming unite
CM	Cryptocrystalline magnesite
CO_2	Carbon dioxide

COMAG A.Ş.	Continental Madencilik Anonim Şirketi
Cu	Copper
ddATP	2, 3-dideoxyadenosine triphosphate
ddCTP	2, 3-dideoxycytidine triphosphate
ddGTP	2, 3-dideoxyguanosine triphosphate
ddNTP	2, 3-dideoxynucleotide
dH2O	Distilled water
DNA	Deoksiribo Nucleic Acid
dNTP	Deoxynucleotide
DTT	Dithiothreitol
dTTP	2, 3-dideoxythymidine triphosphate
EDTA	Ethylene Daimine Tetraacetic Acid
EF	*Enterecoccus feacalis*
F primer	Forward primer
Fe	Iron
Fe2O3	Iron (III) oxide
FeCO3	Siderite
g	Gram
GY	Glucose-Yeast extract
GYC	Glucose-Yeast extract-Calcium
GYM	Glucose-Yeast extract-Magnesite
HCl	Hydrocloric acid
HCT	Hematocrit
HGB	Hemoglobine
HNO_3	Nitric acide
HPLC	High Performance Liquid Chromotography

H_2SO_4	Sulphiric acid
ICP-MS	Inductively Coupled Plasma – Mass Spectrometer
K1	*Staphylococcus warneri*
kb	Kilobase
KÜMAŞ	Kütahya Manyezit Anonim Şirketi
L	Liter
MAŞ	Manyezit Anonim Şirketi
Max	Maximum
MCH	Mean corpuscular hemoglobin
MCHC	Mean corpuscular hemoglobin concentration
MCV	Mean corpuscular volume
Mg	Magnesium
$MgCl_2$	Magnesium cloride
$MgCO_3$	Magnesium carbonate
$MgFeCO_3$	Breunerite
mL	Mililiter
mM	Milimolarity
Mn	Manganese
MPV	Mean platelet volume
MTA	Maden Tetkik ve Arama
N	Normality
NA	Nutrient Agar
Né	Newton number
nm	Nanometer
Np	Power number
NT	*Neurospora tetrasperma*

OD_{600}	Optic Density at 600 nanometer wavelength
PAGE	Polyacrylamid Gel Electrophoresis
Pb	Lead
PCR	Polymerase Chain Reaction
PCT	Platelet crit
PDA	Potato dextrose agar
PDW	Platelet distribution width
pH	power of Hydrogen
PLT	Platelet
P-LCR	Platelet-Large cell ratio
p-NPA	p-Nitrophenyl acetate
P/VL	Force per volume
ppm	Parts per million
RBC	Red blood cells
RDW-SD	Red cell distribution width-Standard Deviation
RDW-CV	Red cell distribution width
Re	Reynolds number
R primer	Reverse primer
rpm	Revolution per minute
rps	Revolution per second
rRNA	Ribosomal Ribonucleic acid
SDA	Sabroud Dextrose Agar
SDS	Sodium Dodecyl Sulphate
Si	Silisium
SiO_2	Silisium oxide
SM	Sparry Crystalline Magnesite

Sn	Spelter
Tm	Melting temperature
TSA	Tryptic Soy Agar
TSB	Tryptic Soy Broth
US	United States
USA	United States of America
USD	United States Dollars
WBC	White blood cells
Zn	Zinc

1. INTRODUCTION

1.1. MAGNESITE

The mineral sector that supplying raw materials to domestic industry is one of the leaders in the field. Turkey is one of the world's richest countries in terms of mineral variety with 53 operable minerals and metals and 4,500 mineral deposits, excluding petroleum and coal.

Turkey's geology is very complex and this complexity provides the diversity of its mineral deposits. Magnesite has ranked at level 8 among the economically most important minerals produced in Turkey including boron minerals, feldspar, marble, baryte, celestite, emery, limestone, magnesite, perlite and pumice [1].

Magnesite ($MgCO_3$) theoretically contains 48,8 percent MgO and 52,2 percent CO_2 [2]. Magnesite is the primary source for production of magnesium and its compounds, which are widely used in divers fields from basic refractory bricks to pharmaceutical and from catalyst to fertilizer industries [3].

World's magnesite reserves are approximately 2200 million tons. Turkey is the fifth country with about 168,4 million tons magnesite reserves on the world after Russia, North Korea, Brazil and China [4][1].

Most of Turkey's magnesite reserves are concentrated in the Konya-Kütahya-Eskişehir triangle. In addition, some reserves are located in Erzincan and Çanakkale (Fig 1.1.1.). The cities, which have sedimentary magnesite ore in Turkey, are Balıkesir (Dursunbey), Çankırı (Orta), Kütahya (Kınık), Eskişehir (Mihallıççık), Denizli (Hırsız Dere-Çambaşı Köy ve civarı), and that have vein stock work are Isparta (Değirmenderesi), Datça-Muğla (Kızlar Köyü), Fethiye-Muğla (Göcek), Erzincan (Çayırlı and Refahiye), Bursa (Mustafa Kemalpaşa ve Orhaneli), Erzurum (Aşkale), Bolu (Mudurnu), Konya (Meram-Yunak), Seyhan-Adana (Haruniye) and Bilecik [5]

According to the 2012 Sector Report of Economy Ministry

Raw magnesite, dead burned and caustic calcined magnesite are produced in Turkey. Several small companies also produce raw magnesite. Some of them provide raw magnesite to the large domestic dead burned magnesite producers or to the ceramic industry, while others export their products. Magnesite is exported as raw magnesite, calcined, sintered and burned. Magnesite is also exported as bricks which are used in the iron and steel industry. In 2011, magnesite exports were about US$ 90 million, and Austria, Ireland and Germany were the major markets for Turkish magnesite. In 2011, Turkey ranked second in magnesite exports in the world with a share of 32 percent. [1]
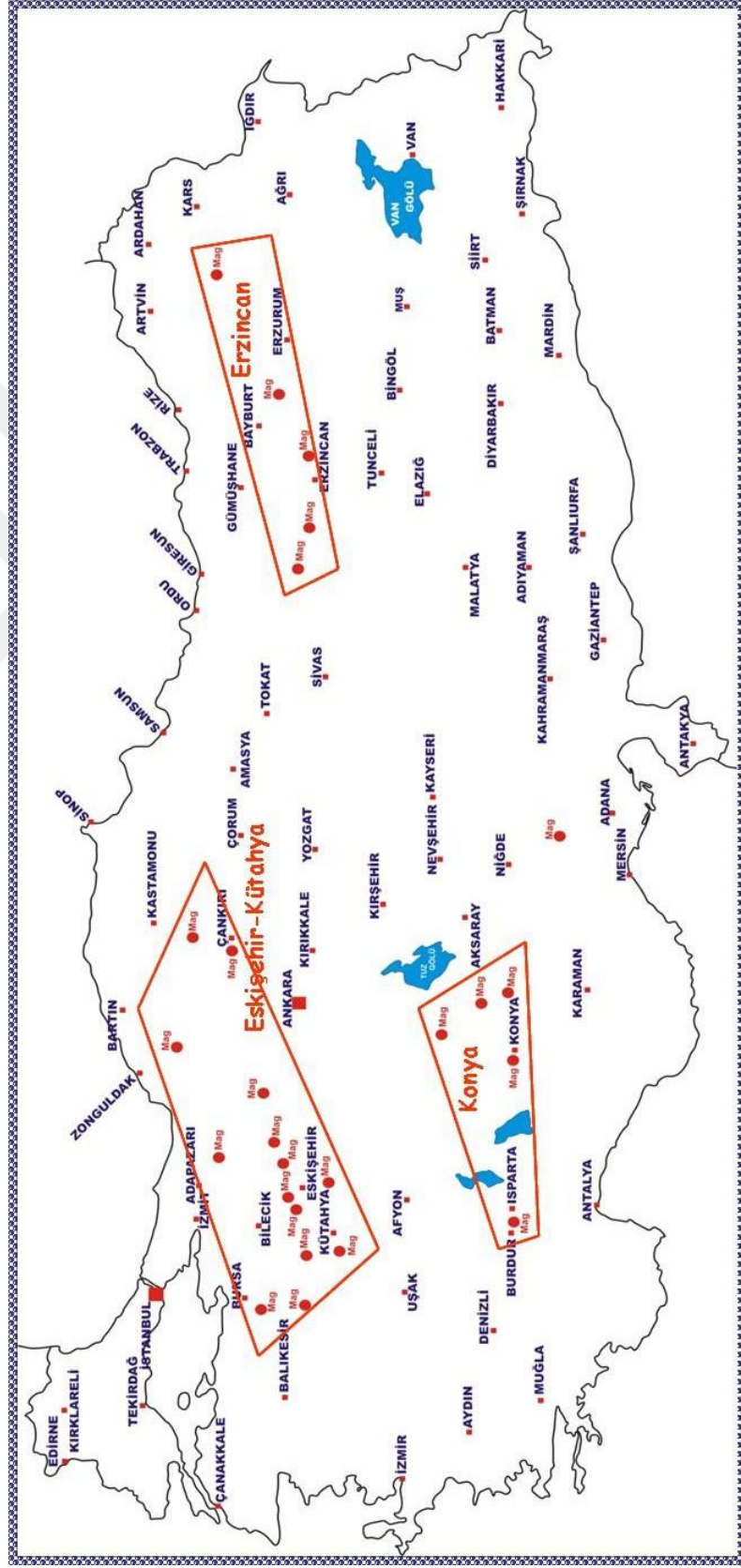
Figure 1.1. Distribution of Turkey's magnesite reserves [5]

Magnesite occurs in two mineralogical modifications as mineral and ore. They are fine to coarse grained crystalline Sparry crystalline magnesite (SM) with crystals up the size of several cm and Cryptocrystalline magnesite (CM), also referred as amorphous with crystals in the range of $1 - 10$ μm. Quantity of main magnesite resources and main magnesia producers are shown in **Table 1.1.**

Table 1.1. Magnesia producing countries: magnesite resources and types used [6]

COUNTRY	MAGNESITE RESOURCES BY TYPE (MILLION TONES)			MAGNESIA PRODUCTION BY TYPE (Kt) ('000 TONNES)		
	Sparry	Cryptocrystalline	Total	Sparry	Cryptocrystalline	Total
AUSTRALIA	132,3	549,7	682		240	240
AUSTRIA	30		30	445		445
BRAZIL	862		862	453		453
CANADA	64		64		64	64
CHINA	3.318	120,8	3.439	4.100		4.100
GREECE		30	30		200	200
INDIA	186	59	245	173	86	259
IRAN		3,3	3,3		65	65,0
NORTH KOREA	3.000		3.000	185		185
POLAND		12	12		10	10
RUSSIA	2.745		2.745	1.055		1.055
SERBIA		13,8	13,8		20	20,0
SLOVAKIA	1.240		1.240	465		465
SOUTH AFRICA	18		18		85	85
SPAIN	205		205	215		215
TURKEY		162	162		474	474
USA	66		66	140		140
TOTAL	11.867	951	12.817	7.231	1.244	8.475

93 percent of the world's magnesite resources is in the Sparry (coarse) type and just 7 percent of the world's magnesite resources is in cryptocrystalline type as indicated in **Table 1.1.** However, consumption of cryptocrystalline is higher than the resources with 15 percent [6]

Cryptocrystalline magnesite can be formed in three ways. In the first way, CO_2 rich waters alter magnesium-rich serpentinite; the second is the weathering of serpentine by CO_2-laden waters and in the last formation way magnesia rich fluids attack dolomite or limestone.

Sparry crystalline magnesite is formed by replacement of limestone and dolomite. In this formation type, magnesia rich fluids attack dolomite or limestone. While density of cryptocrystalline type magnesite is 2,95 gr/cm^3, density of Sparry crystalline magnesite is 3,05 gr/cm^3. Magnesite ores contain Ca, Si, Fe, Mn and Al elements in variable amounts. Cryptocrystalline type magnesite is often high quality with low CaO, Fe_2O_3 than Sparry magnesite (**Table 1.2.**).

Table 1.2. Comparison of main properties of magnesite mine [6]

CRYPTOCRYSTALLINE / AMORPHOUS MAGNESITE	MACROCRYSTALLINE / SPARRY / BONE MAGNESITE
Massive with a characteristic conchoidal fracture	Marble like crystallinity
Often of high quality with low CaO, Fe_2O_3	Higher Fe_2O_3 and impurities
Generally white color	Various colors, but doesn't reflect grade
Tends to occur in smaller and shallow deposits	Present in huge deposits
Present in veins and stockworks	
Fine crystal size 1-10 micron	Large crystal size in cms

The carbonates are removed as carbon dioxide as calcite and dolomite, when magnesite is heated up, and the magnesium oxide is produced. Magnesite does not react with cold hydrochloric acid. On the contrary dolomite reacts weakly and calcite reacts strongly. This property facilitates to discern the magnesite from dolomite and calcite. Magnesite is in the trigonal carbon hydrates group and this group contains calcite ($CaCO_3$), dolomite ($CaMg(CO_3)_2$), magnesite ($MgCO_3$), breunerite ($MgFeCO_3$) and siderite ($FeCO_3$).

The carbonates are removed as carbon dioxide and the dense and rigorous sintered magnesite is produced, when magnesite is heated up to 1400–1800°C. Sintered magnesite is an important refractory material which could be used for producing fire-resistant products widely used in, ceramic, and chemical and metallurgy industries. When magnesite mineral is heated up to 700–1000°C, calcined magnesite be formed. Calcined magnesite could be used for producing insulating materials, wear-resisting materials, soundproof materials, and pharmaceutical products [7].

Raw Magnesite: Raw Magnesite is produced by mining, sorting and grinding of magnesium carbonate ($MgCO_3$) from natural deposits. After that, it can be used in the ceramic and chemistry sectors. In order to use for applications in ceramics, raw material should have very low iron content while CaO and SiO_2 impurities are not important. In the chemistry sector, it is used to produce magnesium sulphide disregarding the quality.

Sintered Magnesite: As a result of burning magnesite at temperatures above 1600°C, dead burnt magnesite is produced. This product has extremely low reactive properties. Dead burnt magnesite is also called Sintered Magnesite. This product is suitable for basic refractories shaped and unshaped products. Its usage areas are iron foundries as a refractory material, refractory industry for manufacture of refractory bricks, slag splashing in arc furnaces and steel industry as coating material.

Calcined Magnesite: Calcined Magnesite is produced by sintering raw magnesite in a temperature controlled manner (650-1100°C). Although, sintered magnesite has very low reactive properties, Calcined Magnesite is chemically reactive product. This product is used in the pharmaceutics and medicine as drug, in the agriculture industry as fertilizers and animal

feed, in the chemical industry as preliminary substrate of magnesium compounds, and in the polishing industry and production of Sorel cement.

In the Cryptocrystalline type magnesite, content has to be;

- Plain Quality: Max 1,00 percent SiO_2, max percent 1,30 CaO ve max 0,50 percent Fe_2O_3
- Adverse Quality: Max 1,70 percent SiO_2, max percent 0,80 CaO ve max 0,30 percent Fe_2O_3.

In the Sparry type magnesite, content has to be;

Max 3,00 percent SiO_2, max 2,00 per cent CaO and max 4,00 per cent Fe_2O_3 [8].

The natural magnesite contains some impurities such as carbonates, silicates and oxides. These can affect the usage of obtained products negatively [2]. For instance, in brick industry the raw material which has high melting point, is defined as high quality? Optimized ratio of MgO-CaO/SiO_2 and minimized ratio of Fe_2O_3 increases melting point of raw material. CaO-MgO-SiO_2 composition will have low melting temperature (Tm = 1495 ∘C) when CaO/SiO_2 ratio is about 1 which decreases refractoriness. The microstructure of a brick with CaO/SiO_2 ratio about 2 includes usually more refractory crystal phases such as CaO-SiO_2 and has higher melting point (Tm = 2130˚C) while the brick with CaO/SiO_2 ratio about 3 has low melting point (Tm = 1575˚C). As a result, the further increase in the CaO/SiO_2 ratio (~2) leads to abrasion, infiltration and decline in refractoriness. Moreover, a great quantity of silicate in the brick causes to a decline in the resistance to spalling and refractoriness. While, firing at the outlet of sintering zone, Fe_2O_3 is also converted to FeO. This formation causes decreasing of volume and leads to spalling and destruction of the brick. Therefore, magnesia-based brick refractory for the cement industry should therefore have as little Fe_2O_3 as possible (<1 percent). A remarkable amount of Al_2O_3 can also provide an improvement in thermal shock resistance of the brick, on the other hand this leads to decrease in refractoriness and cause spalling. Thus, the Al_2O_3 content should be as low as possible for elasticity of the brick but adequate. Generally, when the highest quality raw materials are used, resultant in the optimum MgO and Al_2O_3 content, the decreased Fe_2O_3 and the optimum CaO/SiO_2 ratio prevent the formation of low-melting compounds with brick and kiln feed components [9].

Beside the increasing quality of the products of magnesite, beneficiation of magnesite is also important to increase its commercial value. As MgO percent of magnesite increases, the unit price increases as well. For instance, while sintered magnesite consisting of 90 percent MgO unit price is 300 USD/ton, consisting of 97 percent MgO unit price is 450 USD/ton, and consisting of 99 percent MgO unit price is 700 USD/ton.

Therefore, natural magnesite ($MgCO_3$) is enriched by using a variety of methods to produce a high-grade product which can be used in the manufacture of refractories, magnesium metal, or other products. Thus, physical and chemical methods are usually preferred for recovery of products, such as hand sorting hand sorting the heavy medium separation, magnetic separation and flotation [2] [10].

Heavy medium separation method depends on differences of density between magnesite and gang minerals. Very intensive media material ferrosilicon (6,8 gr/cm^3) is used for this process. While low density material floats on the media, the dense ones sink.

Hand/ manual sorting is a visual method dependent on man labour. Magnesite is separated from gang minerals according to the color differences.

Magnetic separation method sorts the minerals according to their magnetic properties. Since magnesite is a nonmetallic and nonmagnetic mine, magnetic separation is used to remove the ferromagnetic and paramagnetic gang materials from magnesite.

Floating is another enrichment method to separate magnesite from calcium carbonate and silica by the use of oleic acid and small amounts of carbon dioxide as a conditioner. The main drawback of this method is its cost. Due to the high cost, magnetic separation and manual sorting are more preferred methods.

In the magnesite plants in Turkey, natural magnesite is generally processed by crushing, screening, scrubbing, calcination and magnetic separation. Only 474,000 ton of 164 million ton magnesite reserves are handled in Turkey. The tailings of Turkey still contain a significant amount of usable very low grade magnesite [3]. Handling low grade magnesite ores by classical methods is not commercially convenient because of high cost.

Due to the disadvantages of classical methods including low sensitivity, high energy demand, and negative effects of extensive chemicals use it is required to determine efficient, economical and safer alternative methods. Biomining is a novel biotechnological approach widely used in the commercial scale for the enrichment of copper, gold, uranium, zinc and nickel. Moreover, it could provide enrichment of magnesite.

1.2. BIOMINING

In the environment, heavy metals often present as free elements. But, in most instances some minerals such as pyrrhotite, arsenopyrite, chalcopyrite and pyrite encapsulate these metals chemically. The recovery of the metal ion via conventional methods is prevented by this encapsulation since it generates a physical barrier. In many countries, application of biotechnology in mining has been investigated by researchers over the last 40 years [11]. Biomining is the process of using microorganisms to extract valuable metals from mineral ores and mine tailings [12] [13]. According to Siddiqui et al. (2009), use of microbes to solve a lot of mineral ores is an old process that goes back to Roman times in the first century BC. Microbial activity was used to leach copper from ore by those early miners without being aware that microbes were involved in the process [14] [15]. But nowadays with increasing research trend in mineral biotechnology, the use of microorganisms to simplify the lineage and recovery of precious and base metals from primary ores, has developed into a successful and widening area of biotechnology [12].

Biomining has applications as an option to traditional physical-chemical mineral processing methods [16]. There are some reasons for this. While high-grade surface mineral deposits are mining by the traditional pyrometallurgy-based metal recovery processes, this processes is not adequate for the remaining lower-grade mine ores for economic reasons. This prompted the mine producers to find new methods to process the lower-grade mine ores. In the extraction of metals from many low-grade mine sources, microbial processes have clear economic advantages. For instance, during controlled irrigation of the dump, low-grade ores or dumps have been processed and large quantities of copper have been extracted while they are not

exploitable materials for traditional mining operations. Microbial metal-extraction applications are generally more environmentally friendly than chemical and physical processes. Microbial metal extraction processes do not use the large amounts of energy as it is required in roasting or smelting which means lower sulfur dioxide and other harmful gaseous emissions. Moreover, physicochemical processes produce wastes and these wastes might be biologically percolated with mine residues when exposed to rain and air, producing unwanted acid and metal pollution. Tailings from biomining operations are chemically less active and the biological activity is reduced by the extent to which they have already been bioleached [15]. Shortly, biomining processes can be operated with a simple infrastructure, less labour, and energy costs compared to the other technologies. Biomining provides Green Technology via low gaseous emission, cleaner tailings, mine high or low grade ores and economically viable tailings than traditional methods [13].

The modern period of bioleaching began in the mid-1940s with the discovery of the bacterium, *Thiobacillus ferrooxidans* (now *Acidithiobacillus ferrooxidans*) and the initial understanding of this microbe's involvement in extraction of copper. In 1958, the use of *Thiobacillus ferrooxidans* for copper extraction is patented by Kennecott Mining Company. *Thiobacillus ferrooxidans* was used in the bio hydrometallurgical process for extracting copper from low-grade copper ores from the Bingham Canyon Mine near Salt Lake City, Utah, USA [16]. There are previous reviews concerning methods of bioleaching and their application in several countries. This biotechnology is especially important in Chile. Because Chile is the main copper producer in the world, producing about 400,000 ton of copper per year via biomining [17].

When microorganisms are in contact with solid metal-containing particles or metals in solution, several metabolic reactions may occur, regarding the presence of mineral and metallic compounds in waste. **Table 1.3** shows an overview on possible reactions and mechanisms resulting in the mobilization of solid metals or immobilization of solubilized metals. Mineralytic effects of bacteria and fungi on minerals are based mainly on three principles, namely acidolysis, complexolysis, and redoxolysis. Microorganisms are able to mobilize metals via the formation of organic or inorganic acids (e.g., citric acid, sulfuric acid), via oxidation and reduction reactions; and by the excretion of complexing agents (e.g.,

cyanide) and via proton pumping. In the presence of ligands under acidic conditions proton-promoted and ligand-promoted mineral solubilization can occur simultaneously [18].

Table 1.3. Microbial reactions leading either mobilization or immobilization of metals [18].

Process	Mechanism	Description of the reaction
Mobilization	Redoxolysis	Metals are microbially oxidized or reduced during oxidation-reduction processes. As result, metal mobility is increased depending on the type of metal and its oxidation state.
	Acidolysis	The mechanism is also called proton-induced metal solubilization. Microbial secretion of protons results in changes of the metal mobility. Under these conditions protons are bound to the surface resulting in the weakening of critical bonds as well as in the replacement of metal ions leaving the solid surface.
	Complexolysis	The mechanism is also termed ligand-induced metal solubilization. Microbial formation of complexing or chelating agents leads to an increase of metal mobility. Complexes are formed on metal surfaces by ligand exchange polarizing critical bonds and facilitating the detachment of metals species from the surface. Organic ligands of bi- or multi-dentate nature are particularly effective.
	Alkylation	Alkyl groups are enzymatically transferred to the metal and covalently bound. The process is often described as metal volatilization, because alkylated metals show an enhanced volatility as compared to their elemental or ionic forms. Methylation is the best known alkylation process.
Immobilization	Biosorption	Biosorption is defined as a passive process of metal sequestering and concentration by chemical sites (functional groups such as carboxyl, sulfonate, phosphate, hydroxyl, amino, or imino residues) naturally present on the surface of living or dead microbial biomass. Metal sorption can be more or less selective depending on the organisms used and environmental conditions (e.g., pH, salinity).
	Bioaccumulation	Soluble metals are actively transported through the cell membrane and accumulated within the cells as solid particles or in vacuoles.
	Redox reaction	Metals are microbially oxidized or reduced during oxidation-reduction processes. As result, metal mobility is decreased depending on the type of metal and its oxidation state.
	Complex formation	Soluble metal species are immobilized (precipitated) by microbially formed complexing agents, e.g., sulfide. Metal sulfides show very low solubility products, so that metals are efficiently precipitated even at low sulfide concentrations. Additionally, the bacterial activities can result in a reduction of the acidity in an environment leading to the precipitation of metals as hydroxides.

A variety of mineral oxidizing readily found bacteria are able to oxidize iron and sulfur containing minerals easily. These include the iron- and sulfur-oxidizing *Acidithiobacillus ferrooxidans* (previously, *Thiobacillus ferrooxidans*), *Acidithiobacillus caldus* (previously, *Thiobacillus caldus*), the sulfur-oxidizing *Acidithiobacillus thiooxidans* (previously *Thiobacillus thiooxidans*), and the iron-oxidizing *Leptospirillum ferrooxidans* and *Leptospirillum ferriphilum.*

Some species of fungi can be used for biomining. According to the previous studies, two fungal strains that are called *Aspergillus niger* and *Penicillium simplicissimum* could mobilize Cu and Sn by 65 percent and Al, Ni, Pb and Zn by more than 95 percent [14].

1.2.1. Mechanism of Biomining

A generalized reaction of the biological oxidation involved in leaching of a mineral sulfide can be expressed as

$$MS + 2O_2 \rightarrow MSO_4 \tag{1.1}$$

where, M is a bivalent metal [11]. However, the mineral dissolution reaction is not exactly the same for all metal sulfides. The oxidation of different metal sulfides proceeds via different intermediates has been observed. They proposed two different mechanisms: thiosulfate mechanism for the oxidation of acid-insoluble metal sulfides, for instance pyrite (FeS_2), molybdenite (MoS_2) or tungstenite (WS_2), and a polysulfide mechanism for acid-soluble metal sulfides, such as; sphalerite (ZnS), chalcopyrite (Cu_2S) or galena (PbS).

In the thiosulfate mechanism, solubilization is accomplished ferric iron attack on the acid-insoluble metal sulfides, with thiosulfate being the main intermediate and sulfates the main end-product. Using pyrite as an example, the reactions proposed by Schippers and Sand are [19]:

$$FeS_2 + 6Fe^{3+} + 3H_2O \rightarrow S_2O_3^{2-} + 7Fe^{2+} + 6H^+ \tag{1.2}$$

$$S_2O_3^{2-} + 8Fe^{3+} + 5H_2O \rightarrow 2SO_4^{2-} + 8Fe^{2+} + 10H^+ \tag{1.3}$$
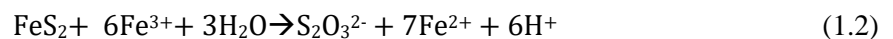
Main intermediate. This elemental sulfur is relatively stable, but can be oxidized to sulfate by sulfur-oxidizing microbes. (1.4)– (1.6).

$$MS + Fe^{3+} + H^+ \rightarrow M^{2+} + 0.5H_2S_n + Fe^{2+} \qquad\qquad (n\geq2) \ (1.4)$$

$$0.5H_2S_n + Fe^{3+} \rightarrow 0.125S_8 + Fe^{2+} + H^+ \qquad\qquad (1.5)$$

$$0.125S_8 + 1.5O_2 + H_2O \rightarrow SO_4^{2-} + 2H^+ \qquad\qquad (1.6)$$
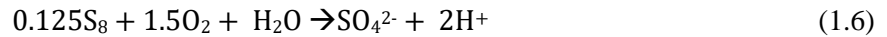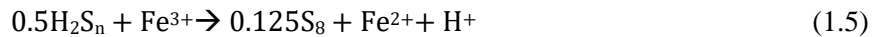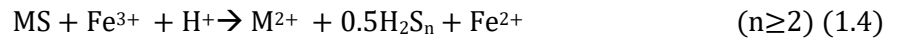
This explains why only sulfur-oxidizing bacteria, such as *At. thiooxidans* or *At. caldus* are able to leach some metal sulfides but not others.

The role of the microorganisms in the solubilization of metal sulfides is, therefore, to provide sulfuric acid (1.6) for a proton attack and to keep the iron in the oxidized ferric state (1.7) for an oxidative attack on the mineral

The ferrous iron produced during metal dissolution and bioleaching might also be reoxidized by iron-oxidizing organisms to ferric iron (1.7) [15] [14].

$$2Fe^{2+} + 0.5O_2 + 2H^+ \rightarrow 2Fe^{3+} + H_2O \qquad\qquad (1.7)$$
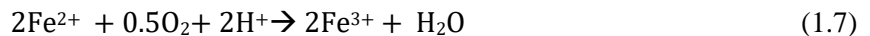
1.2.2. Commercial Applications Of Biomining

In 1950s bioleaching process was called biohytrometallurgy and the first implementation was copper bioleaching at the Kennecott Copper Bingham Mine. Nowadays, copper bioleaching and pretreatment of refractory gold ores and concentrates are commercial application samples of biomining. In the period of 1984–2005, production of copper in the world has increased continuously from 9 Mt to 16 Mt per annum. Now, over 20 percent of that copper production is performed via biomining. After the copper, the second large-scale application of biomining has been demonstrated for uranium. There is quite big potential for bioleaching and bio beneficiation pretreatment of a wide range of base metal and platinum-group metals. At bench scale it has been showed that bioleaching could be effective for the base metal sulfides of Ga, Zn, Mo, Ni, Co and Pb at bench scale. And also, biomining pretreating of sulfide minerals encapsulating platinum group metals (Ru, Pt, Rh, Pd, Ir and Os) could possible [16].

For the present, commercial scale biomining applications can be classified in two types which are stirred tank-type process and irrigation-type process. Irrigation-type processes include the percolation of a lixiviant through a static bed, whereas stirred tank-type processes include agitation of finer particle sizes in a lixiviant. In the large-scale commercial operations of bioleaching, percolation leaching is preferred [11].

1.2.2.1. *Irrigation Type Processes*

Irrigation type processes could be classified in three main methods, such as *in situ,* heap, dump and vat leaching.

In situ method means treating the broken ore in-place without transferring it for mining. For this leaching process mine is exploded to make it permeable. After that, air under pressure and a solution are pumped to ore bodies and mine. The resultant solution which includes metal is collected to wells under the ore. Suitable types of ore bodies for in situ leaching could be divided in three: deep deposits below the water table, surface deposits below the water table and surface deposits above the water table. The ores that has a large buffering capacity are not suitable for this method. All of these restrictions make *in situ* leaching a relatively challenging and hardly form of metal recovery.

Dump leaching process refers to bacterial oxidation of low-grade ore dumps and uncrushed waste. This application doesn't require any encouragement. But it is sometimes harmful for the environment. The dumps are built on a durable base so as to contain the bacterial oxidation solution and on the in a valley or side of a slope so that the solution flows through via gravity, and as a result does not require any liquid/solid mechanical separation.

The preparation of the ore is required for heap leaching, firstly size reduction, in order to maximize mineral–lixiviant interaction and the laying of an impervious base to prevent pollution of water bodies and lixiviant loss [14] [11]. **Fig. 1.2.** [15] shows a copper containing ore that is enriched by a typical heap leaching process. In this process firstly ore is crushed. After that, sulfuric acid is used for acidification. Then, to bind fine particles to large grained

particles it piled up in rolling drums. Solubilization of copper is performed by bacteria on the ore via oxidation ferrous iron to ferric iron. After that, the solution which is saturated with copper is regain from the heap.
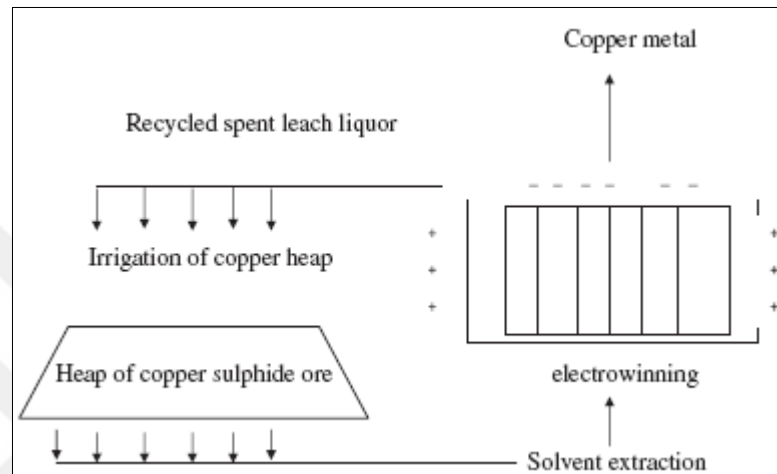
Figure 1.2. Copper ore heap leaching process scheme [15]

Vat leaching is a currently used a leaching method. Decomposition of broken minerals in a tank is required for oxidation of ores. More controls can be applied for enhanced recovery by the use of bioreactors, although these result in higher costs. However, this method is being considered in an active manner for ore concentrates and valuable metals [14].

Table 1.4 Industrial heap bioleaching applications on the world for secondary copper ores and mixed oxide/sulfide ores (without Copper dump bioleach operations) [20].

Industrial heap bioleach plant and location/owner	Cathode copper production/(t.a^{-1})	Operational status
Lo Aguirre, Chile/Sociedad Minera Pudahuel Ltda	15 000	1980-1996 (mine closure due to ore deposit depletion)
Mount Gordon (formerly Gunpowder), Australia/Western Metals Ltd.	33 000	1991-Present
Mt. Leyshon, Australia/(formerly Normandy Poseidon)	750	1992-1995 (stockpile depleted)
Cerro Colorado, Chile/BHPBilliton	115 000	1993-Present
Girilambone, Australia/Straits Resources Ltd & Nord Pacific Ltd.	14 000	1993-2003 (ore depleted)
Ivan-Zar, Chile/Compañía Minera Milpro	10 000-12 000	1994-Present
Punta del Cobre, Chile/Sociedad Punta del Cobre, S.A.	7 000-8 000	1994-Present
Quebrada Blanca, Chile/Teck Cominco Ltd.	75 000	1994-Present
Andacollo Cobre, Chile/Aur Resources, del Pacifico & ENAMI	21 000	1996-Present
Dos Amigos, Chile/CEMIN	10 000	1996-Present
Skouriotissa Copper Mine (Phoenix pit), Cyprus/Hellenic Copper Mines	8 000	1996-Present
Zaldivar, Chile/Barrick Gold Corp.	150 000	1998-Present
Lomas Bayas, Chile/XSTRATA plc	60 000	1998-Present
Cerro Verde, Peru/FreeportMcMoran & Buenaventura	54 200	1997-Present
Lince II, Chile/	27 000	1991-Present (sulfide bioleaching since ~1996)
Monywa, Myanmar/Ivanhoe Mines Ltd, Myanmar No.1 Mining Enterprise	40 000	1998-Present
Nifty Copper, Australia/Straits Resources Ltd.	16 000	1998-Present
Equatorial Tonopah, Nevada/Equatorial Tonopah, Inc.	25 000 (projected)	2000-2001 Failed
Morenci, Arizona/FreeportMcMoran	380 000	2001-Present
Lisbon Valley, Utah/Constellation Copper Corporation	Projected at 27000	2006-Present
Jinchuan Copper, China/Zijin Mining Group Ltd.	10 000	2006-Present
Spence, Chile/BHPBilliton	200 000	Commissioned 2007
Whim Creek and Mons Cupri, Australia/Straits Resources	17 000	2006-Present

There are some important points for biomining technology for treating a definite mineral or mixture of minerals. They are the grade and unit price of the metal content and chemical characteristics of the substrate. In **Table 1.5.**, the specific metals which is adequate for bacterial oxidation and biomining methods are summarized [21].

Table 1.5. The metals which is adequate for biomining

Metal	Tank	Heap	Dump	Vat	*In situ*
Gold	√	√	√	√	x
Silver	x	x	x	x	x
Cobalt	√	√	√	√	√
Uranium	x	√	√	√	√
Nickel	√	√	√	√	√
Molybdenum	√	√	√	√	√
Tin	√	x	x	x	x
Copper	x	√	√	√	√
Antimony	x	x	x	x	x
Zinc	x	√	√	√	√
Lead	x	x	x	x	x

1.2.2.2. Stirred Tank Processes

Stirred tank bioreactors are used for pretreatment processes for the recovery of gold from recalcitrant arsenopyrite concentrates at the most of the commercial operations. Because of gold dividing into mixture of pyrite/arsenopyrite, recalcitrant ores cannot be easily solubilized by the usual cyanidation process. For decomposition of arsenopyrite, cyanide must contact with the gold, since the gold is included in a relatively minor fraction treatment of the ores. The ore is grinded and then preparation of a gold-containing concentrate is made by flotation.

The working principle of bioreactors are continuous-flow mode. For this mode, tanks are arranged in series and continuity is provided by feeding the first tank and over flowing
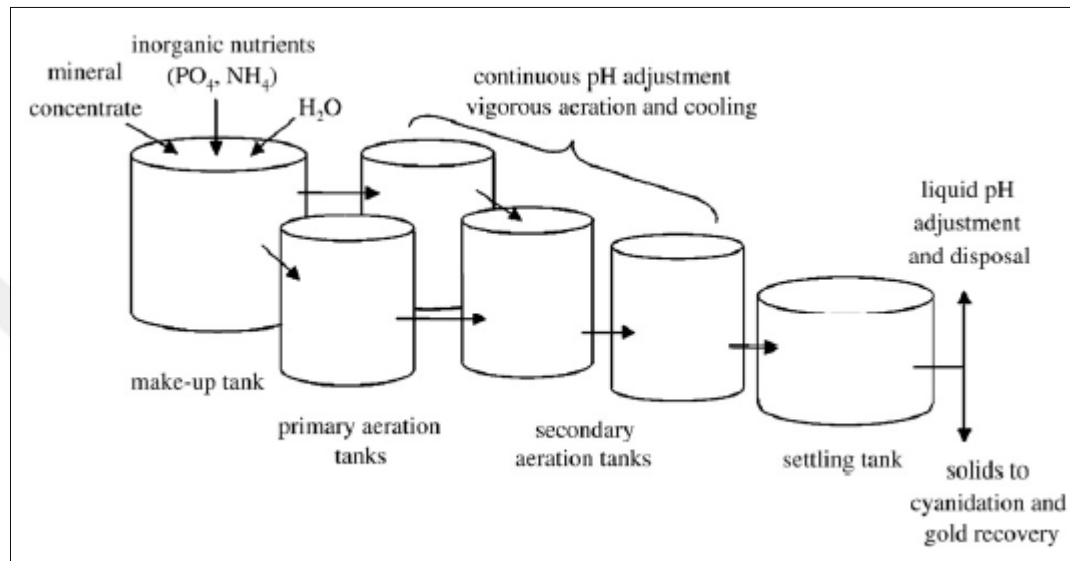
Figure 1.3. Scheme of gold-bearing arsenopyrite pretreatment by continuous-flow bio oxidation process

from tank to tank until bio oxidation of the mineral concentrate is complete efficiently. The bioreactor tanks are generally arranged in parallel for providing suitable retention time for the microbial cell quantity to reach high steady-state levels without being washed out,. **Figure 1.3.** [15] shows the Scheme of gold-bearing arsenopyrite pretreatment by continuous-flow bio oxidation process.

To provide an increase in the rate and efficiency of mineral bio oxidation processes, highly aerated and stirred tank bioreactors are utilized (**Figure 1.3**). However, construction and operation of these reactors are expensive, which inhibits the usage it for high-value ores and concentrates [11].

Table 1.6. Industrial aerated continuous stirred-tank bioleach operations [16].

Industrial stirred-tank bio oxidation/bioleach plant, location and owner	Design capacity/t	Operating years
Fairview, Barberton, South Africa/Barberton Mines Ltd.	55	1986-Present
Sao Bento, Brazil/Eldorado Gold Corp	380	1991-Present
Harbour Lights, Western Australia	40	1991-1994
Wiluna, Western Australia/Agincourt Resources Ltd.	158	1993-Present
Ashanti, Obuasi, Ghana/AngloGold Ashanti Limited	960	1994-Present
Youanmi, Western Australia/Goldcrest Resources	120	1994-1998
Kasese, Uganda/Kases Cobalt Company	250	1999-Present
Tamboraque, San Mateo, Peru/Iamgold Corp. and Minera Lizandro Proano SA	60	1998-2003 Restarted at 2006
Beaconsfield, Tasmania, Australia/Beaconsfield Gold NL	70	2000-Present
Laizhou, Shandong Province, China/Sino Gold Ltd.	100	2001-Present
Suzdal, Kazakhsan/Celtic Resources Holdings Ltd.	196	2005-Present
Fosterville, Victoria, Australia/Perseverance Corporation, Ltd.	211	2005-Present
Bogoso, Ghana/Golden Star Resources	750	2006-Present
Jinfeng, China/Sino Gold Ltd and Guizhou Lannigou Gold Mine Ltd.	790	2006-Present
Kokpatas, Uzbekistan/Navoi Mining and Metallurgy	161069	2008-Present

1.2.3. Microorganisms That Used For Biomining Of Magnesite

In this study, previously isolated and pre-identified *Lactococcus garvieae* and *Enterococcus feacalis* strains were used. They were patented by us as Ca-dissolvers. They belong to lactic acid bacteria group. In previous biomining studies, none of the lactic acid bacteria were used.

The lactic acid bacteria (LAB) are part of a Gram-positive organisms group. These microorganisms are non-sporulating, primarily anaerobic bacteria which produce lactic acid as the principal end product of sugar fermentation [22]. Lactic acid bacteria (LAB) consist of *Oenococcus, Lactococcus, Streptococcus, Enterococcus, Leuconostoc, Lactobacillus, and Pediococcus.*

The *Lactobacillus* genus is rod-shaped, facultatively aerotolerant, gram-positive, catalase negative, non-spore forming and non-motile characteristics. They are able to produce lactic acid by fermenting glucose. *Lactobacillus* bacteria have been isolated from a vast range of fermented food products such as; fermented milk, cheese, raw milk, vegetables, fruits, and meat and they are commonly consumed as probiotics. Beside their morphology, *Lactococcus* bacteria and *Lactobacillus* has no difference [23]. In 1985, Schleifer and colleagues proposed the genus *Lactococcus* while reclassifying some species of the genera *Streptococcus* and *Lactobacillus*. After that, this classification was confirmed by a number of techniques such as; the determination of immunological relationships of superoxide dismutase, the similarity of lipoteichoic acid structures, lipid patterns, and fatty acid and menaquinone compositions. Finally, this calcification has been supported by 16s rRNA sequencing. [24] [25].

The genus *Lactococcus* bacteria are cocci-shaped. Although a number of these bacteria, such as *Lactococcus lactis* and *Lactococcus garvieae* have been isolated from dairy products, the primary origins of *Lactococcus* bacteria are plant and animal skin. *L. lactis* exhibits anti-pathogen activity through media acidification and bacteriocins production. *Lactobacillus* and *Lactococcus* strains isolated from food products can be described as probiotics. Because they are beneficial for health and they are not pathogenic nature. Probiotics are able to decrease the risks of diarrhea, irritable bowel syndrome, antibiotic-related diarrhea, vaginal infections, atopic eczema, and inflammatory bowel disease via regulation of hosts' immune system. Cytotoxic and anti-proliferative effects of probiotics on different cancer cell lines have been reported previously to improve human health. [23] [26].

Enterococcus, which among the LAB, are also Gram positive, coccus shaped, lactic acid producers. Moreover, *Enterococcus* produces some enterocins that are antimicrobial substances and inhibits spoilage organisms. *Enterococcus feacalis* and *Enterococcus feacium*

are commensal organisms that live in human intestines. In 2004, Strompforva et al. and colleagues reported that *Enterococcus feacalis* and *Enterococcus feacium* could be accounted as potential candidates for new probiotic strains [27]. In addition, Alomar et al. (2008), indicated that *Enterococcus feacalis, Lactococcus lactis* and *Lactococcus garvieae* inhibit *Staphylococcus aureus* which is a food borne pathogen in milk [28].

1.3. SCALE UP OF FERMENTATION

In biotechnology, most frequently used shake flasks are the bioreactors. But, very little is known about their characteristics from an engineering viewpoint. Shake flasks are used for various tasks such as; strain screening, establishment of basic process conditions, medium development, etc. Moreover, shake flasks are commonly used since their handling is very easy and many experiments can be carried out concurrently with little supervision [29]. To commercialize the fermentation, the scale-up of laboratory fermentation to pilot scale and industrial scale fermenter are required [30] Unfortunately, the transfer process from shake flasks to fermenter is troublous and poorly understood, mainly since the lack of knowledge related the impression of the operation conditions on mass transfer, power input and hydrodynamics [31].

Usually, the productivity of the desired product is high in flask scale, and is drastically reduced as the scale is enlarged when one attempts to translate the conditions of the flasks to stirred bioreactors. Accordingly, results obtained in the shake flasks can be used only as preliminary indicators. Scale-up studies must be proven in studies carried out in a bench scale fermenter, to determine the conditions for successful industrial production [32].

The scale-up criteria are specific for each system. For the performance of the bioprocess, the most critical point is selecting the scale-up principle depending upon the transport property [33]. The method for scaling up a fermentation system is commonly based on empirical criteria such as pH, temperature, constant power input per unit volume (P/V), a constant mass transfer coefficient, constant mixing time and a constant impeller tip velocity [32].

P/V is especially important in complex two-phase liquid systems as drop diameter depends on power consumption or the maximum energy dispensation rate. Moreover, the extraction efficiency in extractive processes should be influenced by power input as it detects the mean droplet and the distribution of the immiscible extractive organic phase. In this respect, Cull and colleagues [34] showed that P/V was the best scale-up criteria to keep constant the interfacial area in a two liquid phase bioconversion process using geometrically similar stirred tank reactors. That's why, using the P/V as a scale-up criterion seems moderate for given the two-liquid phase nature of extractive bioprocesses [33].

Although, power input per volume (P/V) is among the most often used parameters for scale-up, the scale-up method to maintain dissolved oxygen (DO) at a constant level became popular by the developing of sensor technologies for DO concentration. Because of applied shear stress, culturing filamentous microorganisms such as fungi or actinomycetes in a large fermenter could expose cells to damage. In parallel with this situation, the product yield is reduced. Therefore, optimization studies need to be performed to achieve a sufficient level of DO with minimum possible shear stress [32].

1.4. NEXT GENERATION SQUENCING

DNA sequencing expanded horizons in the life sciences. Sequencing history is started with Sanger sequencing in 1977. At the same time, Maxam and Gilbert were published chemical degradation method for sequencing. Firstly, Maxam-Gilbert method became preferred method for sequencing, because of application simplicity. But, it did not last long, due to used unsafe chemicals and be out of keeping with large scale applications.

Sanger sequencing depends on the synthesis complementary of single strand DNA via DNA polymerase with the standard 2′-deoxynucleotides (dNTPs) and 2′,3′- dideoxynucleotides (ddNTPs). 2′,3′- dideoxynucleotides (ddNTPs) terminate the reaction irreversibly. When a 2′,3′- dideoxynucleotide (ddNTP) is ligated the oligonucleotide, reaction stops. That's why, different sized oligonucleotides occurs. Separate reaction is need for each ddNTP (ddATP, ddCTP, ddTTP, and ddGTP) type. For separation polyacrylamide gel electrophoresis is used.

Each product is loaded to gel and the sequence of template DNA is detected. This difficulty is solved by using florescent dye and fluorescence detection system. Thus, detection is occurred in one reaction instead of four reactions (**Figure 1.4**) [35].
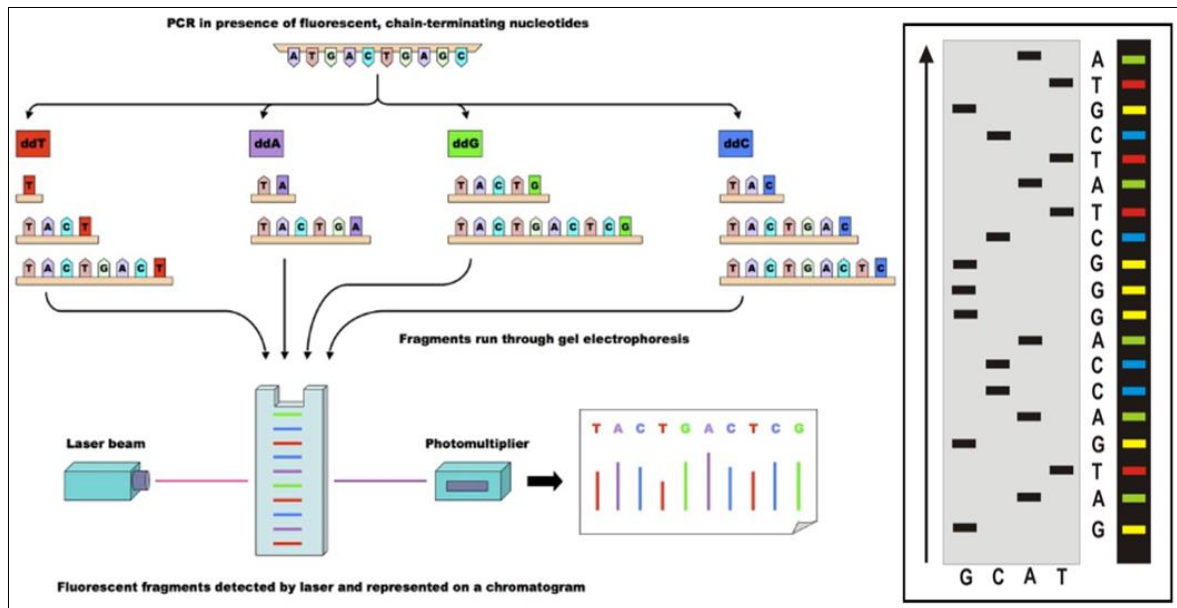
a)   b)

Figure 1.4. a) Sanger sequencing with fluorescent ddNTPs. b) Standard gel electrophoresis (left), Gel electrophoresis of sequences using fluorophores (right) [36].

In time, Sanger sequencing developed via the Human Genome Project. In 1996, H. Kambara and his group developed capillary array DNA sequencer which has higher throughput. Capillary systems produce approximately 1000 bp for each read. Nevertheless, Sanger sequencing still have disadvantages such as; necessity of cloning, using gels for separating of DNA fragments, laborious sample preparation procedures and fewness of parallel analysis. To discard from these limitations new sequencing platforms were developed. These are called Next Generation Sequencing (NGS) systems. In 2008, this technology was started to use commercially. These platforms are the 454 GS20 (Roche App. Sci.), Illumina Genome

analyzer (Illumina, Inc.), the AB SOLID (Applied Biosystems), and the Heliscope from Helicos, Inc. [35] [37].

The basic steps of Next Generation Sequencing are library preparation, cluster generation, sequencing and data analysis.

The 454 Genome Sequencer FLX instrument is the first device of Next-Generation Sequencing technology. It's working principle is based on pyrosequencing. In this device library preparation is achieved by adapter-flanked fragments. Each fragment ligates to a streptavidin bead. Cluster generation is provided via emulsion PCR. Beads with amplicons are transferred and immobilized to picotiter plate. During the reaction chemiluminescent signal releases from each inorganic pyrophosphate (PP_i). Sequence detection is performed during the pyrosequencing (**Figure 1.5.**) [38] [39].
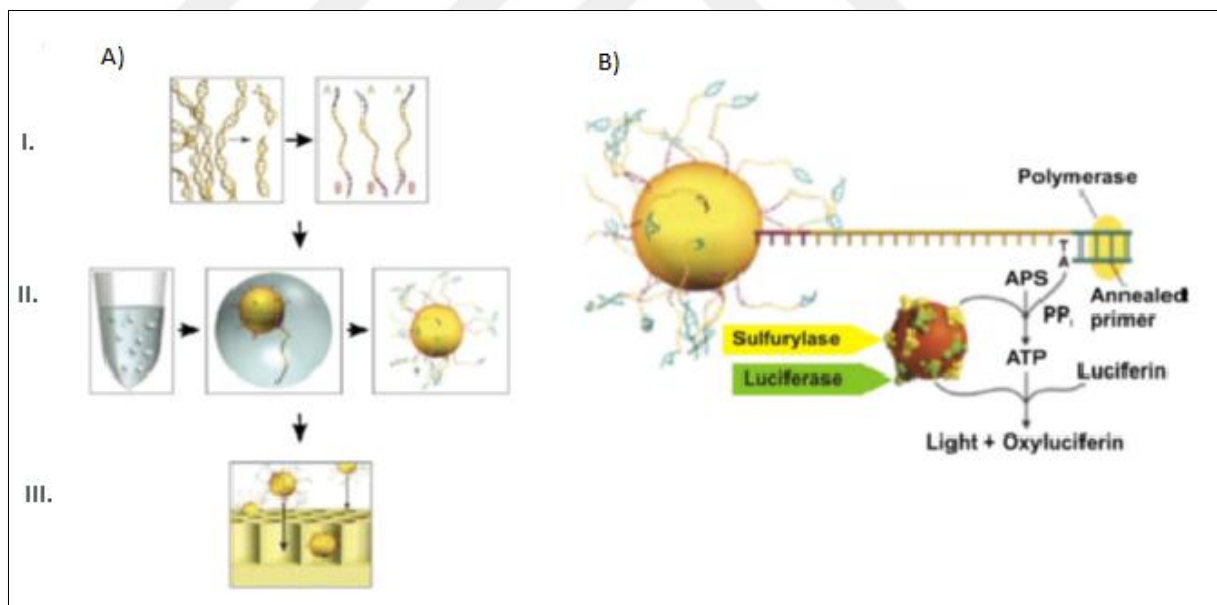
Figure 1.5. (A) G454 DNA sequencer working scheme. (I) Library construction. (II) Emulsion PCR to Amplificate the DNA with beads. (III) Loading the beads to the picotiter plate. (B) Pyrosequencing reaction illustration. [38].

The Illumina Genome Analyzer or Solexa sequencing platform entered into the market in the end of 2006. Its detection principle is sequencing by synthesis as the 454 GS FLX. Library construction is carried out by pair end adapters. Cluster formation is performed by Bridge PCR. When amplification is completed, four fluorescent labelled reversible terminator dNTPs added for sequencing reaction. DNA sequence detected by fluorescence signal. Data analysis is performed by comparing the results with reference genome (**Figure 1.6.**) [35] [40].
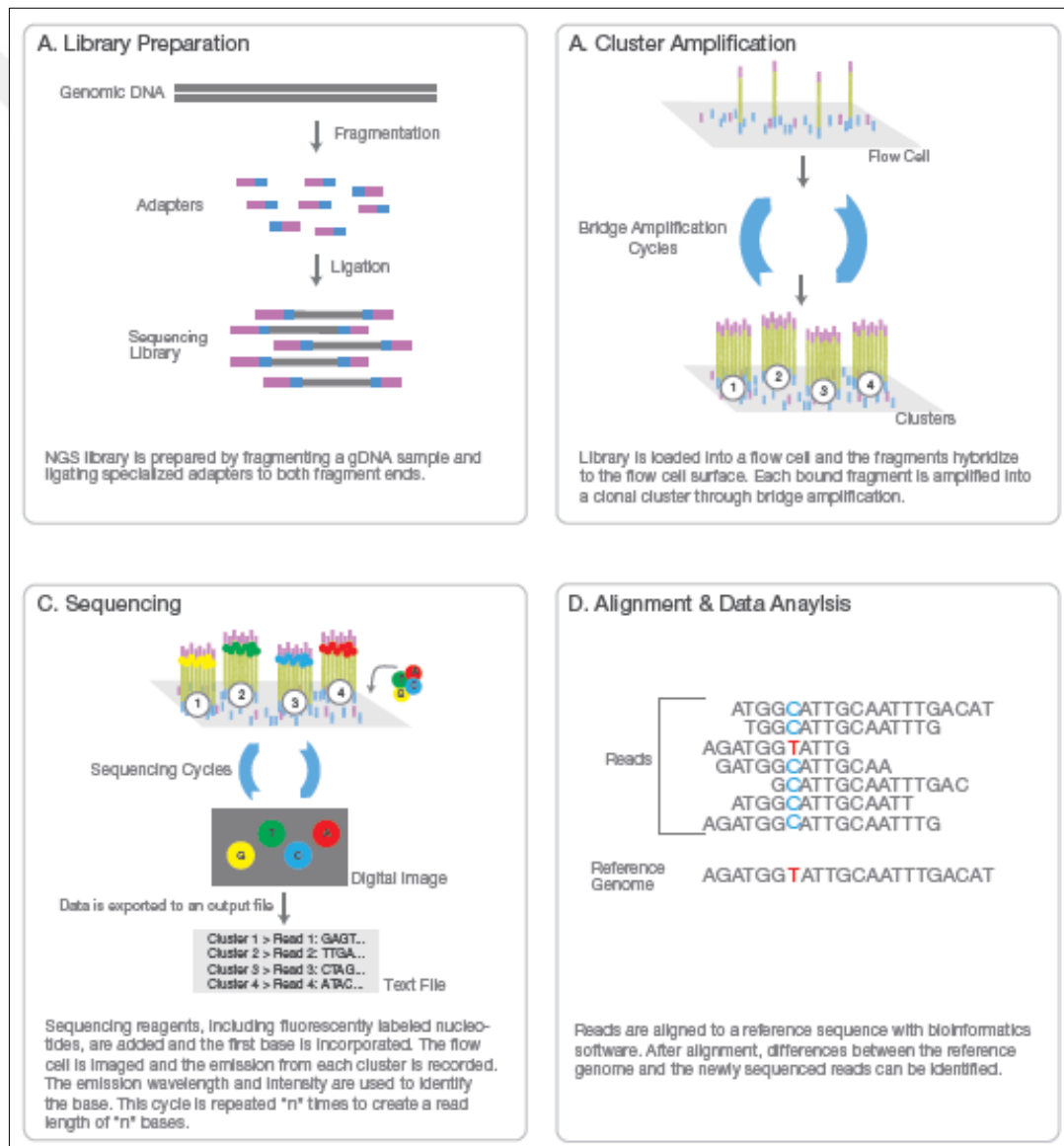
Figure 1.6. The Illumina Genome Analyzer workflow [40].

AB SOLID Sequencer is a platform which its sequencing principle based on DNA ligation. This device has been used since 2007. SOLID is abbreviation of Sequencing by Oligo Ligation and Detection. For library preparation magnetic beads linked adapters are used. After that, emulsion PCR is performed for amplification of DNA fragments. Special glass slide is used as platform for amplicons. Reaction starts by annealing of universal primer. During sequencing fluorescent labeled 8mer dinucleotides (four different dye for each base) are ligated to DNA fragment by DNA ligase. Fluorescence signal provides detecting the DNA sequence (**Figure 1.7.**) [41].
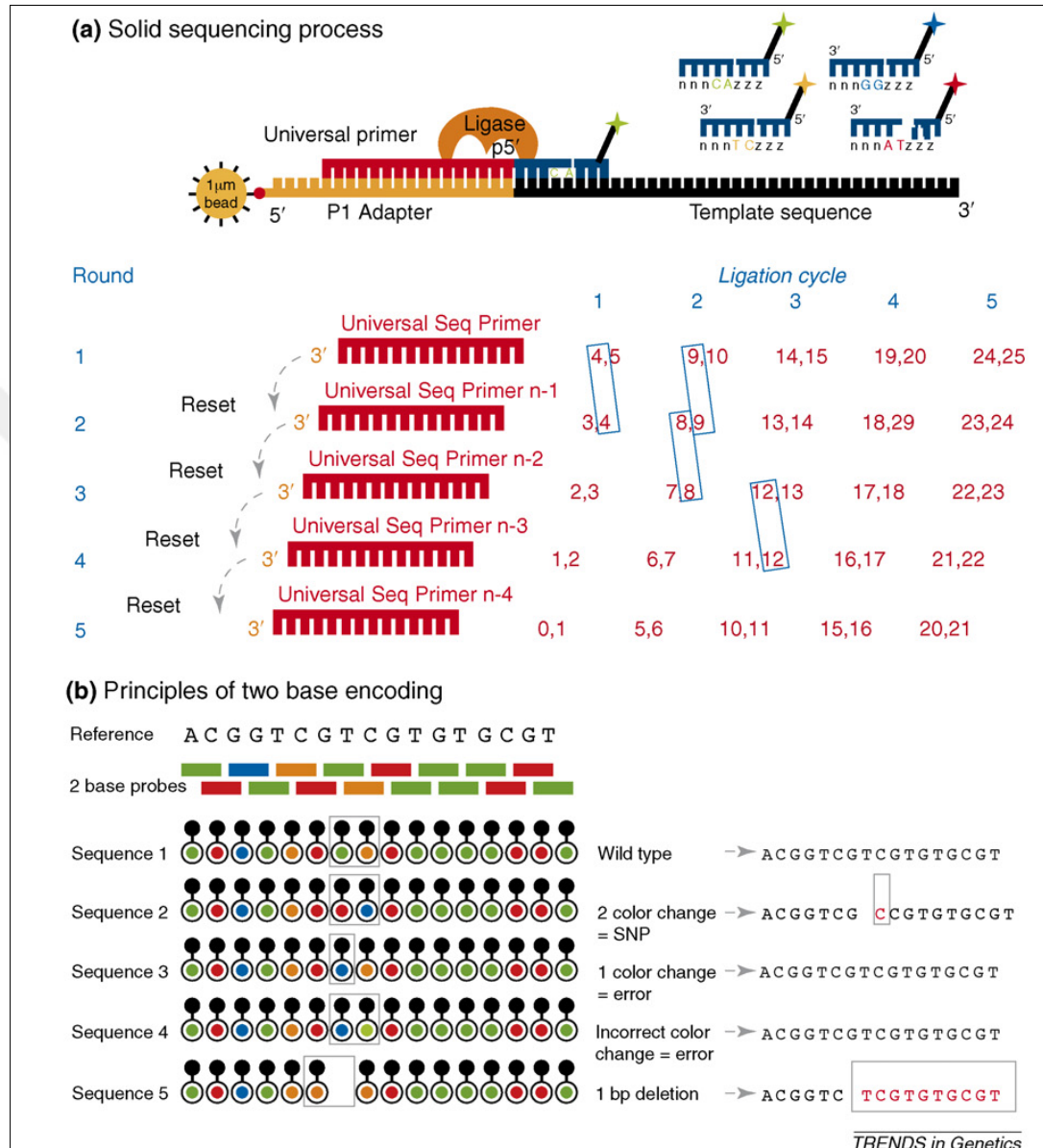
Figure 1.7. AB SOLID Sequencer workflow [41].

The Helicos sequencing system does not include amplification step unlike the other sequencing platforms. Because, this device has very powerful detection system that could detect fluorescence signal of single DNA. Library is constructed by random fragmentation. DNA fragments are ligated to poly-A tails. So, they could hybridize to poly-T treated surface. After immobilization, DNA sequence is detected during the synthesis reaction by the

fluorescent signal of labelled dNTPs [42]. In the table 1.7., Next Generation Sequencers are compared.

Table 1.7. Summary of Next Generation Sequencers [43].

Method	Amplification	Read length (base pairs)	Templates per run	Data production/day	Sequence reaction
ABI 373xl	PCR	~900 to 1100	96	1 Mb	Sanger method
454 FLX Roche	Emulsion PCR	~400	1 000 000	400 Mb/run/	Pyrosequencing
Illumina	Bridge PCR	36 to 175	40 000 000	>17 Gb/run/3 to 6 days	Reverse terminator
ABI SOLID	Emulsion PCR	~50	85 000 000	10 to 15 Gb/run/6 days	Ligation sequencing
Helicos Heliscope	None	35 to 30	800 000 000	21 to 28 Gb/run/8 days	Single molecule sequence by synthesis

The next-generation sequencing technologies application fields can be collected in three headlines; genomics, transcriptomics and epigenomics.

Genomics includes Whole Genome Sequencing, Exome Sequencing and *De Novo* Sequencing. Cost effective the Next Generation Sequencer alternatives make possible the sequencing whole genome, such as human and microorganisms. Exome sequencing may also provide identification the genetic diseases.

Transcriptomics is the other application field of the NGS. RNA sequencing is possible after the converting the total RNA sample to cDNA. Total RNA and mRNA sequencing shows us expression profile of cell/microorganism in a time or condition. Targeted RNA sequencing could be performed with this technology. It provides to detect gene fusions, mRNA isoforms and splice junctions. Moreover, small RNA, noncoding RNA, microRNA which are important

regulatory elements in gene expression, transcription and translation which could be sequenced, rapidly.

Epigenomics searches epigenetic modifications. Epigenetic modifications are reversible. Although, they do not change DNA sequence, they affect gene activity. Methylation of DNA, regulation of DNA by sRNAs and DNA-protein interplay are considered as epigenetic modifications. NGS determines this changes in DNA and RNA [40].

1.5. MASS SPECTROSCOPY

Proteins and peptides are biological macromolecules which are formed of amino acid subunits. Amino acids are linked each other by peptide bonds. Proteins have various functions in biological systems such as, catalyst, transporter, and many others. Proteins and enzymes are also used at industrial and pharmacological sector. That's why, protein characterization analysis are so important for these sectors. Less sensitive methods were used before Mass spectroscopy, such as chromatographic and electrophoretic separation, UV detection and staining [44] [45].

Nowadays, Mass spectrometry is the most used tool for protein characterization. It has preferred because it is sensitive, rapid and versatile method. It is able to determine absolute and relative protein quantities, and identify and quantify thousands of proteins from complex samples by this tool. And characterizing a wide variety of post-translational modifications and determining amino acid sequences of peptides are also possible by mass spectrometry. Due to these abilities, it is useful device for biology projects [46] [47] [48].

Before detection, proteins are degraded by some chemicals or enzymes. Peptides are identified in the gas phase. Ionization of peptides are provided by two soft ionization techniques; electrospray ionization (ESI) and matrix-assisted laser desorption/ionization (MALDI) (**Figure 1.8.**) [46] [49] [50] [51].
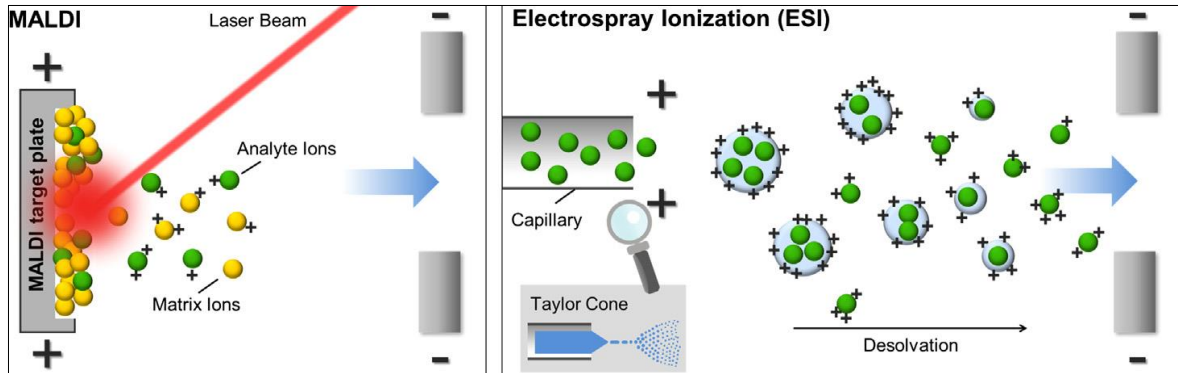
Figure 1.8. Principles of MALDI and ESI ionization [51].

After detection of peptide fragments, theoretical peptide map is generated. Peptide identification is completed by the computational analysis. The coverage of sequence and protein identity are exposed via the comparison with database (**Figure 1.9.**) [51].
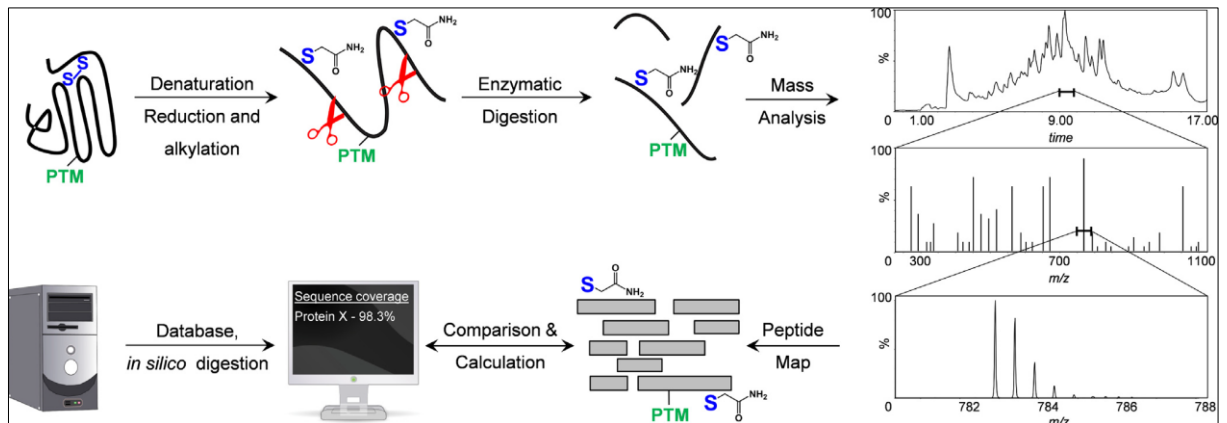
Figure 1.9. Primary structure characterization of a protein [51].

2. MATERIAL

2.1. PRIMERS

Universal 16S rRNA PCR primers, Iontek, TURKEY

27F   AGA GTT TGG ATC ATG GCT CAG
1492R   CGG TTA CCT TGT TAC GAC TT

Universal 18S rRNA PCR primers, Iontek, TURKEY

ITS1 F   CTTGGTCATTTAGAGGAAGTAA
ITS4 R   CAGACTT(G/A)TA(C/T)ATGGTCCAG

2.2. MEDIA AND CHEMICALS

Tryptic Soy Broth (TSB)	MERCK	GERMANY
Tryptic Soy Agar (TSA)	MERCK	GERMANY
Sabroud Dextrose Agar (SDA)	Acumedia	USA
Potato Dextrose Agar (PDA)	MERCK	GERMANY
Nutrient Agar (NA)	MERCK	GERMANY
Calcium Carbonate	SIGMA	USA
Yeast Extract	MERCK	GERMANY
Glucose mono hydrate	Riedel-de Haën	GERMANY
Lactose mono hydrate	MERCK	GERMANY
Mannose	Fluka	SWITZERLAND

Sucrose Carlo Erba	Carlo Erba	ITALY
96 per cent Ethanol	MERCK	GERMANY
Agarose	SIGMA	USA
2X master mix PCR solution	Fermentas	USA
Primestar Taq polymerase	Takara	JAPAN
Generuler1 kb DNA ladder	Fermentas	USA
PageRuler Plus Presatined Protein Marker	Thermo Scientific	USA
Imperial Protein Stain	Termo Scientific	USA

2.3. EQUIPMENTS AND DEVICES

Erlenmayer Flask	ISOLAB	GERMANY
Petri Dish	ISOLAB	GERMANY
Eppendorf	ISOLAB	GERMANY
ICP-MS XSeries-2	Thermo Scientific	USA
Incubator	Memmert	GERMANY
Incubator Shaker Certomat IS	Sartorius Stedim	GERMANY
Labculture Sterile Cabin Class II Type A2	ESCO	SINGAPORE
Centrifuge Allegra 64R	Beckman Coulter	USA
Benchtop centrifuge 1-14 SIGMA	SIGMA	USA
Magnetic stirrer	Heidolph	GERMANY

Fridge	Artico	DENMARK
Autoclave HICLAVE HV-85	HIRAYAMA	JAPAN
Water bath	Memmert	GERMANY
Vortex MX-S	DragonLAB	CHINA
Power supply PowerPac Basic	BIO-RAD	USA
Electrophoresis System	Cleaver Scientific ltd.	ENGLAND
Microwave	ARÇELİK	TURKEY
Spectrophotometer Ultrospec 3000	Pharmacia Biotech	SWEDEN
Plate reader Multiscan Spectrum	Thermo Labsystems	USA
Thermal cycler My Cycler	BIO-RAD	USA
Thermal Block Mixing block	BIOER	CHINA
3 L Fermentor Minifors	INFORS HT	SWITZERLAND
30 L Fermentor BIOSTAT C Plus	Sartorius Stedim Biotech	GERMANY
HPLC 1260 Infinity	Agilent	USA
DV-III Ultra Programmable Rheameter	Brookfield	USA
Sonicator Digital Sonifier 250	Branson	USA
Mini PROTEAN Tetra cell Electrophoresis Chamber	BIO-RAD	USA
HT Gas Analyzer	INFORS	SWITZERLAND

2.4. KITS

Genomic DNA Isolation Kit, Invitrogen

InnuPrep Total RNA Isolation Kit, Analytic Jena, Germany

2.5. PREPARED SOLUTIONS

SDS-PAGE Running Buffer (1L)

- 2,02 g Tris
- 14,4 g Glisin
- 0,5 g SDS
  Adjust volume to 1L with dH2O

Phosphate Buffer Saline (PBS)

- 1,4 M NaCl
- 27 mM KCl
- 101 mM Na2HPO4
- 18 mM KH2PO4

Wash solution

- 10 mL of methanol
- 9 mL of water.
- 1 mL of acetic acid

Destain solution

- 100mM 5 mL Ammonium bicarbonate

- 5 mL Acetonitrile

Trypsin Solution

- 1 mL ice cold 50 mM ammonium bicarbonate
- 20 µg sequencing-grade modified trypsin.

Extraction Buffer

- 10 ml acetonitrile
- 9 mL of water
- 1 mL of formic acid

3. METHODS

3.1. OBTAINING MAGNESITE SAMPLES AND BIO-SOLUBILIZATION OF CACO₃ BY BACTERIA STRAINS

Magnesite samples were ordered from three mining companies. Grained magnesite ore samples were provided from different magnesite ores in Turkey (Konya Krom A.Ş. (Konya), KÜMAŞ (Kütahya), Turkmag A.Ş. (Erzurum).

In this study, pre-identified *Enterococcus* spp. and *Lactococcus* spp. bacterial strains were used. Bacteria were grown in sterilized TSB (Tryptic soy broth) with 150 ml working volume in the 250 ml Erlenmeyer flask. Then, *Enterococcus feacalis* (EF) and *Lactococcus garviaea* (A1) bacterial cultures were inoculated sterilized calcium carbonate medium (5g Yeast extract, 5g Glucose, 6g Calcium carbonate ($CaCO_3$) and 500ml dH_2O) to demonstrate the $CaCO_3$ dissolving potential [52]. Flasks were incubated in the shaking incubator at 30^oC and 150 rpm. Samples were taken from these cultures for analyzing free Ca amount with ICP-MS. After that, magnesite ore enrichment will be performed with this medium by putting magnesite sample in place of $CaCO_3$. This experiment was performed as three repeats.

Samples were filtered through 0.2 μm membrane filters and diluted 200 μL/10 mL (filtrate/ 2 percent HNO_3 solution). All elemental analysis for determining free Mg and Ca amount will be performed by Inductively Coupled Plasma Mass Spectrometry (ICP-MS) device at Instrumental Analysis Laboratory of Yeditepe University Genetics and Bioengineering Department [53] [54].

3.2. ISOLATION, IDENTIFICATION OF MICROORGANISMS FROM NATURAL FLORA OF MAGNESITE ORE AND DETERMINATION OF MAGNESITE ENRICHMENT CAPACITY OF THE MICROORGANISMS

3.2.1. Isolation of Microorganisms From Natural Flora of Magnesite Ore

Magnesite samples were added to sterile phosphate buffer (pH: 7,2) and shaken for an hour, to isolate and identify natural flora of magnesite ore. After that, a 100μl sample from buffer was inoculated to TSA (Tryptic Soy Agar), SDA (Sabroud Dextrose Agar), and NA (Nutrient Agar) media at aseptic conditions. After purification, each bacteria colony and fungi that grew on agars were inoculated sterilized calcium carbonate agar (5g Yeast extract, 5g Glucose, 6g Calcium carbonate ($CaCO_3$), 7,5g agar and 500ml dH2O) and broth (5g Yeast extract, 5g Glucose, 6g Calcium carbonate ($CaCO_3$) and 500ml dH_2O) to determine $CaCO_3$ dissolving potential.

3.2.2. Identification of Isolated Microorganisms From Natural Magnesite Ore Flora

The bacteria and fungi having $CaCO_3$ dissolving potential were selected and their molecular identification was done. Molecular identification was made by using 16S rRNA analysis [55] for bacteria and 18S rRNA analysis for fungi [56]. Genomic DNA isolation from bacteria was performed by commercial kit (Invitrogen). Genomic DNA isolation from fungi was performed by CTAB method [57]. 16S rRNA and 18S rRNA PCR was made with isolated DNA samples. Universal 16S rRNA primers (**Table 3.1**) and universal 18S rRNA primers (**Table 3.2**) were used. 16S rRNA PCR reaction at the **Table 3.3** and **Table 3.4** was performed by 2X Master mix PCR solution (Fermantas). 18S rRNA PCR reaction at the **Table 3.5** and **Table 3.6** was performed Primestar Taq polymerase (Takara). After agarose gel electrophoresis imaging PCR products were sent Macrogen Inc. for sequencing.

Table 3.1. Universal 16S rRNA PCR primers

27F	AGA GTT TGG ATC ATG GCT CAG
1492R	CGG TTA CCT TGT TAC GAC TT

Table 3.2 Universal 18S rRNA PCR primers

ITS1 F	CTTGGTCATTTAGAGGAAGTAA
ITS4 R	CAGACTT(G/A)TA(C/T)ATGGTCCAG

Table 3.3. 16S rRNA PCR reaction

Master Mix	12,5μl
F Primer	0,5 µl
R Primer	0,5 µl
Template DNA	2 µl
dH$_2$O	9,5 µl
Total reaction volume	25 µl

Table 3.4. 16S rRNA PCR reaction program

94°C	3 min	1 x
4°C	30 sec	
55°C	30 sec	35 x
72°C	2 min	
72°C	8 min	1 x

Table 3.5 18S rRNA PCR reaction

Buffer	10 µl
F Primer	1 µl
R Primer	1 µl
Template DNA	5 µl
dNTP	1 µl
Enzyme	0,5 µl
dH$_2$O	31,5 µl
Total reaction volume	50 µl

Table 3.6 18S rRNA PCR reaction program

94°C	3 min	1 x
94°C	30 sec	
55°C	30 sec	35 x
72°C	1 min	
72°C	5 min	1 x

3.2.3. Determination Of Magnesite Enrichment Capacity Of The Isolated Microorganisms

Newly isolated microorganisms were inoculated sterilized Magnesite medium GYM (5g Yeast extract, 5g Glucose, 6g Magnesite ($MgCO_3$) and 500ml dH_2O) to determine magnesite dissolving potential. Samples were taken under sterile conditions and free Mg and Ca amount were analyzed by ICP-MS device. This experiment was performed as three repeats.

3.3. DETERMINING OPTIMUM OPERATING CONDITIONS OF PRE-IDENTIFIED BACTERIAL STRAINS AND NEWLY IDENTIFIED STRAINS

Optimum operating conditions of *Enterococcus* spp. and *Lactococcus* spp. bacterial strains and newly identified microorganisms *Staphylococcus warneri* and *Neurospora tetrasperma* from natural flora of magnesite ores were determined by the experiments that were performed under different conditions, such as pH, Temperature, C source, Microbial concentration [12] [14].

3.3.1. Different pH Conditions

TSB (Tryptic Soy Broth) medium was prepared at pH 1, 3, 5, 7, 9, 11 and 13 to detect the optimum pH value for microorganisms. 100 µl from EF, K1 and A1 overnight liquid cultures were inoculated to 10ml TSB medium, separately. After overnight incubation, absorbance values of samples were detected at OD_{600} spectrophotometer.

According to the growth curve, the GYM media were prepared at pH3, pH5, pH7 and pH9. EF, A1, K1 and NT were inoculated to these media. Samples were taken under sterile conditions and free Mg and Ca amount were analyzed by ICP-MS device. This experiment was performed as three repeats.

3.3.2. Different Temperatures

Overnight liquid cultures were inoculated to every 10ml TSB medium, for detection the optimum temperature value for microorganisms 100 µl from EF, K1 and A1. After overnight incubation at 4ºC, 15ºC, 30ºC, 45ºC and 60ºC, absorbance values of samples were detected at OD_{600} by spectrophotometer.

According to the growth curves of A1, K1, NT, EF, GYM medium was prepared and after inoculation all samples were inoculated at 30ºC and 37ºC. Samples were taken under sterile conditions and free Mg and Ca amount were analyzed by ICP-MS device. This experiment was performed as three repeats.

3.3.3. Different C Source

The GYM medium was prepared with four different carbon sources. Glucose, Mannose, Lactose and Sucrose were used as carbon sources. A1, K1, EF and NT were inoculated to

media and were incubated at 30ºC. Samples were taken under sterile conditions and analyzed with ICP-MS device. This experiment was performed as three repeats.

3.3.4. Different Bacterial Concentrations

Different bacterial concentrations were tried to find optimum bacterial concentration for enrichment of magnesite ore 0,1 ml, 1 ml and 5 ml K1, A1, EF culture samples that have OD_{600}: 0,5 absorbance were inoculated 150 ml GYM medium. They were incubated at 30ºC. Samples were taken under sterile conditions and analyzed with ICP-MS device. This experiment was performed as three repeats.

3.3.5. Optimum And Un-optimized Conditions

Optimum operating conditions were defined for each microorganism. For representing the difference between optimum and un-optimized conditions biomining of magnesite experiments were prepared.

Optimum operating conditions for A1, EF and NT is pH3, Temperature: 30ºC, carbon source glucose while carbon source is sucrose for K1.

Un-optimized conditions for A1, EF are pH11, Temperature: 60ºC, carbon source sucrose while carbon source is mannose for K1 and lactose for NT.

In these conditions, media were prepared and microorganisms were inoculated. All of the cultures were incubated at defined temperatures. Samples were taken under sterile conditions and analyzed with ICP-MS device.

This experiment was performed as two repeats.

3.3.6. Mixed Combinations of Microorganisms

Firstly, A1, EF, K1 and NT were inoculated to TSA to see antagonistic effect of them to each other.

After that, 11 different mixed combinations of microorganisms were tried to have stronger dissolving effect. GYM medium was prepared and A1-EF, A1-NT, A1-K1, EF-NT, EF-K1, NT-K1, A1-EF-NT, A1-EF-K1, A1-NT-K1, EF-NT-K1, A1-EF-NT-K1 microorganism combinations were inoculated. Cultures were incubated at 30ºC. Samples were taken under sterile conditions and analyzed with ICP-MS device. This experiment was performed as two repeats.

3.4. ENRICHMENT OF MAGNESITE ORE

According to the optimization experiments results, scale up experiments were performed. Firstly, magnesite ore enrichment was performed 3 L fermenter scale. Then, magnesite ore enrichment was performed 30 L fermenter scale. Samples were taken for five days and were analyzed with ICP-MS

3.4.1. Bioreactor Calculations

Previous experiments resulted A1 and EF as the most effective Ca-dissolver microorganisms. A1- *Lactococcus garvieae* was chosen for scale up. Shaker conditions were 30ºC temperature, 150 rpm and no additional oxygen. To find required impeller speed for 3 L and 30 L fermenter power input per volume (P/V_L) (3.3) was calculated by using Reynolds number (3.1), Newton number (3.2), and Power number. Power number (3.4) was calculated by using reference graph (**Figure 3.1**).

For calculations, density (ρ, kg/m^3) and viscosity (η, kg/m^3) of GYM medium were determined. Density was determined by weighing 5, 10, 15, 20, 25 ml of GYM medium. Viscosity was determined by Rheometer. 500µl GYM medium was put into Rheometer and viscosity was determined when tork was approximately 90 percent.

$$Re = \frac{\rho n d^2}{\eta} \qquad (3.1)$$

$$Né = 70Re^{-1} + 25Re^{-0.6} + 1.5Re^{-0.2} \qquad (3.2)$$

$$\frac{P}{V_L} = Né.\rho \frac{n^3 d^4}{V_L^{2/3}} \qquad (3.3)$$

$$P = N_P . \rho . N^3 D_i{}^5 \qquad (3.4)$$
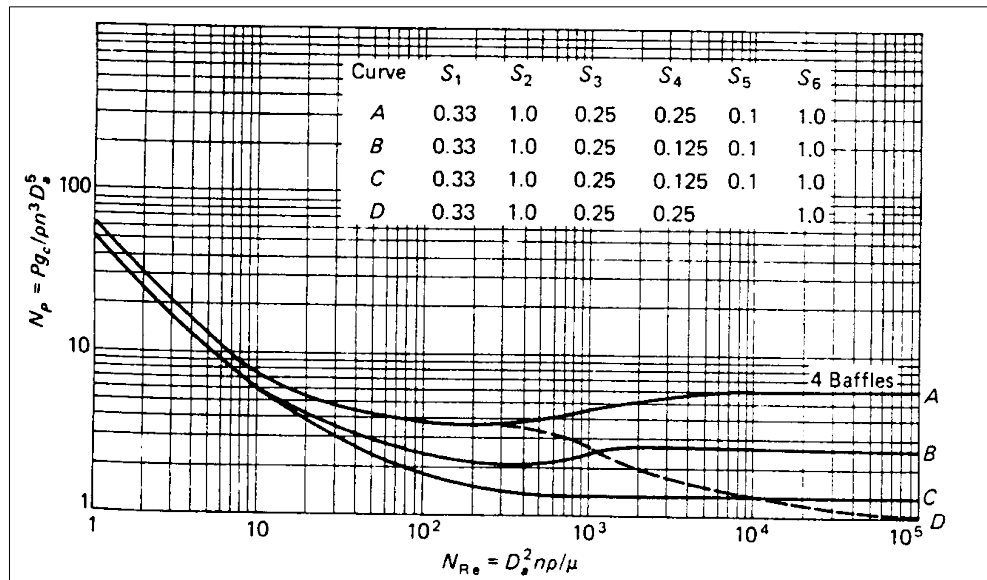
Figure 3.1. Power number and Reynolds number correlation graphic [58]

3.4.1.1. *Phenotypic Analyses of A1 in 3 L Fermenter*

To determine magnesite effect on phenotypic differences, two different fermenter (3L) studies were performed with GYM and GY media for A1 for twice.

Off gas analysis (Exit CO_2 and O_2) were performed online by HT Gas Analyzer (Infors, Switzerland) during the fermentation.

Growth curve was constructed by measuring optic density of cell culture samples by spectrometer at 600nm wavelength.

Lactic acid concentrations were measured for two conditions analyzed with HPLC at Instrumental Analysis Laboratory of Yeditepe University Genetics and Bioengineering Department. Samples were prepared for lactic acid measurement by infiltration with 0,45μm filter and dilution 100 μL/900 μL (filtrate/ 0,1M phosphoric acid solution, pH 2,5).

pH was measured online, using pH probe of fermenter.

3.4.2. Mechanism Of Magnesite Biomining

Measurement of produced lactic acid concentration, Carbonic anhydrase assay, ATPase assay and whole genome analysis, transcriptome analysis and total protein analysis of A1 and EF were performed to determinate magnesite biomining mechanism of A1 and EF microorganisms'.

3.4.2.1. *Measurements of Lactic Acid Concentration*

The GYM medium was prepared and A1 and EF were inoculated to medium. During the incubation at 30ºC, samples were taken at 0h, 4h, 8h, 12h, 16h, 24h, 36h, 48h and 74h.

Samples were prepared for lactic acid measurement by infiltration with 0,45μm filter and dilution 100 μL/900 μL (filtrate/ 0,1M phosphoric acid solution, pH 2,5).

To compare lactic acid efficiency, a magnesite enrichment assay was done with commercial Lactic acid. As GYM medium 1,2 gr magnesite sample added to 100 ml dH$_2$O. Three flasks were prepared and lactic acid was added, till their pH values reach to 1, 3, and 5, respectively. After two hours incubation samples were taken.

Free Mg and Ca amounts were analyzed with ICP-MS device and lactic acid concentrations were detected with HPLC at Instrumental Analysis Laboratory of Yeditepe University Genetics and Bioengineering Department. This experiment was performed as two repeats.

3.4.2.2. ATPase Assay

For ATPase assay, a modified version of Ames 1966 was used. 100μl ATPase assay buffer (25mM Tris-HCl pH:7,4, 5mM MgCl$_2$, 1mM DTT, 1mM ATP) and 10 μl cell lysate were mixed and incubated at 30ºC for 30 minutes. After that, reaction was stopped by adding 200μl 1 percent SDS solution. Then, 100μl 10per cent Ascorbic acid and 600μl 42 percent Ammonium molybdate in 1N H$_2$SO$_4$ were added as color reagent and mixture was incubated at 37ºC for one hour. After the color formation, absorbance measurement was done by spectrometer at 820 nm wavelength. No enzyme added sample was used as blank. [59]

Microorganisms (A1 and EF) have been grown in two types media. One of them is GY (Glucose, Yeast extract) Medium and the other is GYM (Glucose, Yeast extract and Magnesite) Medium. This experiment was performed as three repeats.

3.4.2.3. Carbonic Anhydrase Assay

Time dependent and spectrophotometric Carbonic anhydrase assay, of Caspasa et al 2012, was modified and used for this experiment. For each reaction 600 μl 50mM Tris-HCl, pH 7,4 was used as reaction buffer. 300 μl 3 mM p-NPA (Nitrophenyl acetate) was added as substrate and

100 µl Lysate/ Supernatant were added. No enzyme added sample was used as blank. Absorbance measurements were performed when reaction started (minute 0) and after 10 minute incubation at room temperature (minute 10) at 348 nm wavelength. Difference between minute 0 and minute 10 absorbance values indicated carbonic anhydrase activity. [60]

Microorganisms (A1 and EF) have grown in two types media. One of them is GY (Glucose, Yeast extract) Medium and the other is GYM (Glucose, Yeast extract and Magnesite) Medium. This experiment was performed as three repeats.

3.4.2.4. *Whole Genome Sequencing*

3.4.2.4.1. *Medium for A1 and EF and genomic DNA extraction*

A single colony of A1 and EF grown on TSA (Tryptic Soy Agar) plate was inoculated into 10 ml of GY (Glucose- Yeast extract) broth medium. Broth culture was incubated overnight with shaking at 30˚C. Bacterial cells were collected by centrifugation and genomic DNA extraction was performed with Genomic DNA extraction kit (Invitrogen, USA) according to the manufacturer's instructions.

3.4.2.4.2. *Genome sequencing and annotation*

The genomes of A1 and EF was sequenced by using the Illumina HiSeq 2000 platform (to 100-fold of the sequencing coverage) with paired-end reads at Macrogene Inc. (South Korea). Quality filtered clean reads were assembled by CLC Biology Workbench. The final assembly was automatically annotated with RAST (Rapid Annotation using Subsystem Technology).

3.4.2.5. Transcriptome analysis

3.4.2.5.1. Total RNA isolation

9,5 ml GY and GYM media were prepared for each sample of A1 an EF. 0,5 ml (5 percent of medium) of overnight A1 and EF cultures were inoculated to each medium separately. 3 replicate was prepared for each sample (GY-A1x3, GYM-A1x3, GY-EFx3, and GYM-EFx3). After 19h incubation, cultures were harvested and centrifuged at logarithmic phase +4˚C, 3000 rpm for 10 minutes. Total RNA extraction was performed with InnuPrep RNA Mini Kit (Analytic Jena, Germany) by the manufacturer's instructions. The purified RNA quantity were determined using a Nanodrop. RNA integrity was measured with Agilent 2100 BioAnalyzer (Agilent Technologies, USA) at Macrogen Inc. (Korea).

3.4.2.5.2. RNA Sequencing and Annotation

Transcriptome sequencing was performed by the Illumina HiSeq 2000 platform with pair end reads at Macrogene Inc. (South Korea). Quality filtered clean reads were assembled by CLC Biology Workbench. Annotation for RNASeq was automatically performed with RAST.

3.4.2.6. Protein extraction

Protein extraction protocol of Altin (2009) was modified and performed [61]. 250 ml GY and GYM media were prepared for A1 and EF. 7,5 ml (5 percent of medium) of overnight A1 and EF cultures were inoculated to each medium separately. After five days incubation, cultures were centrifuged at +4˚C, 8000rpm for 15 minutes. Supernatants were discarded and pellets incubated at -80 ˚C overnight. Then, pellets were re-suspended with 4ml 1x PBS by pipetting. 100 µl lysozyme (20mg/ml) was added to all samples. Cell suspensions sonicated with 40

percent amplitude for ten times 30 seconds. Each lysate were centrifuged at +4°C, 14000 rpm for 15 minutes. Supernatants were transferred to new eppendorfs and stored -20 °C [61].

3.4.2.7. SDS Polyacrylamid Gel Electrophoresis

SDS-Page study was performed as [61] protocol. Protein samples were prepared for SDS-PAGE by adding 5 µl 4x Laemmli dye to 15 µL protein sample. Then, samples were heated at 95°C for 5 minutes on heat block. Prepared samples were loaded to polyacrylamide gel and run at 100V for an hour.

3.4.2.8. Staining and Destaining of SDS-PAGE gel

Staining and Destaining were done as explained in manual of Imperial Protein Stain (Thermo Scientific, USA). Gel was put in a suitable container. Gel was incubated three times in ddH$_2$O for 15 minutes on rocking table. Then, gel was incubated in Imperial Protein Stain for an hour on rocking table. For destaining, gel was incubated in ddH$_2$O for 30 minutes.

3.4.2.9. In Gel Digestion for Mass Spectrometric Characterization of Proteins

In gel digestion for mass spectrometric characterization of proteins procedure was performed as Sherman protocol [62]. Protein bands were cut from the gel with a sharp scalpel, and divided into smaller pieces that are approximately 1mm^3 to 2 mm^3. The gel pieces were put in a 1,5 mL eppendorf tube and 200 µL of the wash solution were added on them. The gel pieces were incubated in wash solution for overnight at room temperature.

The following day, wash solution was discarded from the sample with pipette and samples were vortexed with 200 µL of the destain solution. This step was repeated for five times. The destain solution was discarded. After that, for twice 200 µL of acetonitrile was added and the gel pieces were dehydrated for 5 minutes. Acetonitrile was discarded. Then, gel pieces were

dried in a vacuum centrifuge for 2 minutes at room temperature. 30 µL of 10 mM DTT was added to the gel pieces and reduced the protein for 30 minutes at room temperature in a dark place. Then, DTT was discarded. The gel pieces were incubated with 30 µL of 100 mM iodoacetamide at room temperature for 30 minutes. The iodoacetamide solution was discarded. After this step, 200 µL of acetonitrile was added and the gel pieces were dehydrated for 5 minutes. Acetonitrile was discarded. For rehydration, the samples were incubated in 200 µL of 100 mM ammonium bicarbonate for 10 min at room temperature. Ammonium bicarbonate was removed from the samples. 200 µL of acetonitrile was added and the gel pieces were dehydrated for 5 minutes at room temperature. Acetonitrile was discarded. Then, gel pieces were dried completely in a vacuum centrifuge for 2 minutes at room temperature. 30 µL of the trypsin solution was added to the sample and the gel pieces were rehydrated on ice for 10 min with occasional vortex mixing. Samples were centrifuged for 30 seconds and trypsin was discarded by pipette. 5 µL of 50 mM ammonium bicarbonate was added to the sample and mixed with vortex mix. Samples were centrifuged for 30 seconds and for the digestion they were incubated overnight at 37 °C.

After overnight incubation, 30 µL of 50 mM ammonium bicarbonate was added to the digest and samples were incubated for 10 min with occasional gentle vortex mixing. Samples were centrifuged for 30 seconds. After the centrifugation, supernatants were collected and transferred to a new 0,5 ml eppendorf. 30 µL of the extraction buffer was added to the tube containing the gel pieces and samples were incubated for 10 min with occasional gentle vortex mixing. Then, samples were centrifuged for 30 seconds. After the centrifugation, supernatants were collected and combined the extract in the 0,5 ml eppendorf tubes. This extraction buffer step was repeated again. 30 µL of the extraction buffer was added to the tube containing the gel pieces and samples were incubated for 10 min with occasional gentle vortex mixing. Then, samples were centrifuged for 30 seconds. After the centrifugation, supernatants were collected and combined the extract in the 0,5 ml eppendorf tubes. The volume of the extracts were reduced to <20 µL by evaporation in a vacuum centrifuge at ambient temperature. After this step, proteins were ready for analysis.

3.4.2.10.Mass Spectrometric Characterization of Proteins

Mass spectrometric characterizations of proteins were performed with Waters SYNAPT G2-si HDMS and Waters Acquity UPLC M-Class at the Proteomic Laboratory of Medipol University.

3.5. TOXICOLOGY EXPERIMENTS

Toxicology examinations for A1 and EF bacteria were performed at Medicine Faculty Toxicology laboratory of Yeditepe University.

The study was carried out according to Prieur et al. (1973), Ghosh (1984) and Jia et al. (2011). To investigate the subchronic toxicity of A1 and EF, 15 days-feeding study was conducted in wistar rats. Experimental animals were randomly divided in five groups (5rats/group); such as A1 low dose group, A1 high dose group, EF low dose group, EF high dose group and negative control group. A1 and EF overnight cultures were precipitated by centrifuge. Media was removed and pellets suspended with dH_2O to adjust the cell concentration $OD_{600}=2$ for high dose (approximately equivalent to 8.10^9cfu/ml for A1 and 1.10^{10}cfu/ml for EF) and $OD_{600}=0,4$ for low dose (approximately equivalent to $1,6.10^9$cfu/ml for A1 and $1,1.10^9$cfu/ml for EF). Animals were treated with 500μl of sterile dH_2O for negative control groups and 500μl test material for high dose and low dose groups by gavage for 15 days. Blood samples were obtained to tubes containing ethylene diamine tetra acetic acid (EDTA) anticoagulant on day 15 for the measurement of hematology and clinical chemistry parameters. Following parameters were measured: red blood cell count, hemoglobin, platelet count, white blood cell count, differential blood cell count, and alanine aminotransferase. Animals were euthanized for necropsy. At the end of the experiment, macroscopic and microscopic pathological differences in the animals' liver, stomach, kidney, lien, and small intestine were examined. Histological examination was performed on all tissues from animals in the control, low dose groups and high dose groups [63], [64], [65].

4. RESULTS

4.1. BIO-SOLUBILIZATION OF CACO₃ BY BACTERIA STRAINS

Free Ca amount determined for Ca dissolving capacity of *Enterococcus* spp. and *Lactococcus* spp. High dissolving capacity was determined at both of microorganisms (**Figure 4.1** and **Figure 4.2**). High dissolving capacity was determined at both of microorganisms on CaCO₃ agar, too (**Figure 4.3.** and **Figure 4.4.**). After that, these microorganisms were used at magnesite enrichment. According to the ICP-MS results, high enrichment performance was determined for the both of the microorganisms (**Figure 4.5** and **Figure 4.6**).
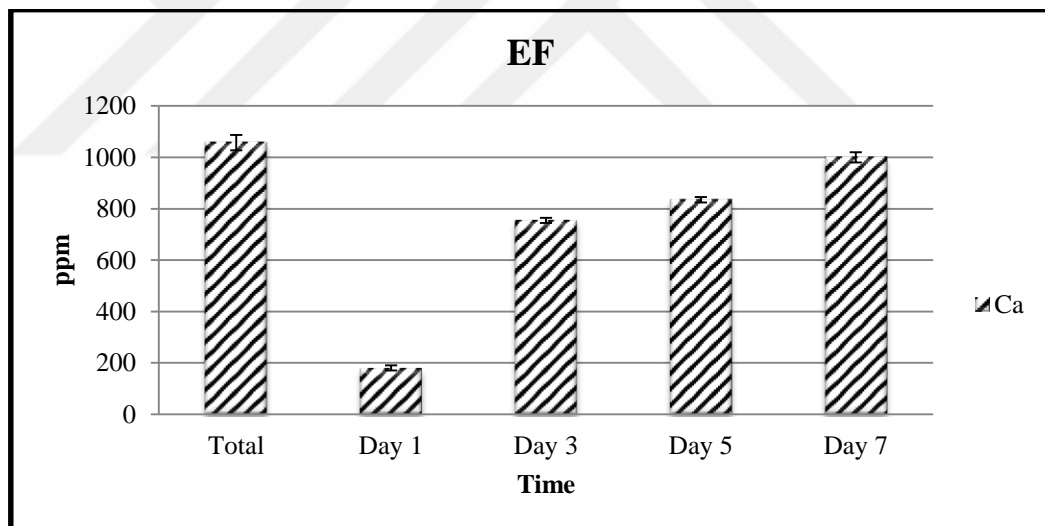
Figure 4.1. *Enterecoccus feacalis* Ca dissolving capacity
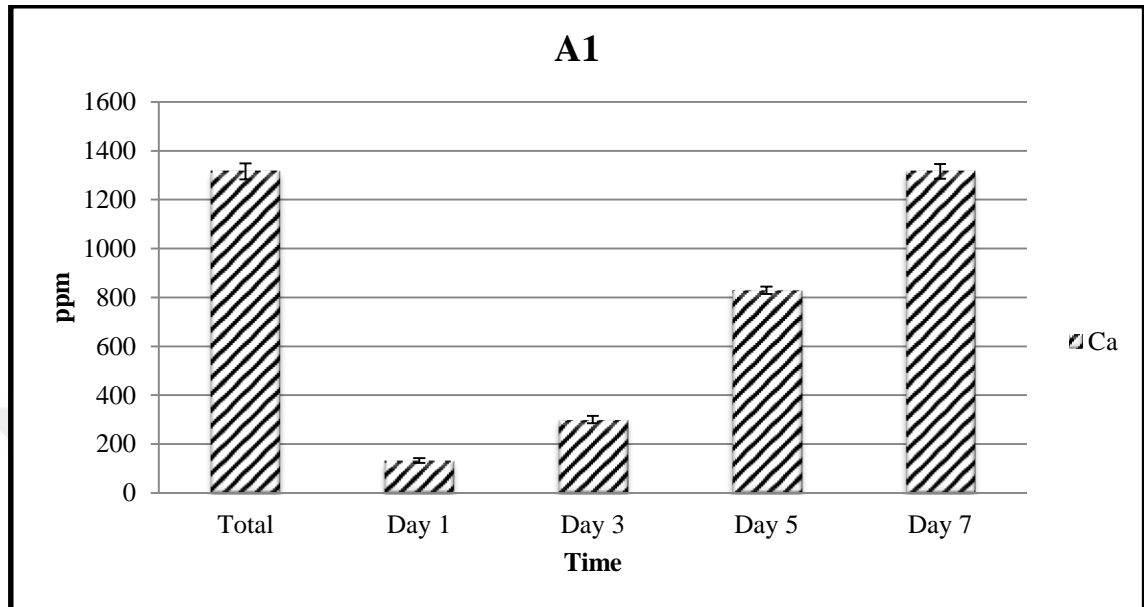
Figure 4.2. *Lactococcus garviaea* Ca dissolving capacity

Figure 4.3 *Enterecoccus* spp. Mg and Ca dissolving capacity on $CaCO_3$ agar

Figure 4.4. *Lactococcus* spp. Mg and Ca dissolving capacity on CaCO$_3$ agar
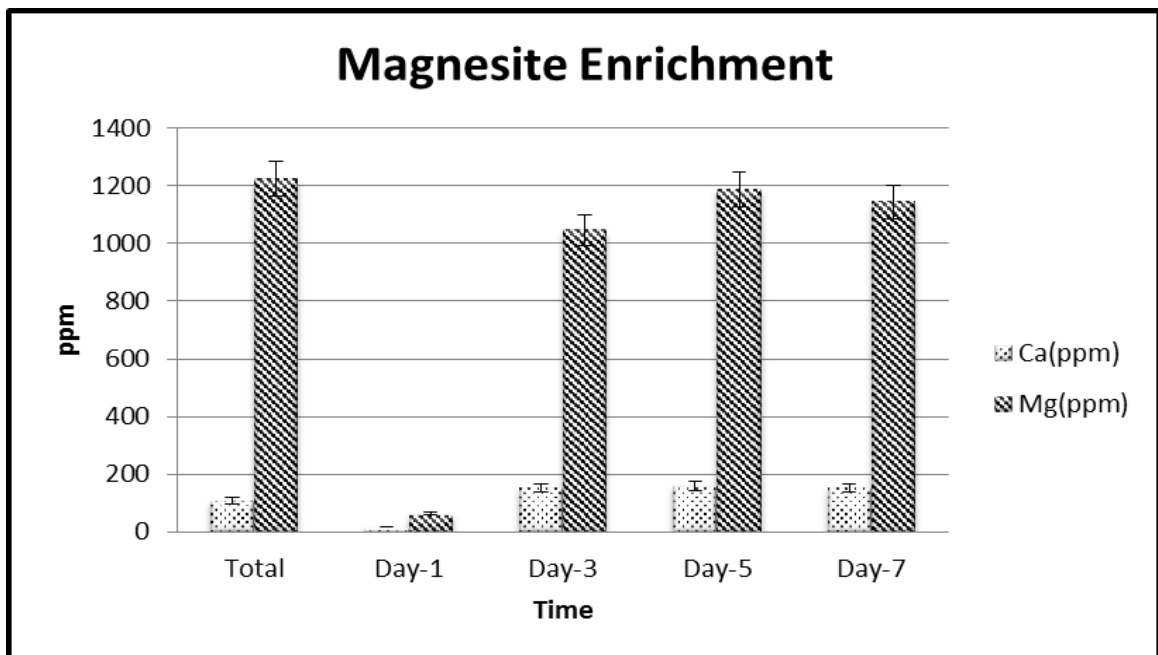
Figure 4.5. *Enterecoccu*s spp. Mg and Ca dissolving capacity
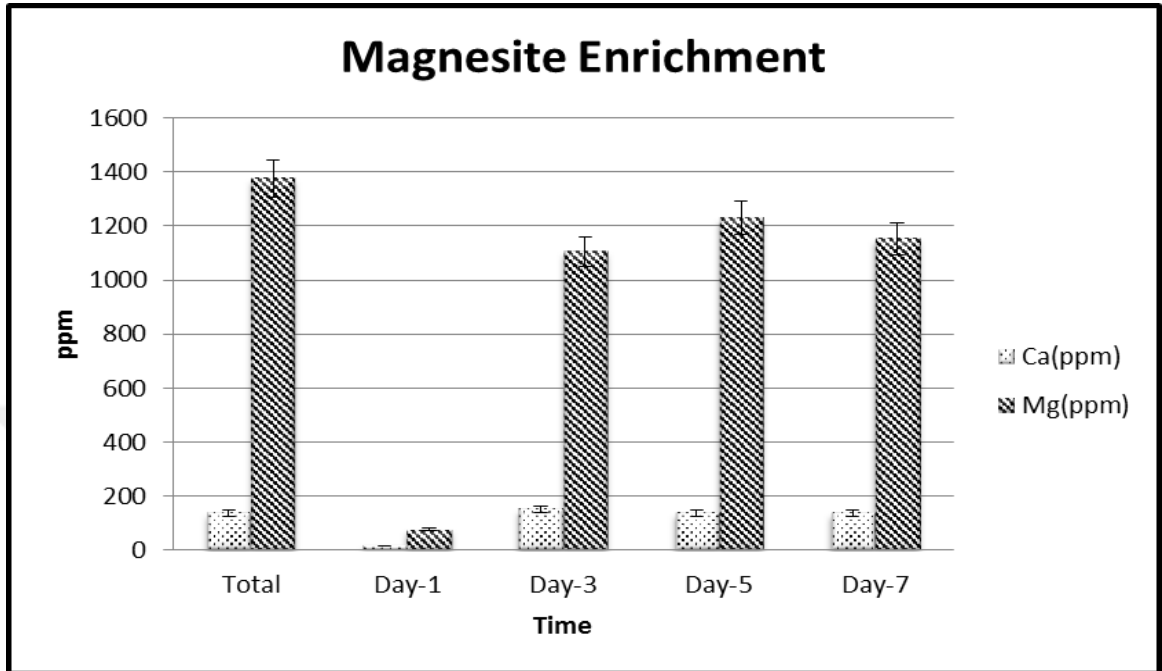
Figure 4.6. *Lactococcus* spp. Mg and Ca dissolving capacity

4.2. ISOLATION, IDENTIFICATION OF MICROORGANISMS FROM NATURAL FLORA OF MAGNESITE ORE AND DETERMINATION OF MAGNESITE ENRICHMENT CAPACITY OF THE MICROORGANISMS

4.2.1. Isolation Of Microorganisms From Natural Flora Of Magnesite Ore

As a result of microorganism isolation study from different magnesite ore, two bacterial strains and a fungi that have $CaCO_3$ dissolving capacity were isolated. Fungi and one of the bacteria were isolated magnesite ore from Erzurum, and the other bacterium was isolated magnesite ore from Kütahya. They were called as G1, K1 and E1, respectively (**Figure4.7**, **Figure 4.8** and **Figure 4.9**).

Figure 4.7. New Ca-dissolver fungi strain from magnesite of Erzurum, called NT (on the left).
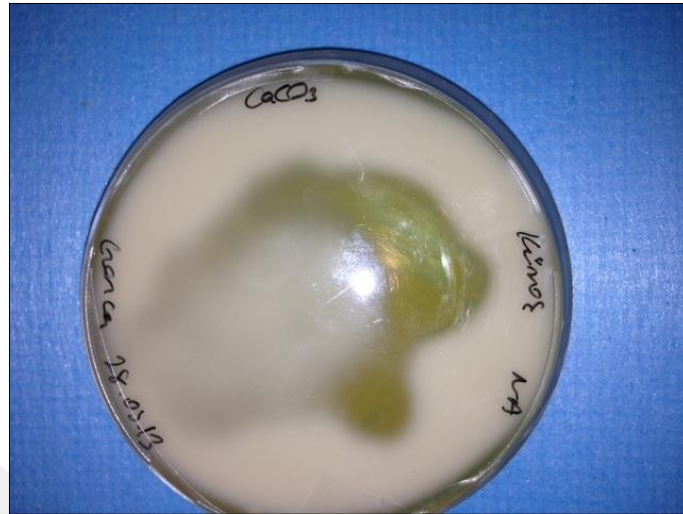
Figure 4.8. New Ca-dissolver strain from magnesite of Kütahya, called K1
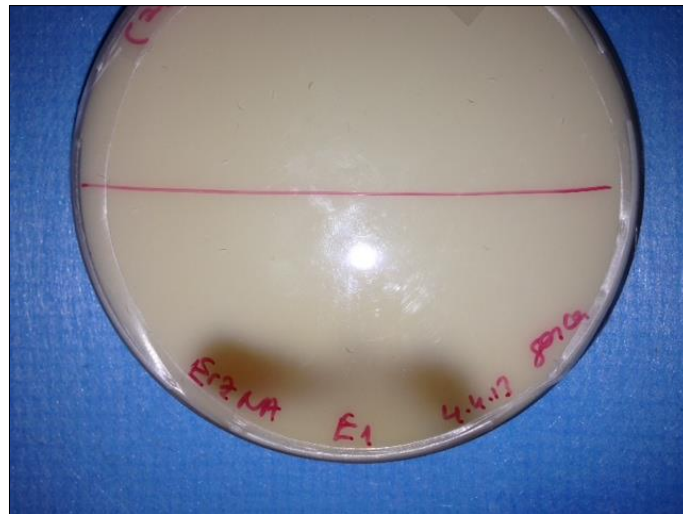
Figure 4.9. New Ca-dissolver strain from magnesite of Erzurum, called E1

4.2.2. Identification Of Isolated Microorganisms From Natural Magnesite Ore Flora

16S rRNA PCR and 18S rRNA PCR were performed for identification of the isolated microorganisms. As a result of 16S rRNA PCR, approximately 1500 bp fragments were determined (**Figure 4.10**) and 18S rRNA PCR product was approximately 600bp fragment (**Figure 4.11**), as expected.
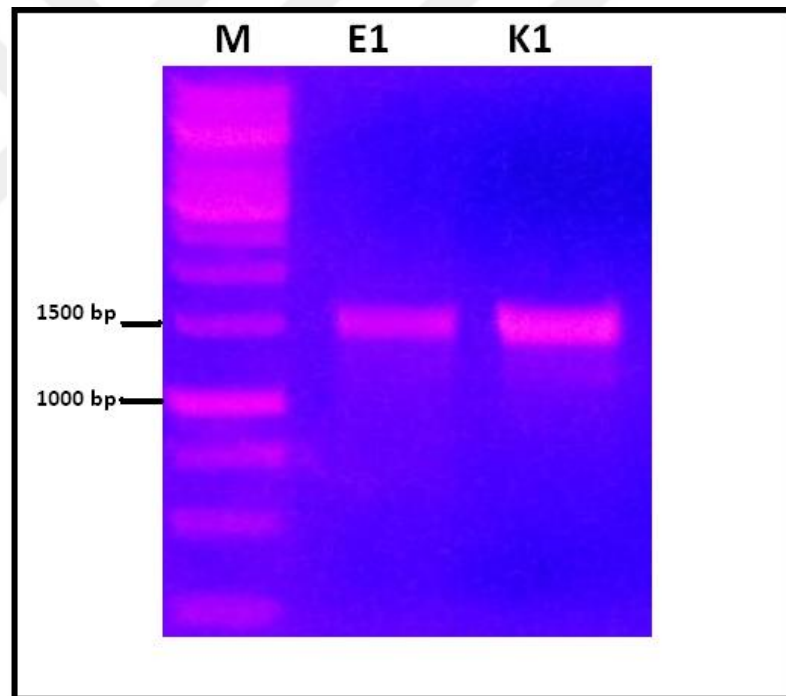
Figure 4.10. 16S rRNA PCR results. M; Generuler1 kb DNA ladder, E1; the bacterium isolated from magnesite of Erzurum and its 16S rRNA PCR product, K1; the bacterium isolated from magnesite of Kütahya and its 16S rRNA PCR product.
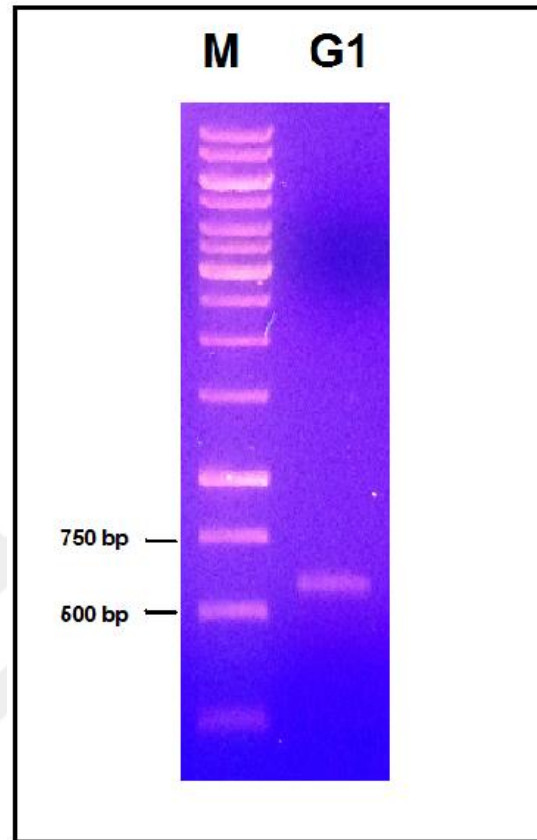
Figure 4.11. 18S rRNA PCR result M; Generuler1 kb DNA ladder, G1; the fungi isolated from magnesite of Erzurum and its 18S rRNA PCR product

PCR products were sequenced at Macrogen Inc. Sequences were aligned with NCBI database by BLAST and CLC Main Workbench program. According to the alignment results, both of the bacteria belong to the same strain, *Staphylococcus warneri* (K1) **(Figure 4.12** and **Figure 4.13)** and fungi belongs to *Neurospora tetrasperma* (NT) strain **(Figure 4.14).**

Id	Description	Overlap	%Identity	%Positive	%Gaps
485099103	Staphylococcus warneri SG1 strain SG1 16S ribosomal RNA, complete sequence	99,51	99,44	99,44	0,28
219846332	Staphylococcus warneri strain AW 25 16S ribosomal RNA, partial sequence	99,51	99,37	99,37	0,28
219856850	Staphylococcus pasteuri strain ATCC51129 16S ribosomal RNA, partial sequence	99,51	98,94	98,94	0,28
219856849	Staphylococcus lugdunensis strain ATCC 43809 16S ribosomal RNA, partial sequence	99,37	98,03	98,03	0,42
310975040	Staphylococcus epidermidis strain Fussel 16S ribosomal RNA, partial sequence	99,37	98,03	98,03	0,42
444439680	Staphylococcus epidermidis RP62A strain RP62A 16S ribosomal RNA, complete sequence	99,37	97,95	97,95	0,42

Figure 4.12. BLAST result for E1

Id	Description	Overlap	%Identity	%Positive	%Gaps
485099103	Staphylococcus warneri SG1 strain SG1 16S ribosomal RNA, complete sequence	99,51	99,44	99,44	0,28
219846332	Staphylococcus warneri strain AW 25 16S ribosomal RNA, partial sequence	99,51	99,37	99,37	0,28
219856850	Staphylococcus pasteuri strain ATCC51129 16S ribosomal RNA, partial sequence	99,51	98,94	98,94	0,28
219856849	Staphylococcus lugdunensis strain ATCC 43809 16S ribosomal RNA, partial sequence	99,37	98,03	98,03	0,42
444439553	Staphylococcus lugdunensis HKU09-01 strain HKU09-01 16S ribosomal RNA, complete sequence	99,37	97,95	97,95	0,42
444439680	Staphylococcus epidermidis RP62A strain RP62A 16S ribosomal RNA, complete sequence	99,37	97,95	97,95	0,42

Figure 4.13. BLAST result for E1

Descriptions

, Reading indexes 1-5, displaying indexes 1-5

Sequences producing significant alignments:
Select:AllNone Selected:0
Alignments Download GenBank Graphics Distance tree of results Show/hide columns of the table presenting sequences producing significant alignments

Sequences producing significant alignments:

Select for downloading or viewing reports	Description	Max score	Total score	Query cover	E value	Ident	Accession
1 ☐ Select seq gb|KF876831.1|	Neurospora tetrasperma isolate	983	983	99%	0.0	99%	KF876831.1
2 ☐ Select seq gb|JX136749.1|	Neurospora tetrasperma strain O2-6	981	981	100%	0.0	99%	JX136749.1
3 ☐ Select seq gb|GU053979.1|	Uncultured fungus clone LX041197-	981	981	100%	0.0	99%	GU053979.1
4 ☐ Select seq gb|GU053881.1|	Uncultured fungus clone LX040429-	981	981	100%	0.0	99%	GU053881.1

Figure 4.14. BLAST result for G1

4.2.3. Determination Of Magnesite Enrichment Capacity Of The Isolated Microorganisms

Magnesite enrichment capacity of *Staphylococcus warneri* (K1) and *Neurospora tetrasperma* (NT) were determined by free Mg and Ca amounts. Although, enrichment performances are not as high as EF and A1, K1 and NT enrich the magnesite, too.
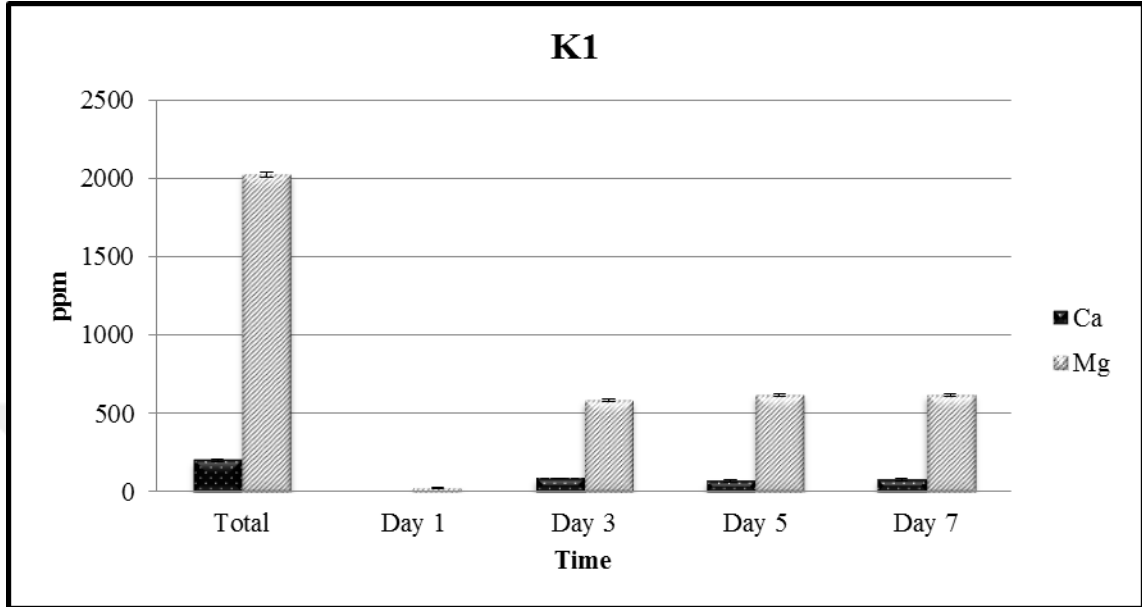
Figure 4.15. *Staphylococcus warneri* (K1) Mg and Ca dissolving capacity
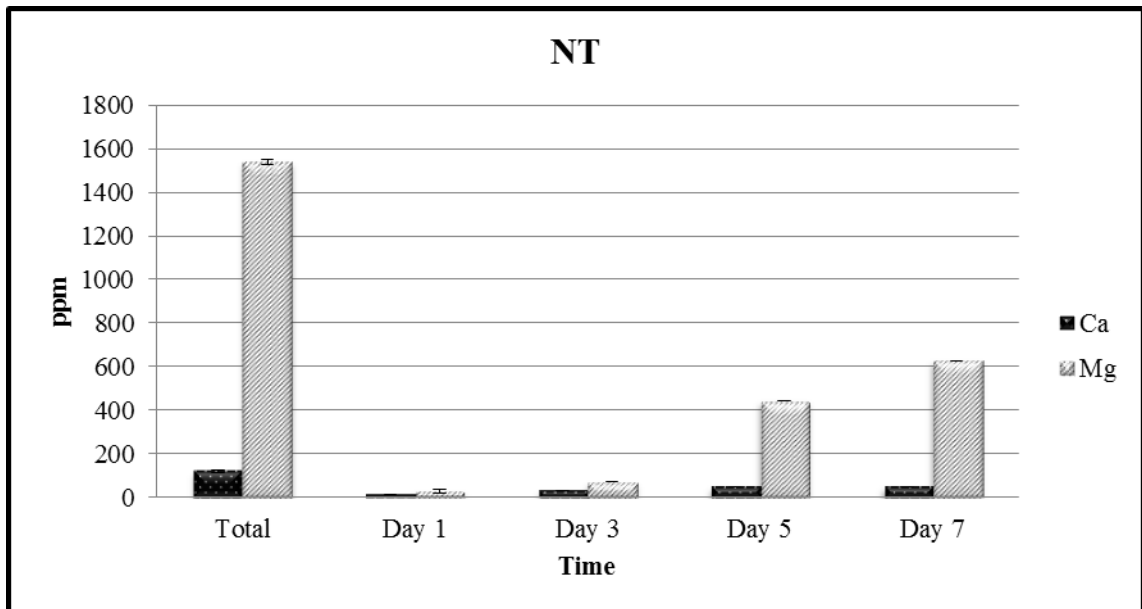
Figure 4.16. *Neurospora tetrasperma* (NT) Mg and Ca dissolving capacity

4.3. DETERMINING OPTIMUM OPERATING CONDITIONS OF PRE-IDENTIFIED BACTERIAL STRAINS AND NEWLY IDENTIFIED STRAINS

4.3.1. Different pH Conditions

According to the curve in **Figure 4.17**, the pH interval that microorganisms could survive was determined between pH 3 and pH 9. Magnesite enrichment was performed with higher performance at acidic pH values than basic pH (**Figure 4.18-4.21**).
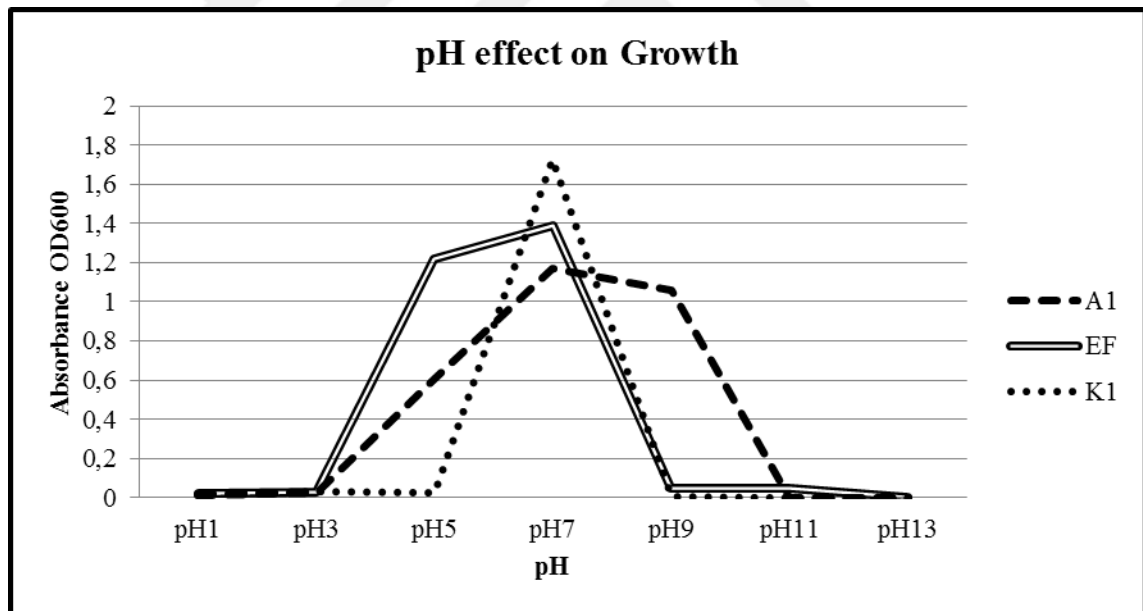
Figure 4.17. pH effects on growth of A1, K1 and EF organisms at different pH values in TSB medium
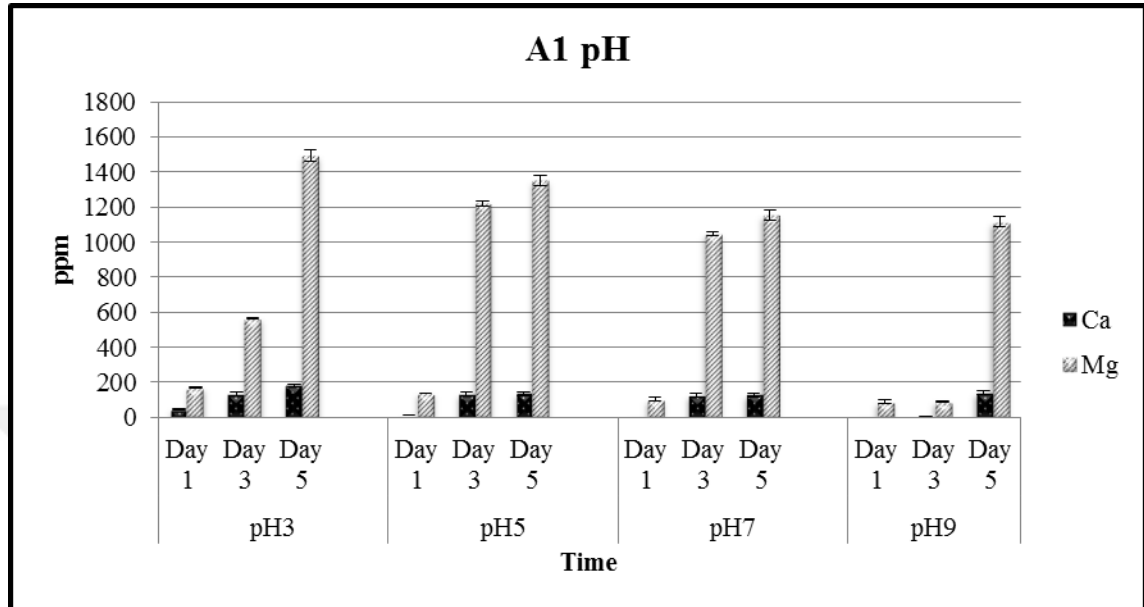
Figure 4.18. Mg and Ca dissolving capacity of A1 at pH values 3,5,7,9.
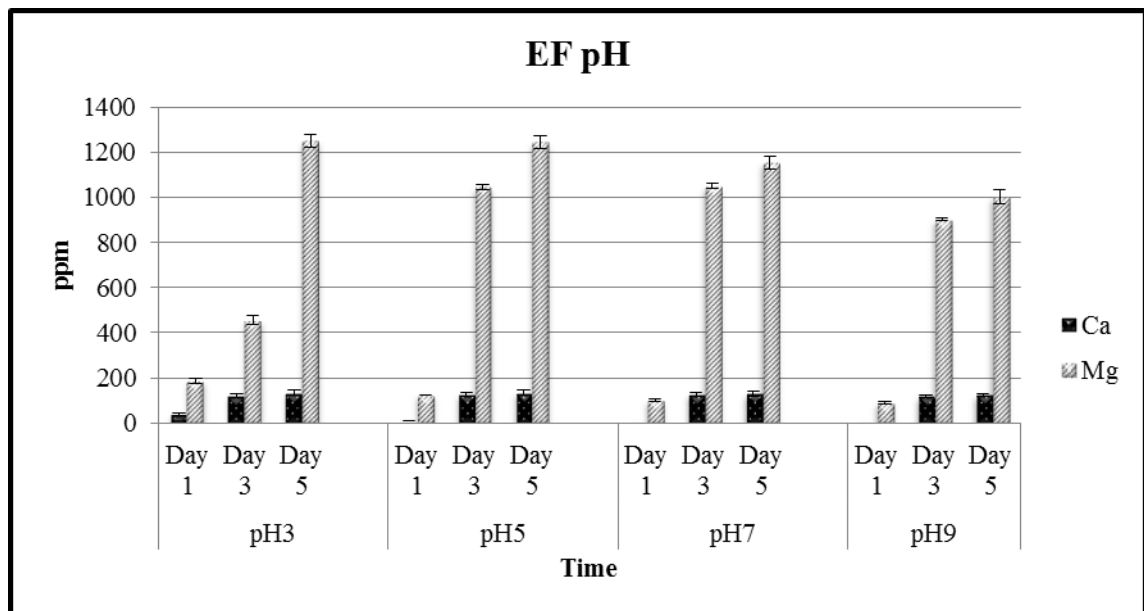
Figure 4.19. Mg and Ca dissolving capacity of EF at pH values 3,5,7,9
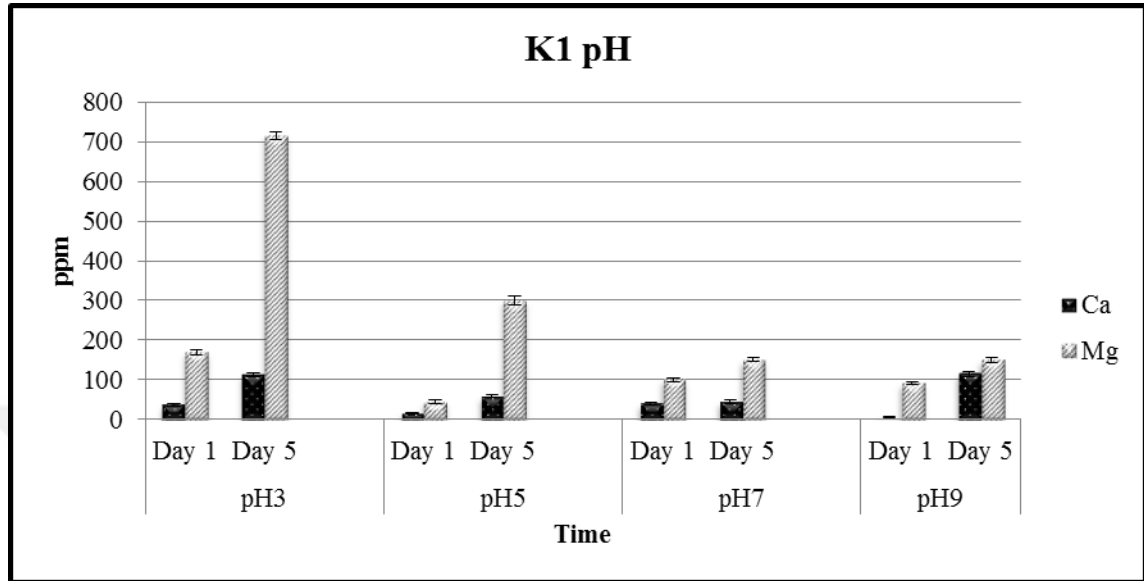
Figure 4.20. Mg and Ca dissolving capacity of K1 at pH values 3,5,7,9
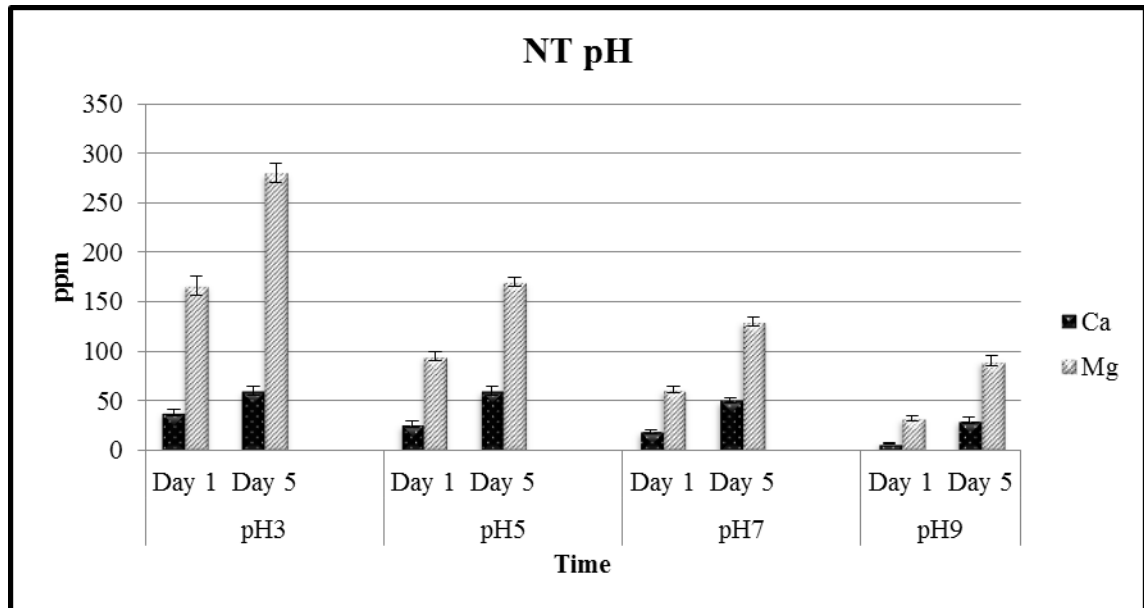
Figure 4.21. Mg and Ca dissolving capacity of NT at pH values 3,5,7,9

4.3.2. Different temperatures

According to the **Figure 4.22**, the temperature interval that microorganisms could survive was determined between 15ºC and 45ºC. As a result 30ºC was determined as optimum temperature for magnesite enrichment (**Figure 4.23-4.26**).
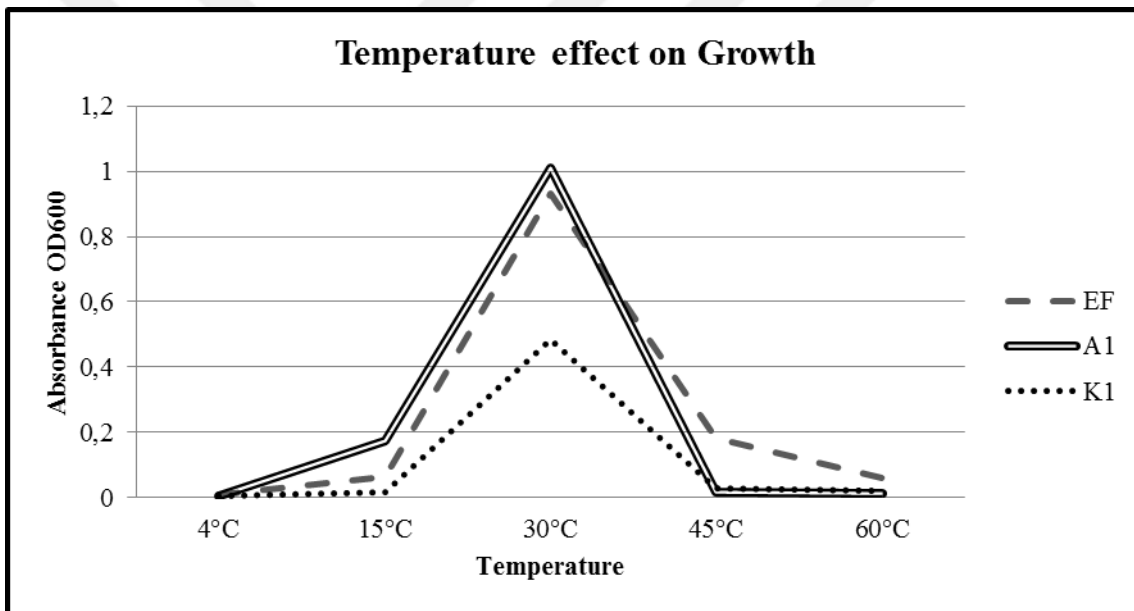
Figure 4.22. Temperature effect on growth of A1, K1 and EF organisms at different temperatures in TSB medium.
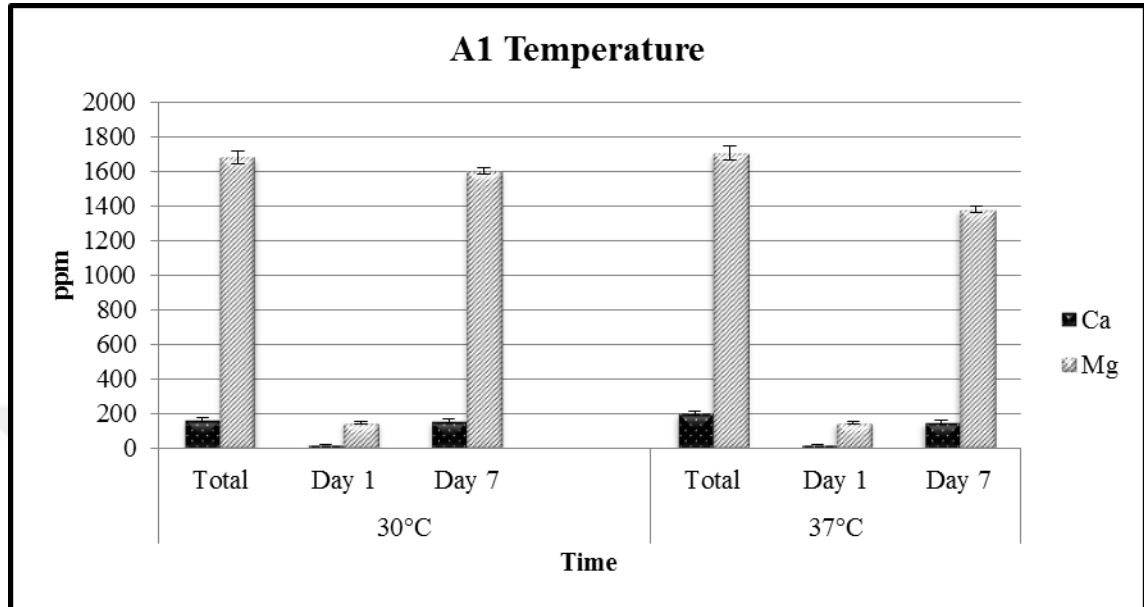
Figure 4.23. Mg and Ca dissolving capacity of A1 at 30°C and 37°C.
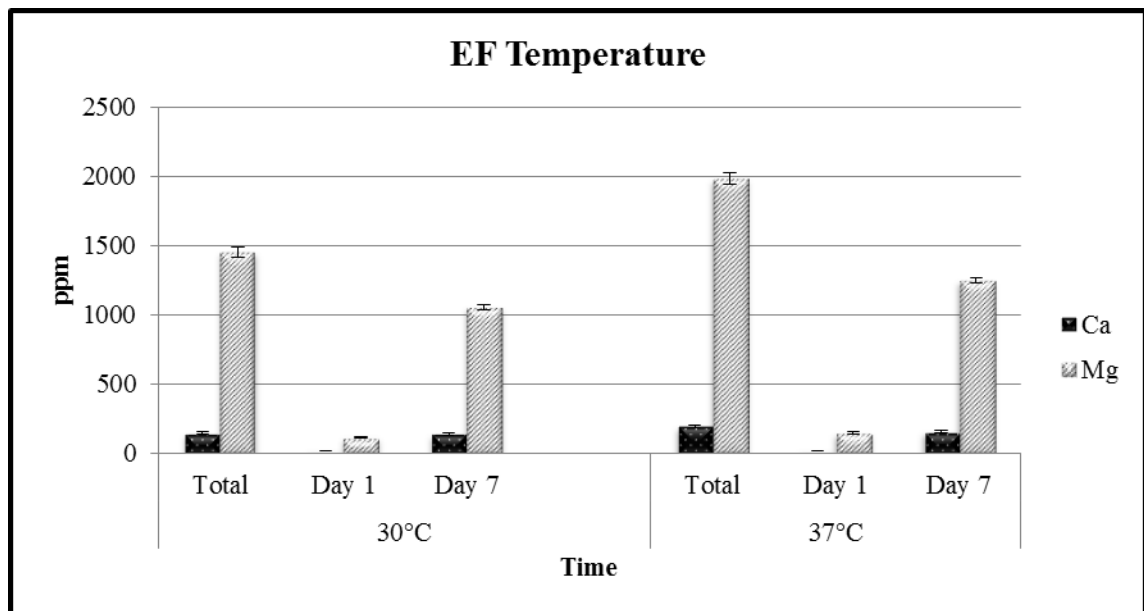
Figure 4.24. Mg and Ca dissolving capacity of K1 at 30°C and 37°C.
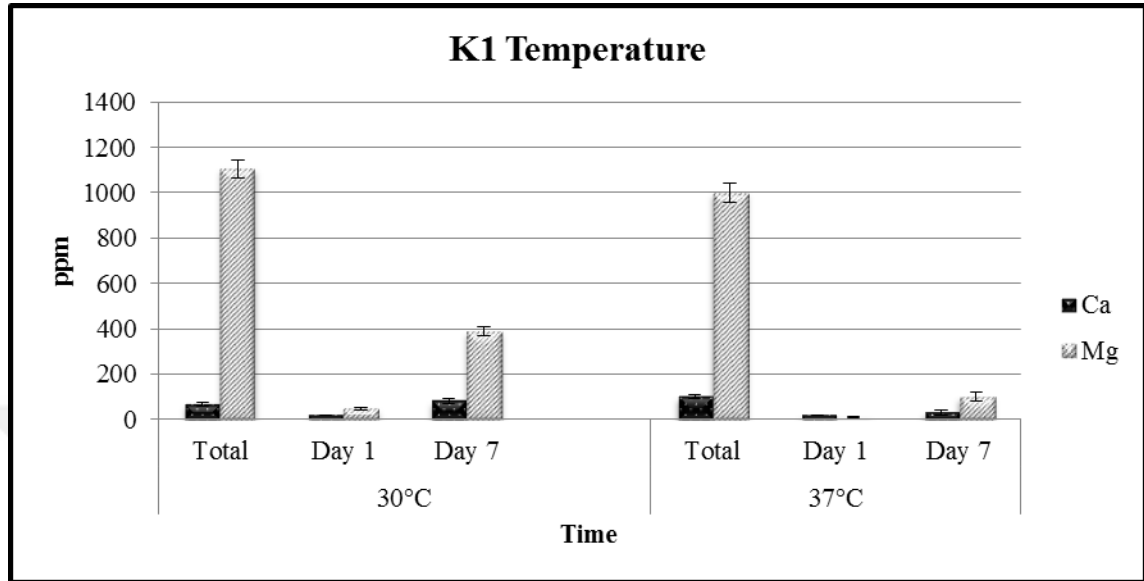
Figure 4.25 Mg and Ca dissolving capacity of EF at 30°C and 37°C.
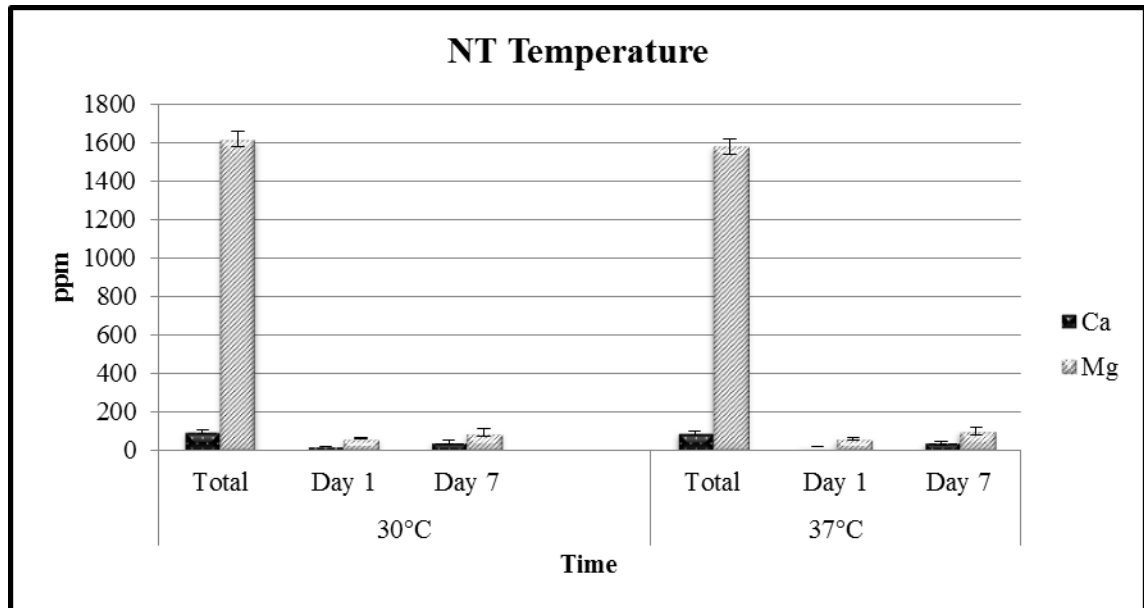
Figure 4.26 Mg and Ca dissolving capacity of NT at 30°C and 37°C.

4.3.3. Different C sources

According to the results in **Figures 4.27-4.30**, Glucose is the optimum carbon source for A1, EF and NT while sucrose is the worst carbon source for A1 and EF and lactose is the worst carbon source for NT. Conversely, Sucrose is the optimum carbon source for K1 with per cent20 dissolving capacity and glucose is the second preferable carbon source after sucrose with percent 18,7 dissolving capacity. The worst carbon source for K1 is mannose.
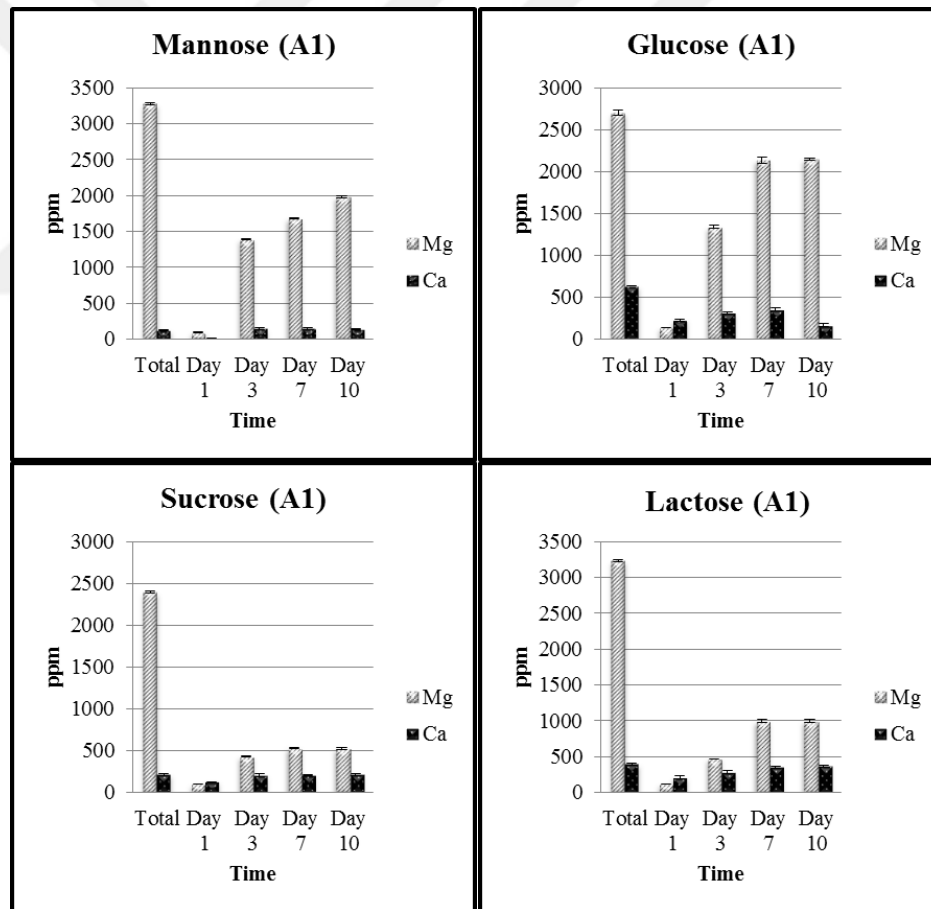
Figure 4.27. Mg and Ca dissolving capacity of A1 with different C sources Glucose, Lactose, Mannose and Sucrose
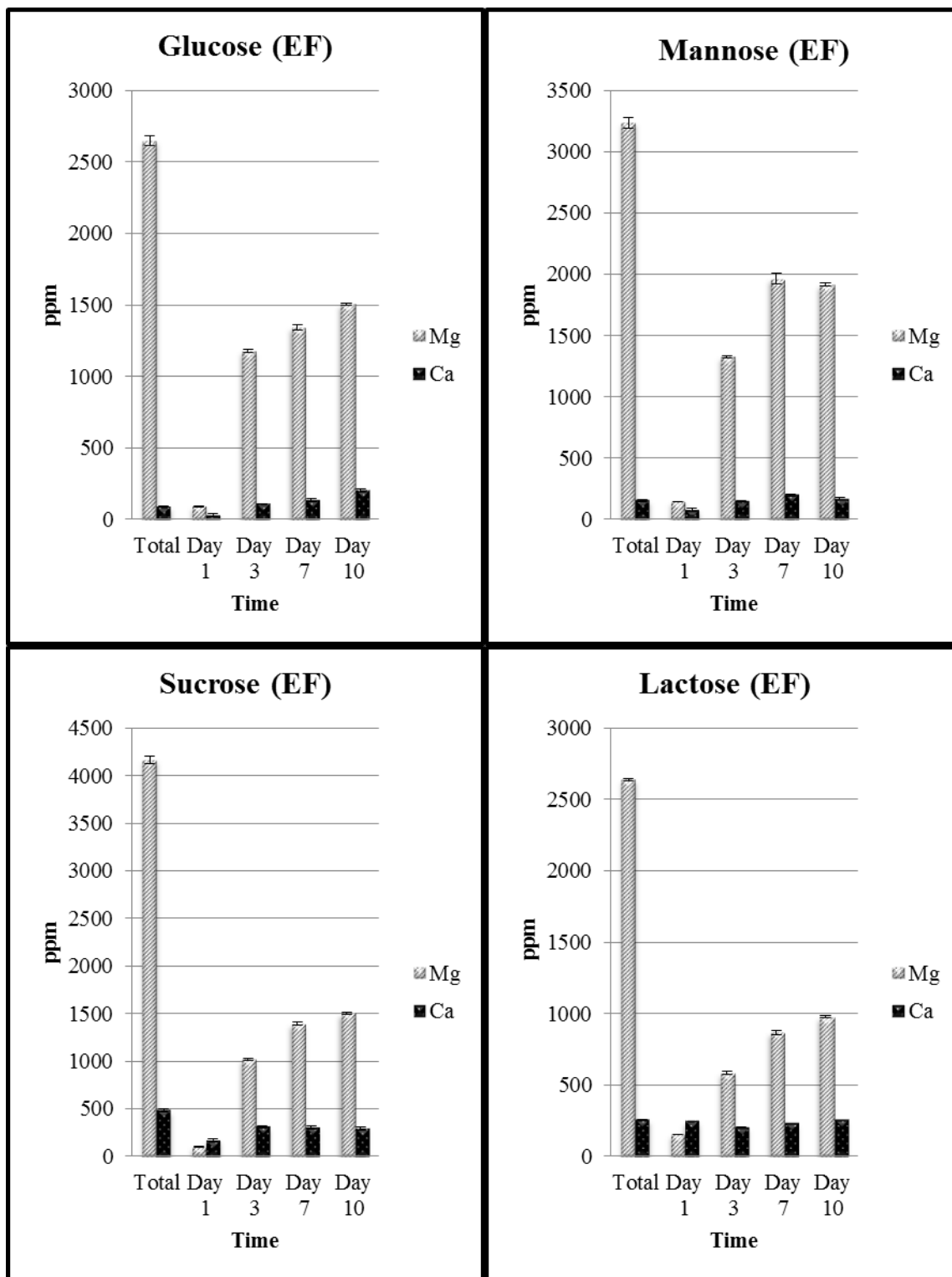
Figure 4.28. Mg and Ca dissolving capacity of EF with different C sources Glucose, Lactose, Mannose, and Sucrose
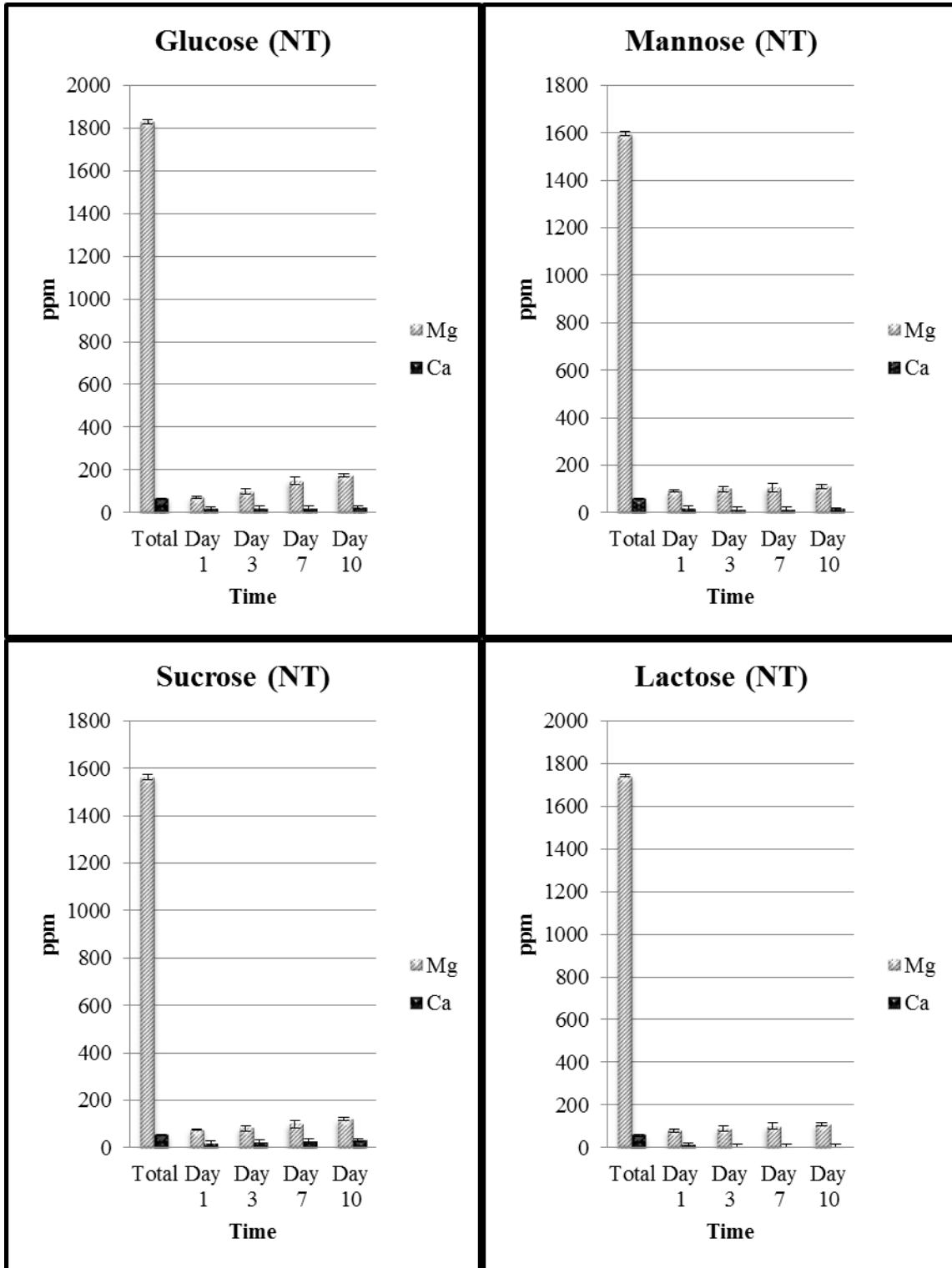
Figure 4.29. Mg and Ca dissolving capacity of NT with different C sources Glucose, Lactose, Mannose, and Sucrose
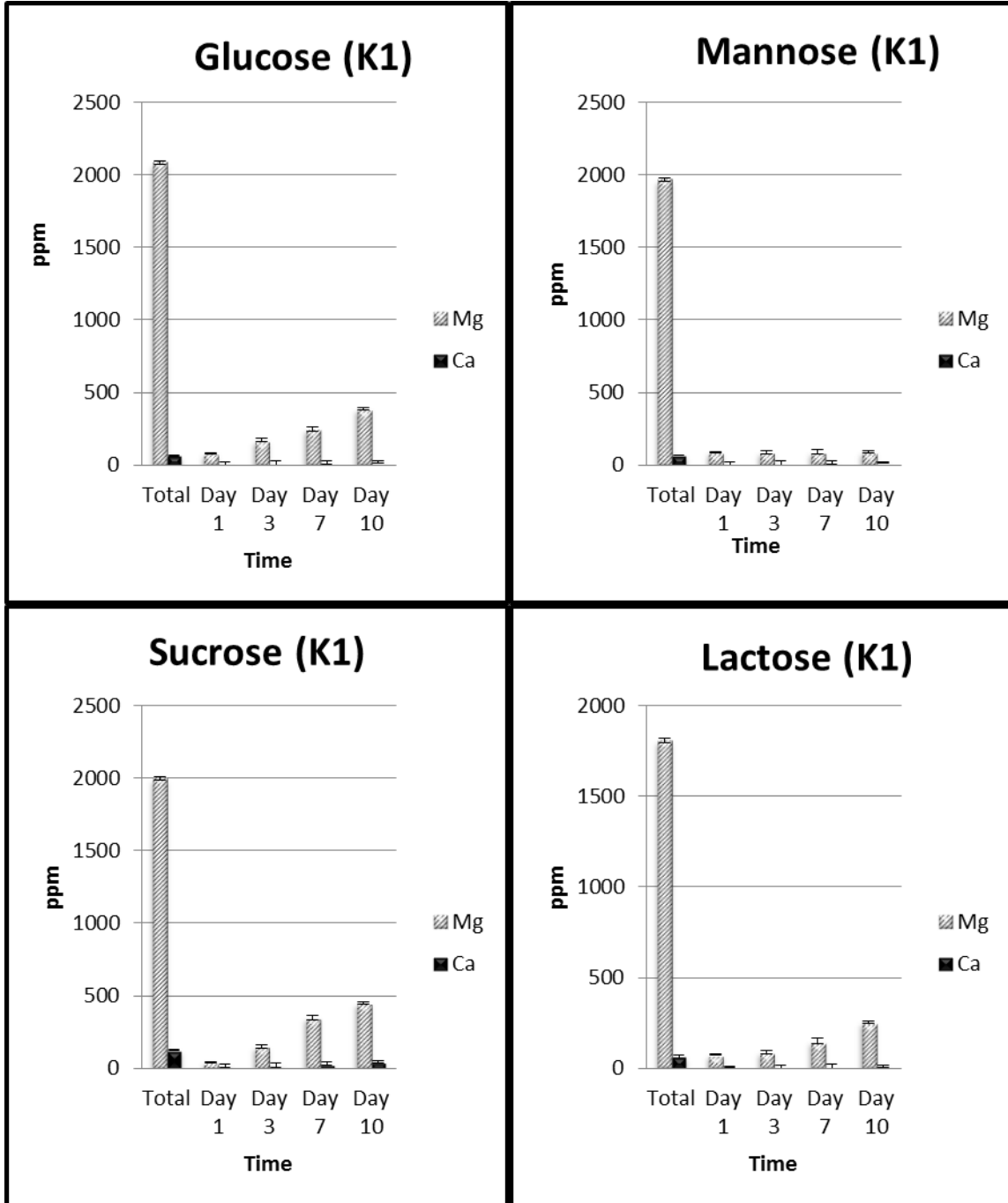
Figure 4.30. Mg and Ca dissolving capacity of K1 with different C sources Glucose, Lactose, Mannose, Sucrose

4.3.4. Different Bacterial Concentrations

There is no noticeable difference that has been observed between Mg dissolving capacity via different bacterial concentrations tested.

4.3.5. Optimum And Un-Optimized Conditions

Magnesite enrichment difference between optimum and un-optimized conditions indicates that optimization was performed successfully (**Figure 4.31-4.38**).

73
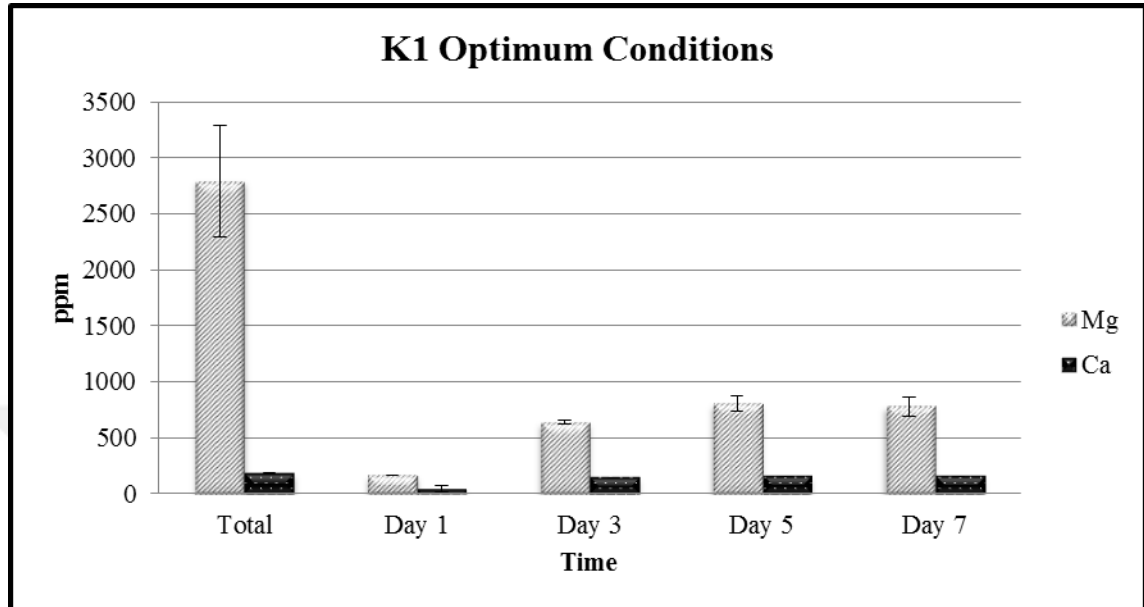
4.31. Mg and Ca dissolving capacity of K1 in optimum conditions
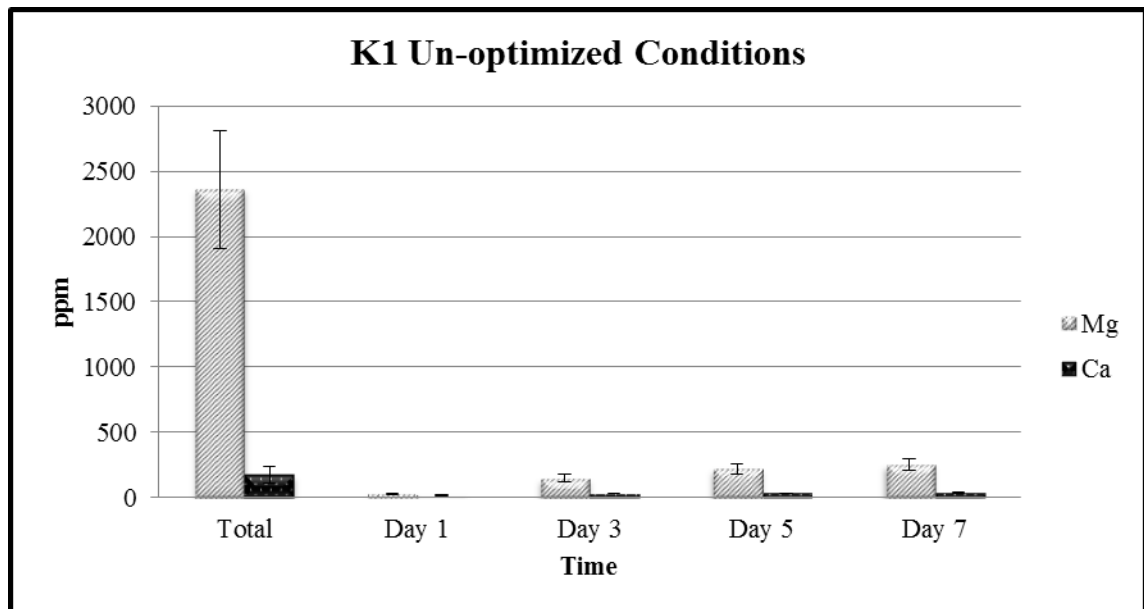
Figure 4.32. Mg and Ca dissolving capacity of K1 in un-optimized conditions
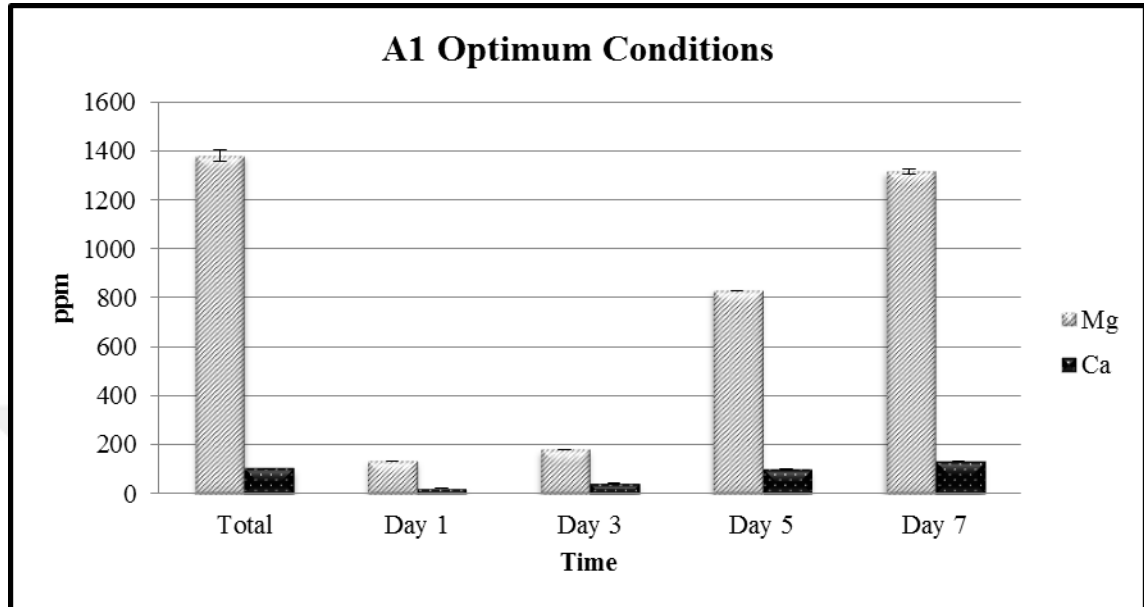
Figure 4.33. Mg and Ca dissolving capacity of A1 in optimum conditions
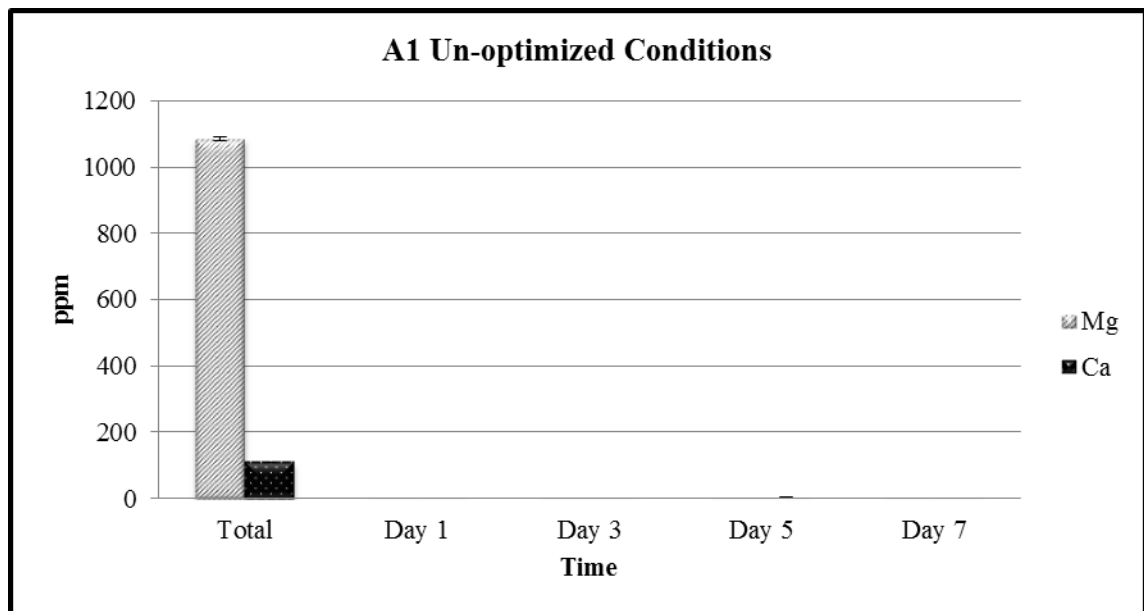
Figure 4.34. Mg and Ca dissolving capacity of A1 in un-optimized conditions
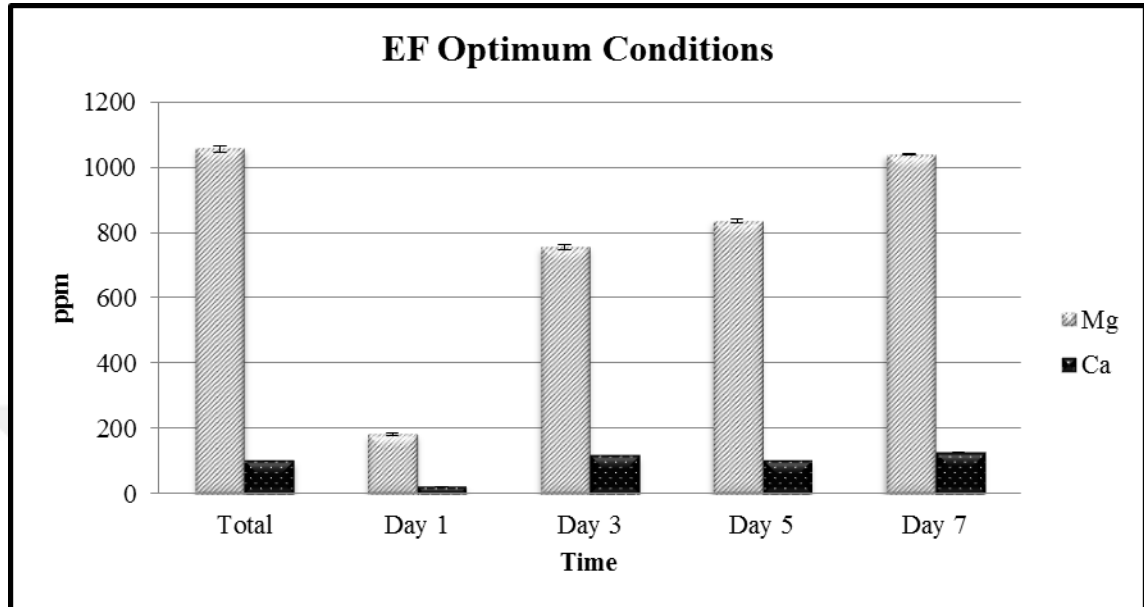
Figure 4.35. Mg and Ca dissolving capacity of EF in optimum conditions
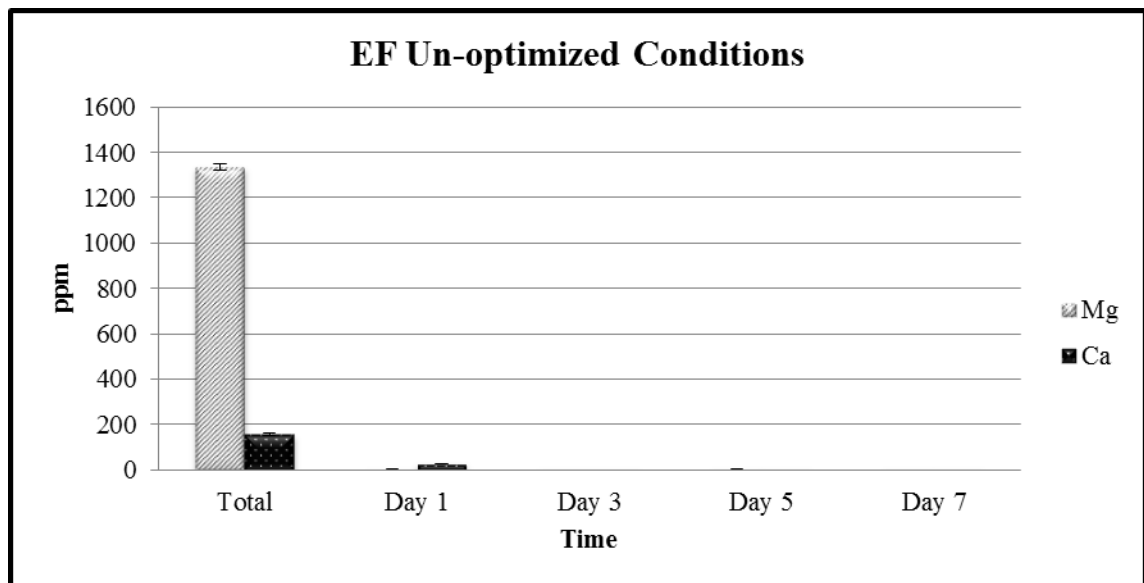
Figure 4.36. Mg and Ca dissolving capacity of EF in un-optimized conditions
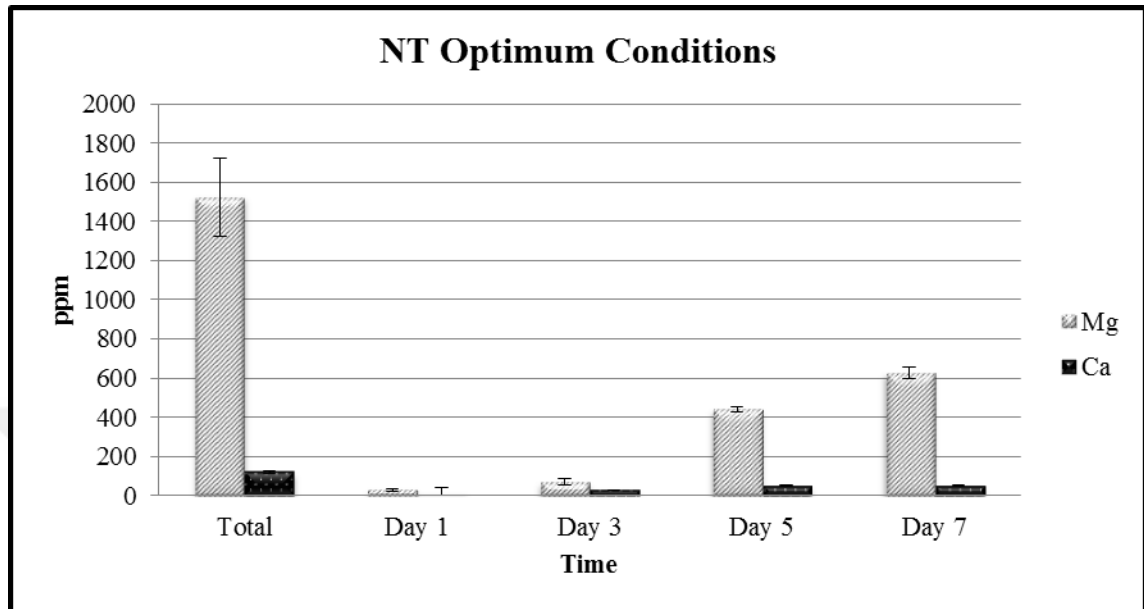
Figure 4.37. Mg and Ca dissolving capacity of NT in optimum conditions
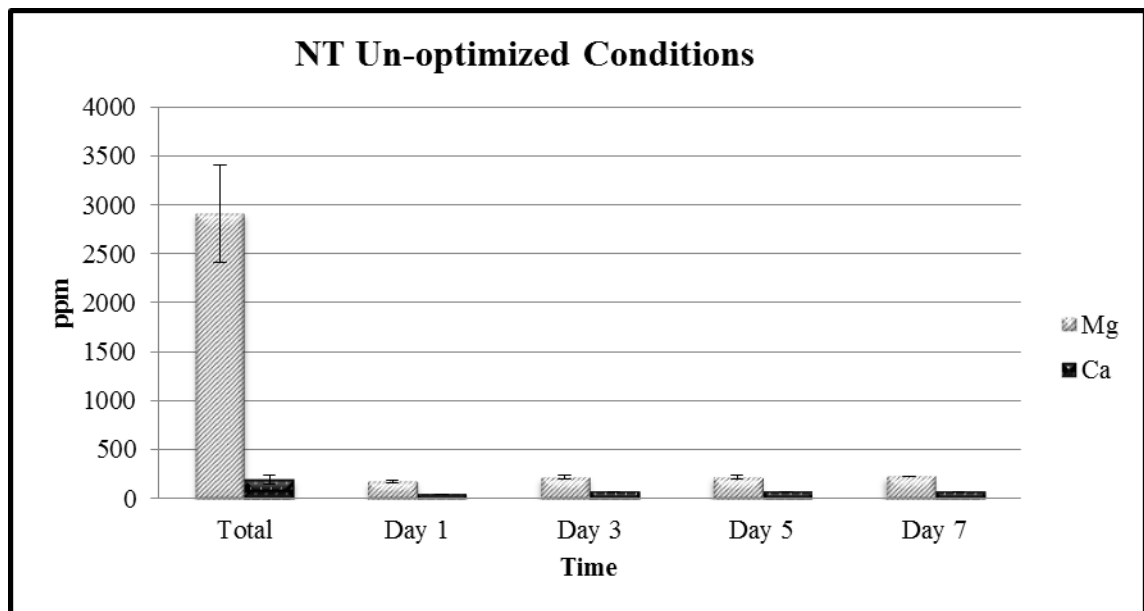
Figure 4.38. Mg and Ca dissolving capacity of NT in un-optimized conditions

4.3.6. Mixed Combinations

No antagonistic effect was determined between microorganisms on TSA (**Figure 4.39**). 11 different combinations of microorganisms' magnesite enrichment capacities were determined to reach a synergic effect. But, none of them has synergic effect. Conversely, the microorganisms in the mixed combinations have decreased each other's dissolving capacity (**Figure 4.40-4.50**).
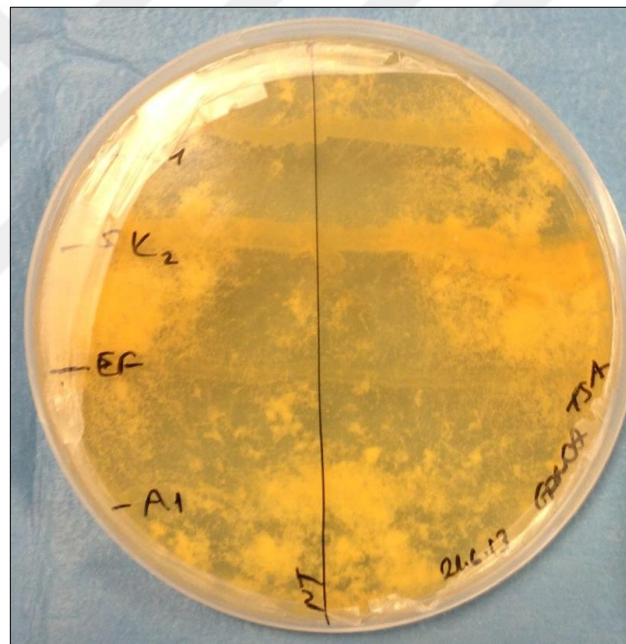
Figure 4.39. A1, EF, K1, NT antagonistic effect determination on TSA

78
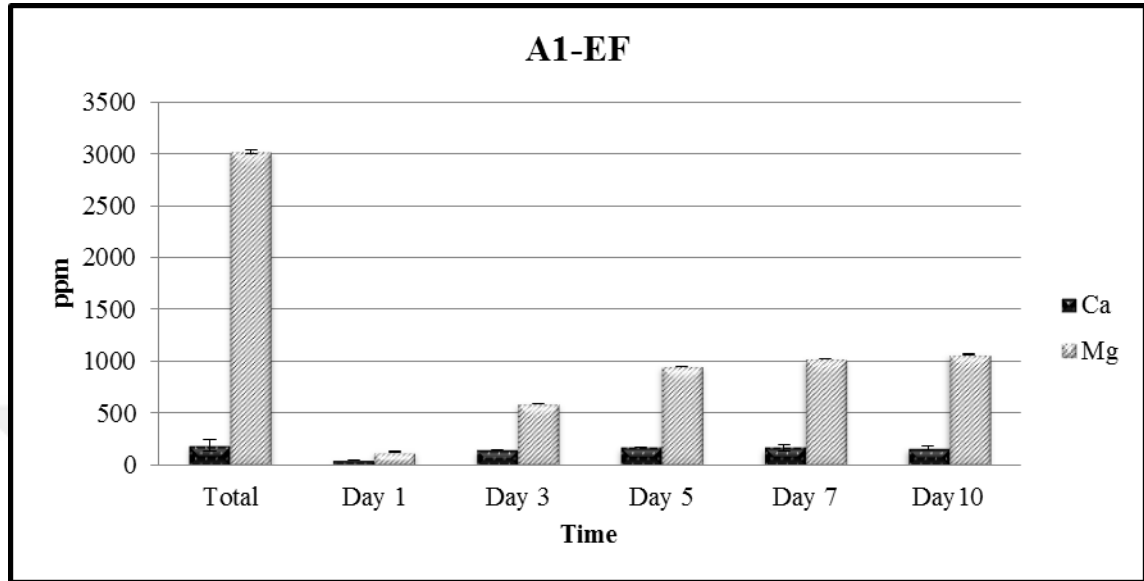
Figure 4.40. Mg and Ca dissolving capacity of A1-EF combination
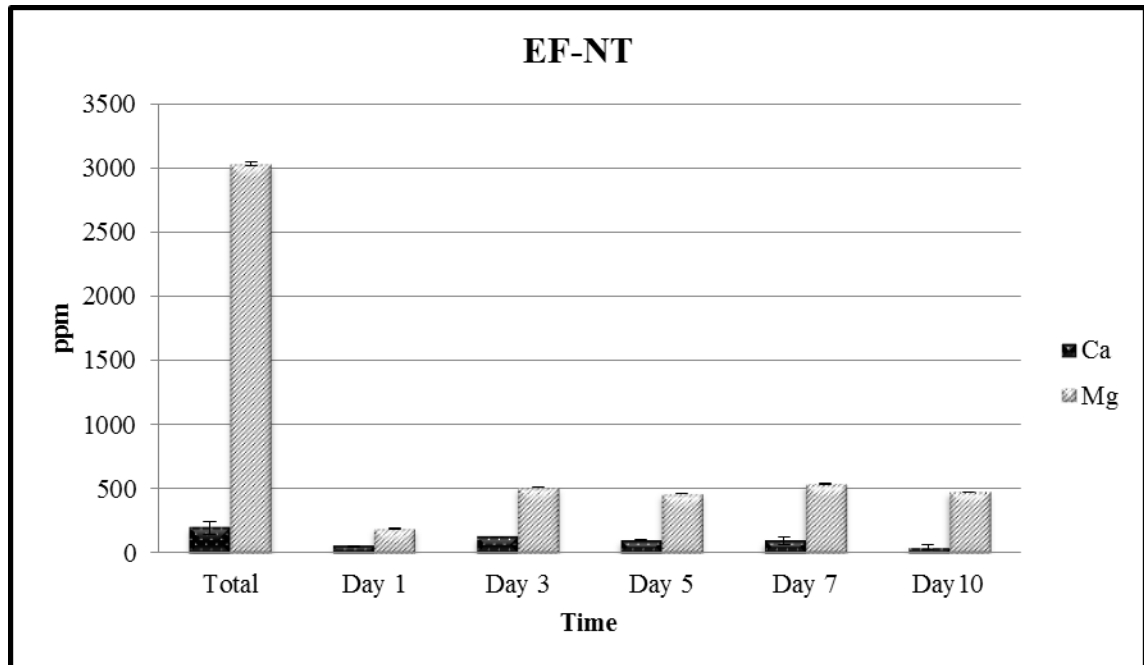
Figure 4.41. Mg and Ca dissolving capacity of EF-NT combination
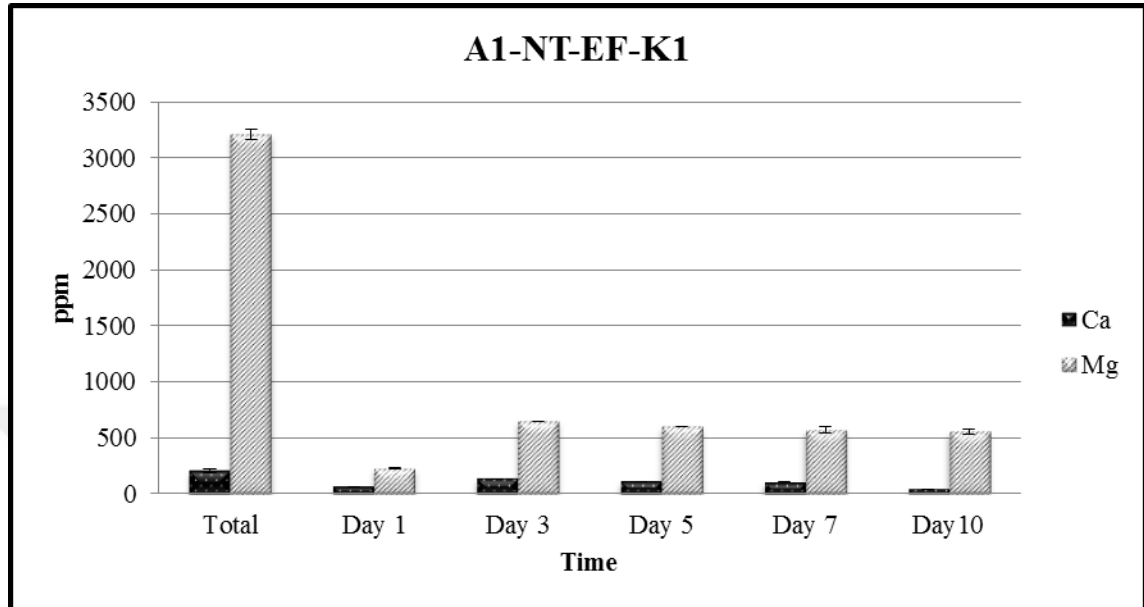
Figure 4.42. Mg and Ca dissolving capacity of A1-NT-EF-K1 combination
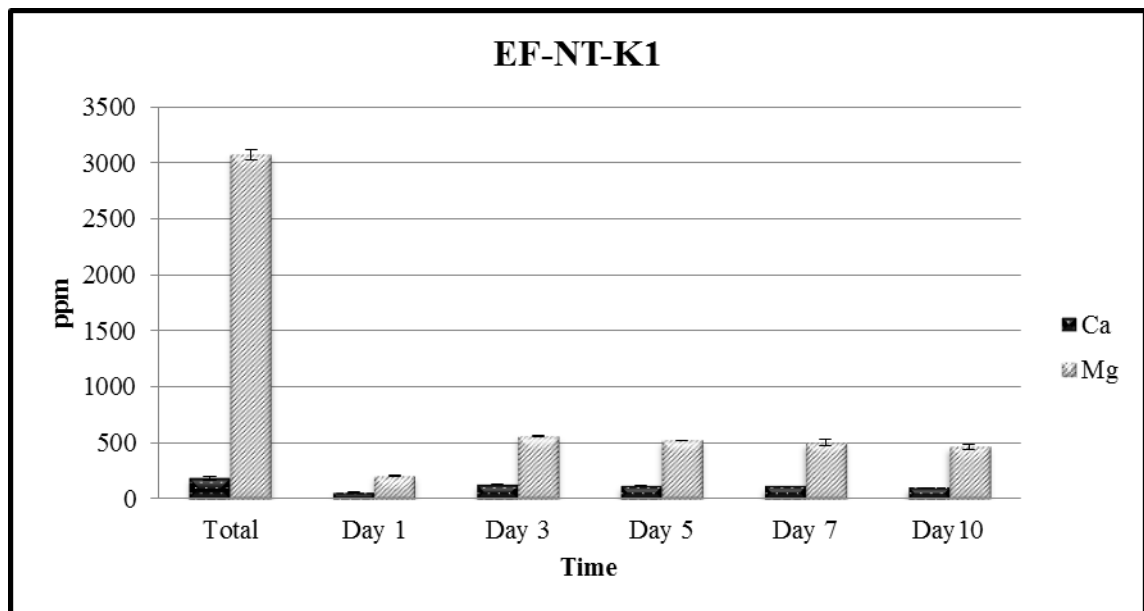
Figure 4.43. Mg and Ca dissolving capacity of EF-NT-K1 combination
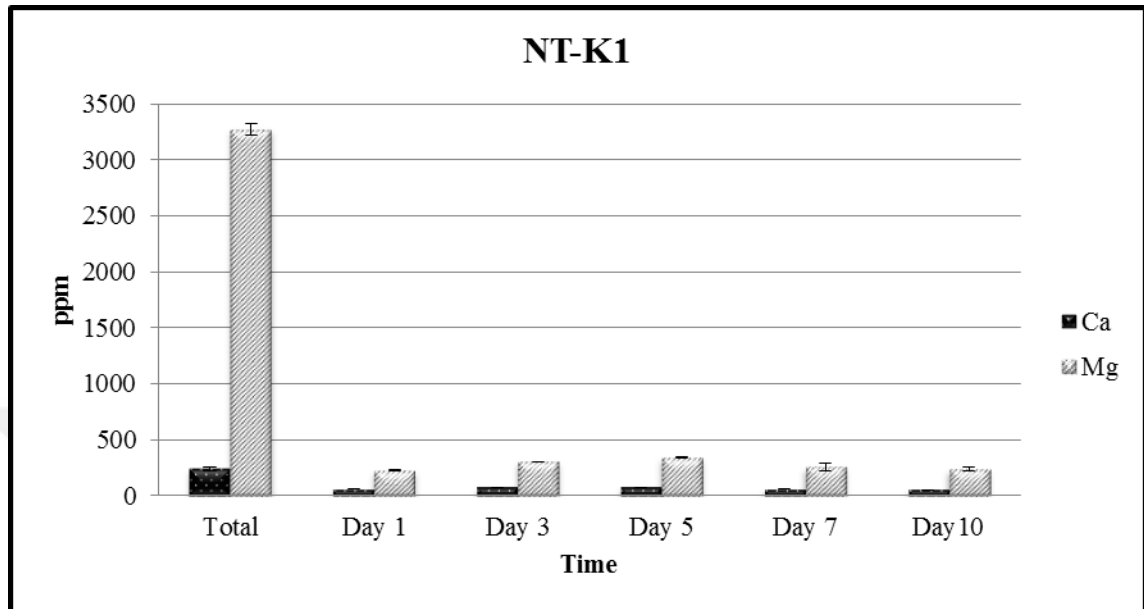
Figure 4.44. Mg and Ca dissolving capacity of NT-K1 combination
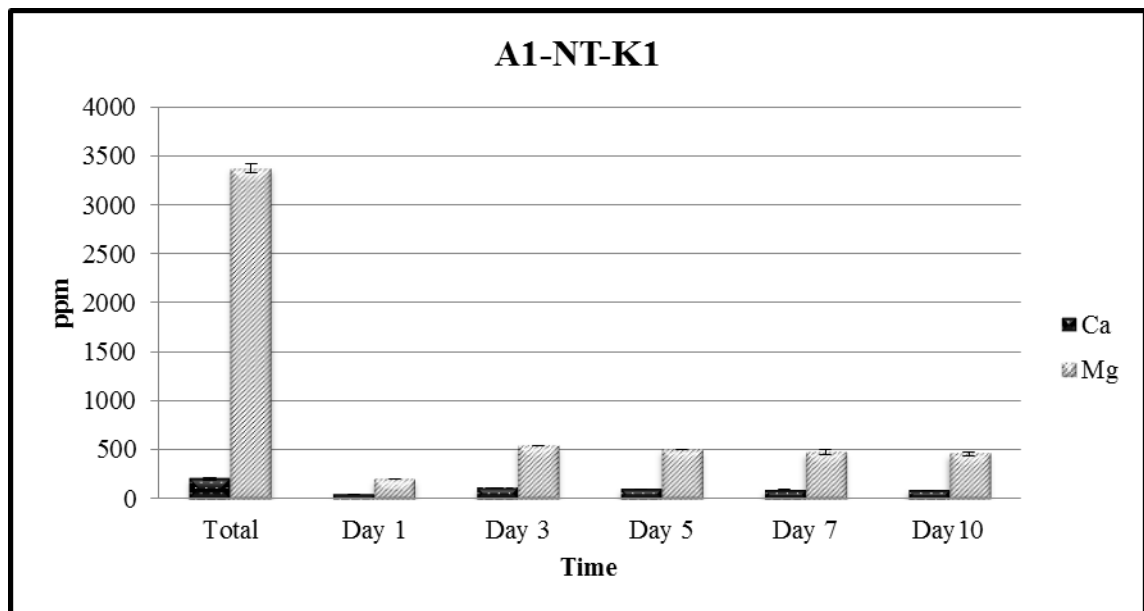
Figure 4.45. Mg and Ca dissolving capacity of A1-NT-K1 combination
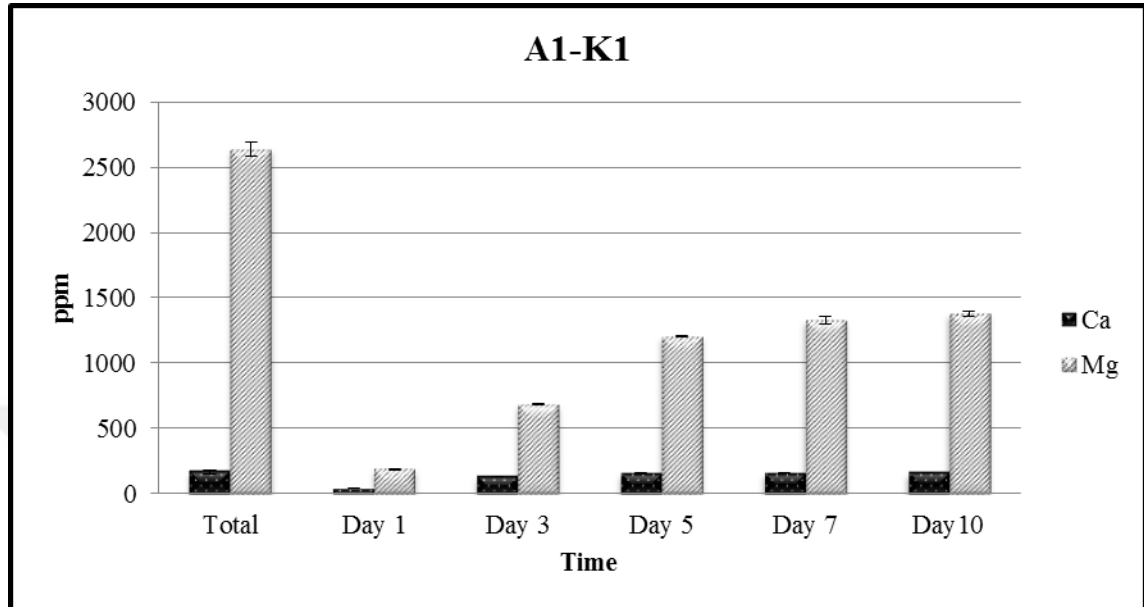
Figure 4.46. Mg and Ca dissolving capacity of A1-K1 combination
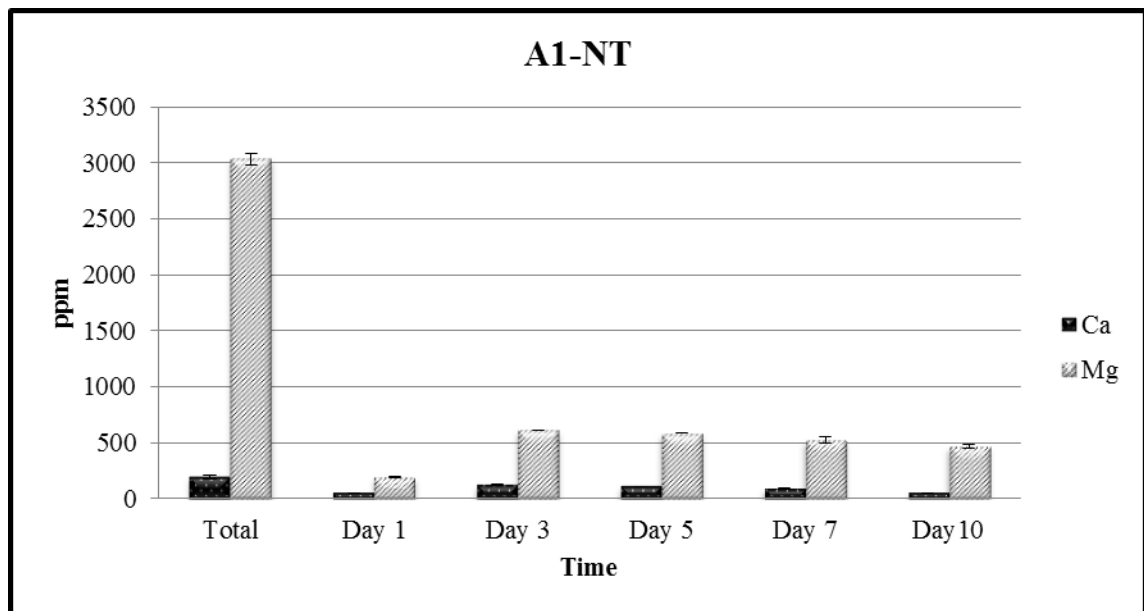
Figure 4.47. Mg and Ca dissolving capacity of A1-NT combination
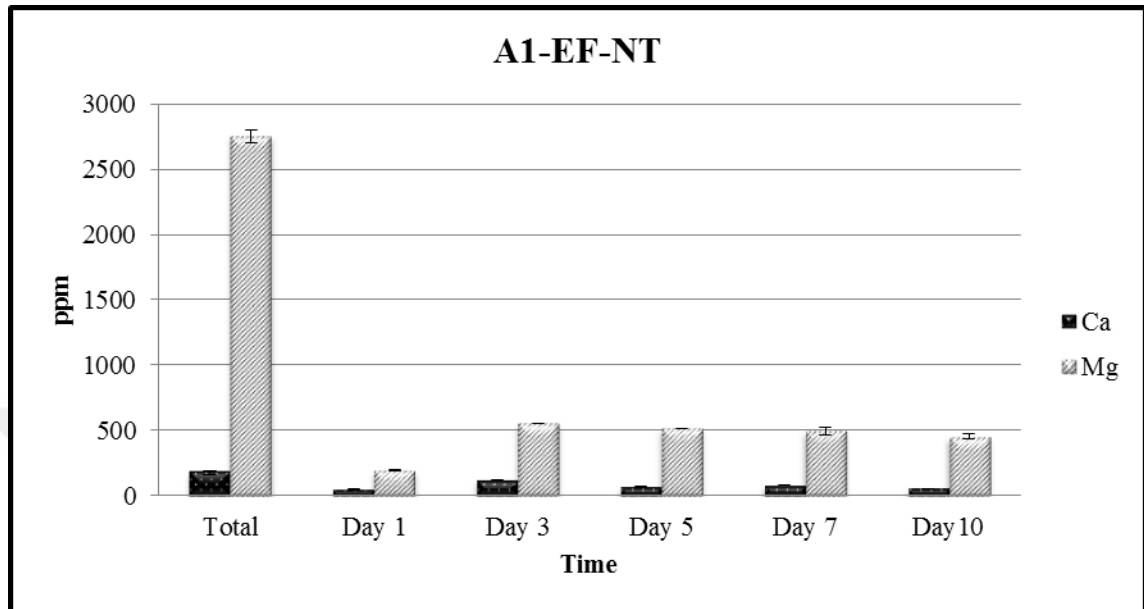
Figure 4.48. Mg and Ca dissolving capacity of A1-EF-NT combination
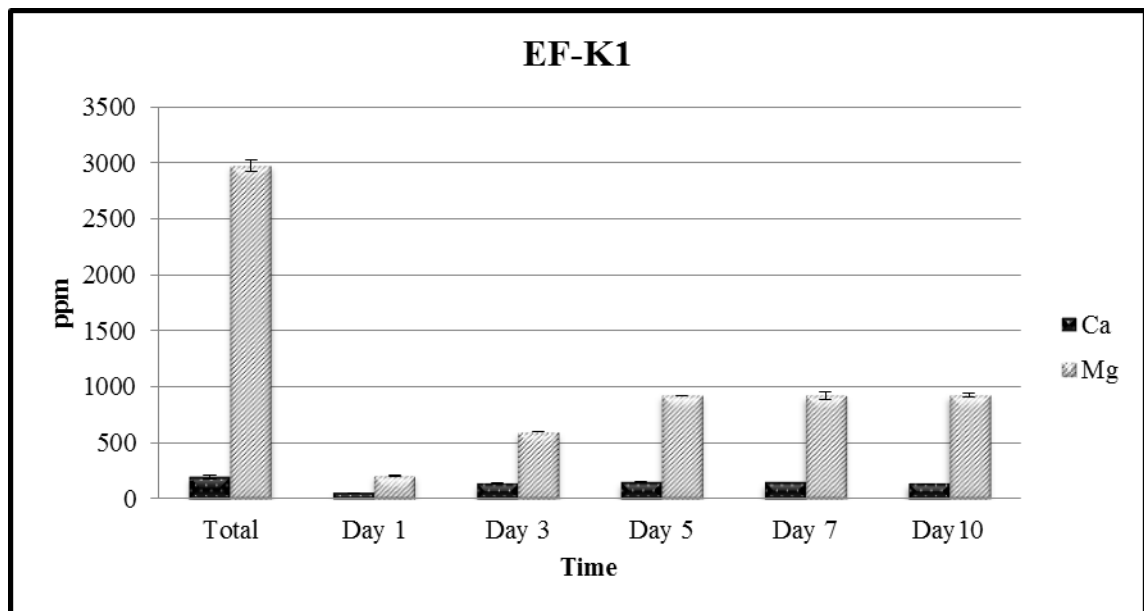
Figure 4.49. Mg and Ca dissolving capacity of EF-K1 combination
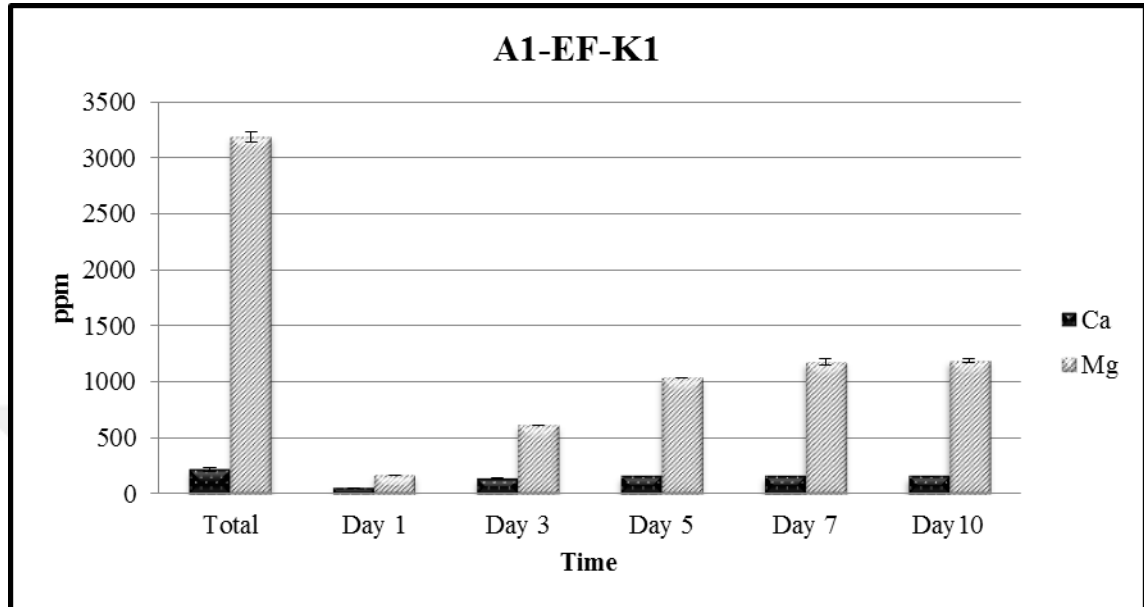
Figure 4.50. Mg and Ca dissolving capacity of A1-EF-K1 combination

4.4. ENRICHMENT OF MAGNESITE ORE

4.4.1. Scale Up Of Magnesite Enrichment

Density of GYM Medium is detected 1026 kg/m^3 (**Figure 4.51**).
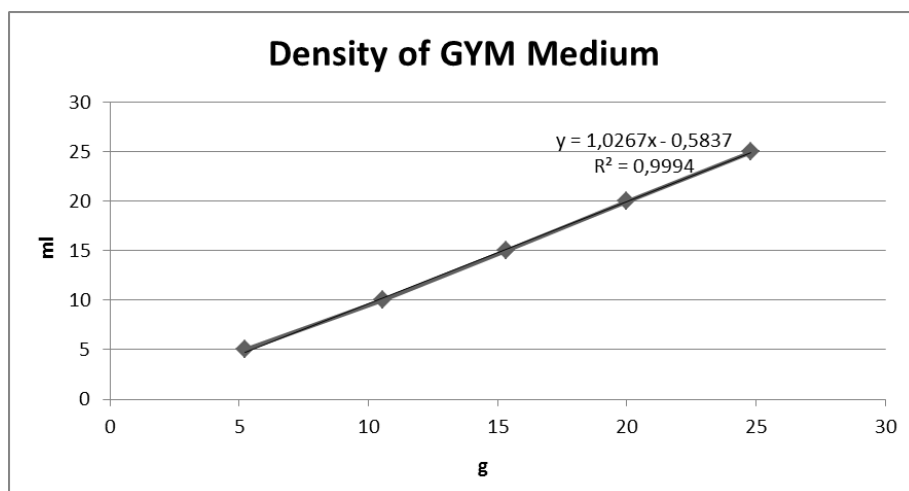
Figure 4.51. Density graphic of GYM Medium

Viscosity of GYM Medium is 3,2 cP (**Table 4.1**).

Table 4.1. Rheometer viscosity results of GYM Medium

rpm	Viscocity	Tork	Shear rate	Shear stress
250	3,2	89,8%	1875	20.7
249	3,2	89%	1867	20.5
248	3,2	89.7%	1860	20.4

Adequate impeller rpm for 3 L fermenter was found 300 rpm and 30 L fermenter was found 107 rpm (**Table 4.2**)

Table 4.2. Bioreactor calculation parameter results

	Re	Né	d	Np	P/V_L	rpm
Shaker	5130	0,4336	0,08	-	210	150
3 L Fermenter	5771	-	0,06	6,5	216	300
30 L Fermenter	20776	-	0,18	6	218	107
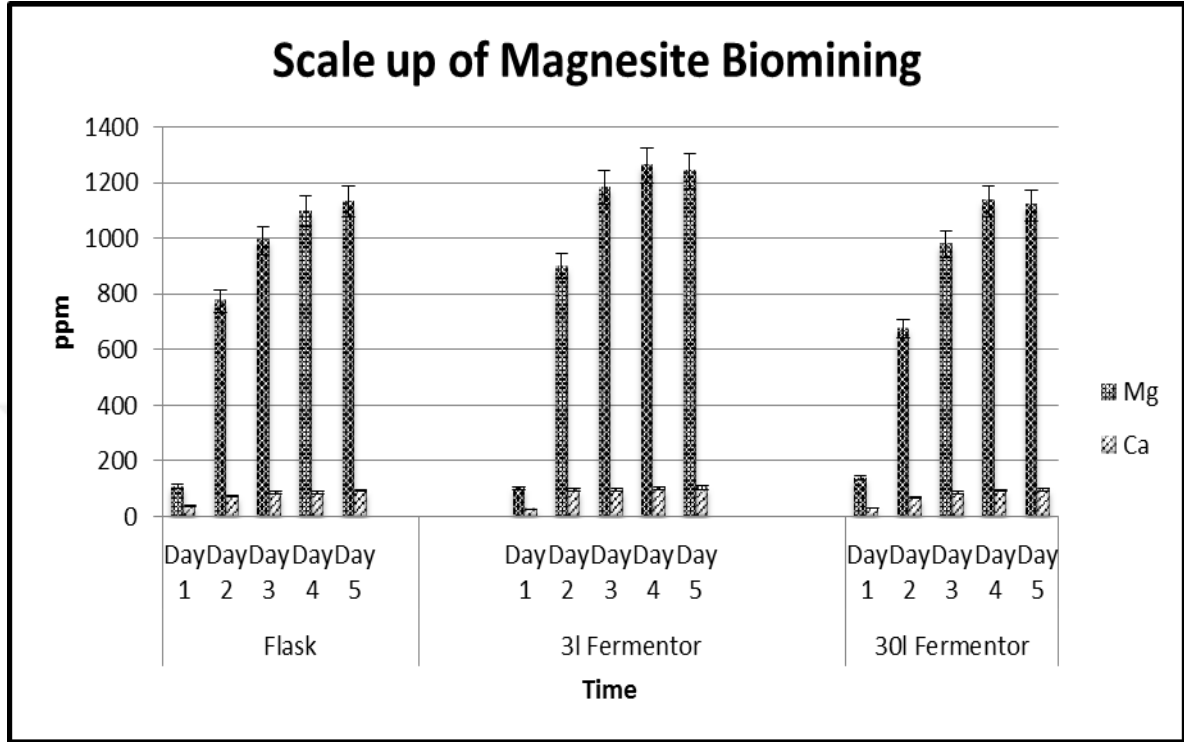
Figure 4.52. *Lactococcus garviaea*'s comparative Mg and Ca dissolving capacity at flask and fermenter scale

According to the ICP-MS results scale up of biomining of magnesite ore was performed successfully (**Figure 4.52**).

4.4.1.1. Phenotypic Analysis of A1 in Fermenter (3L)

According to the phenotypic analysis, exit CO_2, lactic acid production and cell growth increased in A1-Mg. pH values were similar in the culture with and without magnesite (**Figure 4.53**).
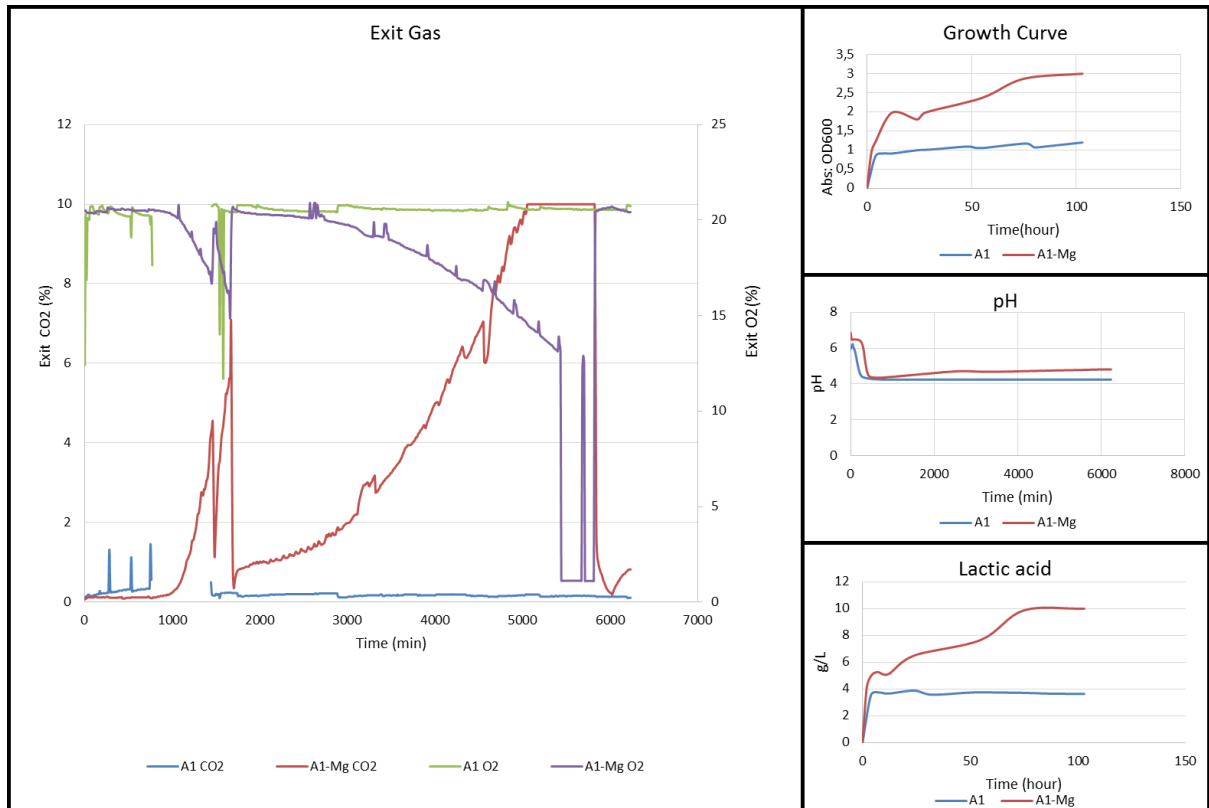
Figure 4.53. Phenotypic analysis result of A1 in 3L fermenter

4.4.2. Mechanism of Magnesite Biomining

4.4.2.1. Lactic Acid Measurements

Measurements of lactic acid production and Mg, Ca dissolving by time was showed in **Figure 4.54** and **Figure 4.55**

For Mg dissolving with commercial lactic acid three magnesite samples were prepared with dH$_2$O. pH of magnesite sample measurement result was 9,5 and to decrease magnesite samples pH value to 1, 3 and 5, 10,881 gr/ml, 6,045 gr/ml, 0,9 gr/ml lactic acid were added, respectively. pH 1 sample could not reach to pH1 value, it only could reach to pH value 2,94.

After two hours, 17 percent of Mg was converted to free Mg at pH 3 sample and 5 percent of Mg was converted to free Mg at pH 5 sample (**Figure 4.56**).
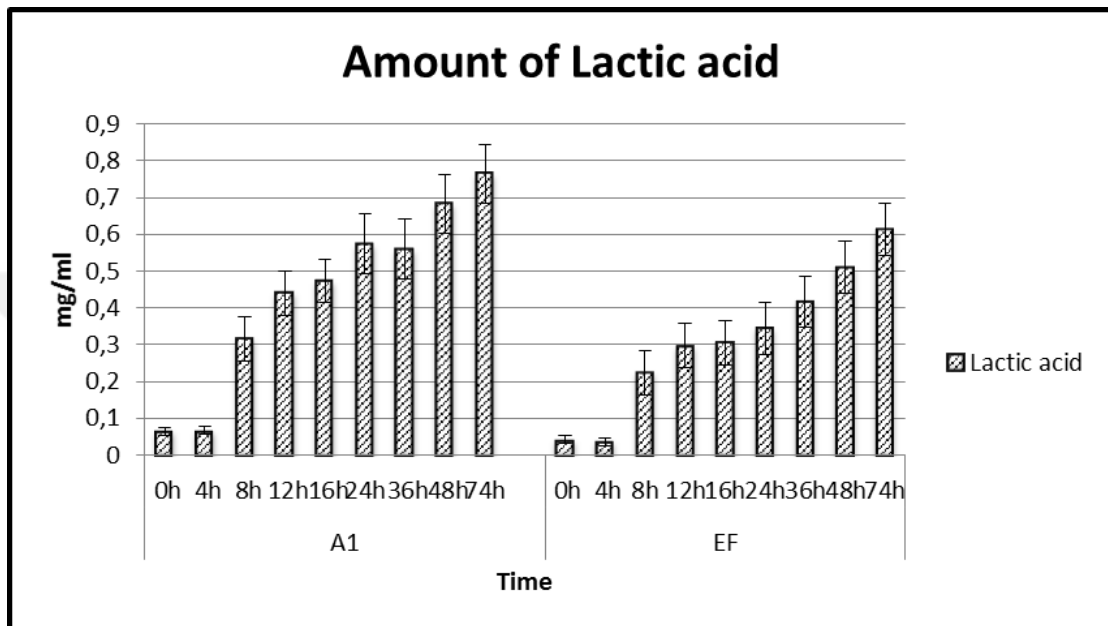
Figure 4.54. Lactic acid production amount of A1 and EF microorganisms during the biomining of magnesite
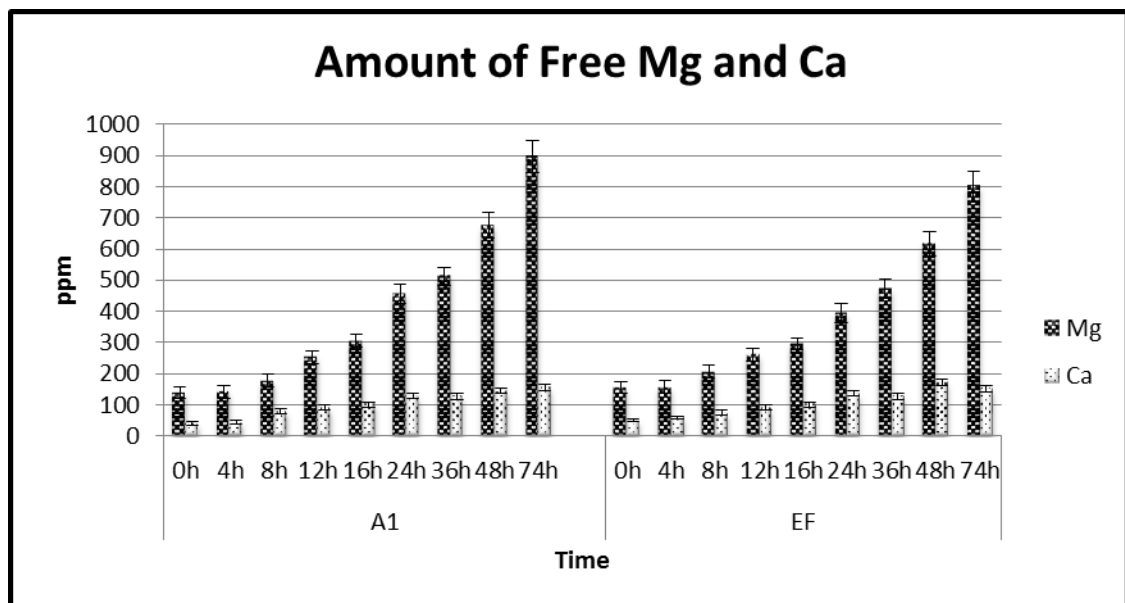
Figure 4.55. Free Mg and Ca amount, during the biomining of magnesite by A1 and EF microorganisms
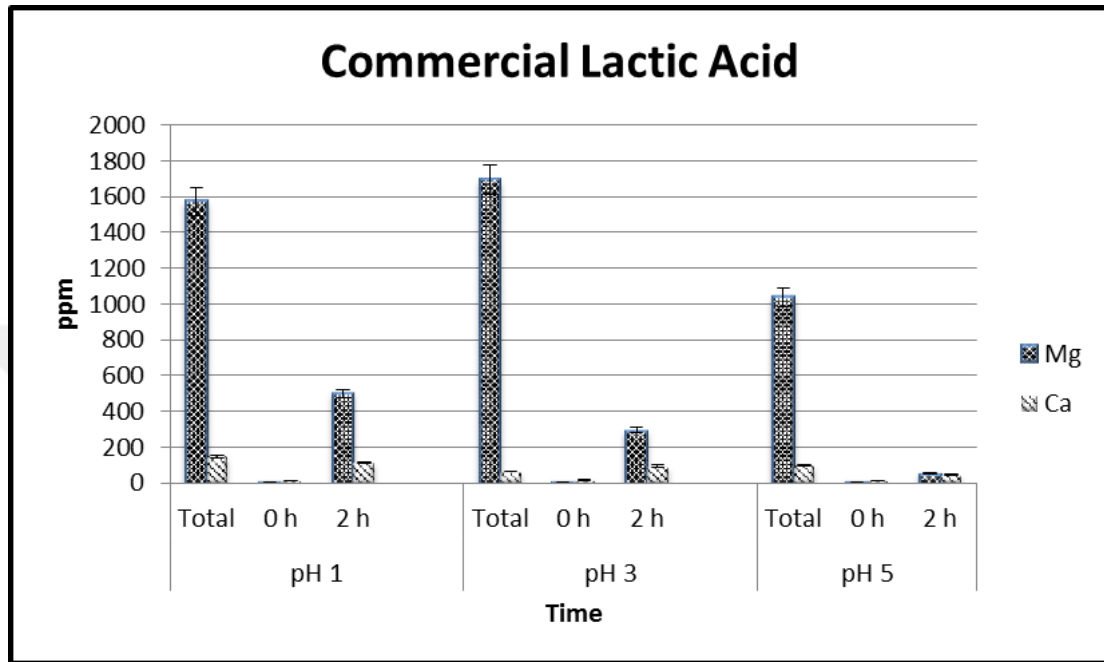
Figure 4.56. Free Mg and Ca amount, after lactic acid addition to magnesite solution

4.4.2.2. ATPase Assay

ATPase activity has detected in the all samples. But, the A1 that have grown in GYM medium, have ATPase activity about 1,2 times more than A1 that have grown in GY medium while no difference was detected between EF that have grown in GYM medium and have grown in GY medium (**Figure 4.57**).
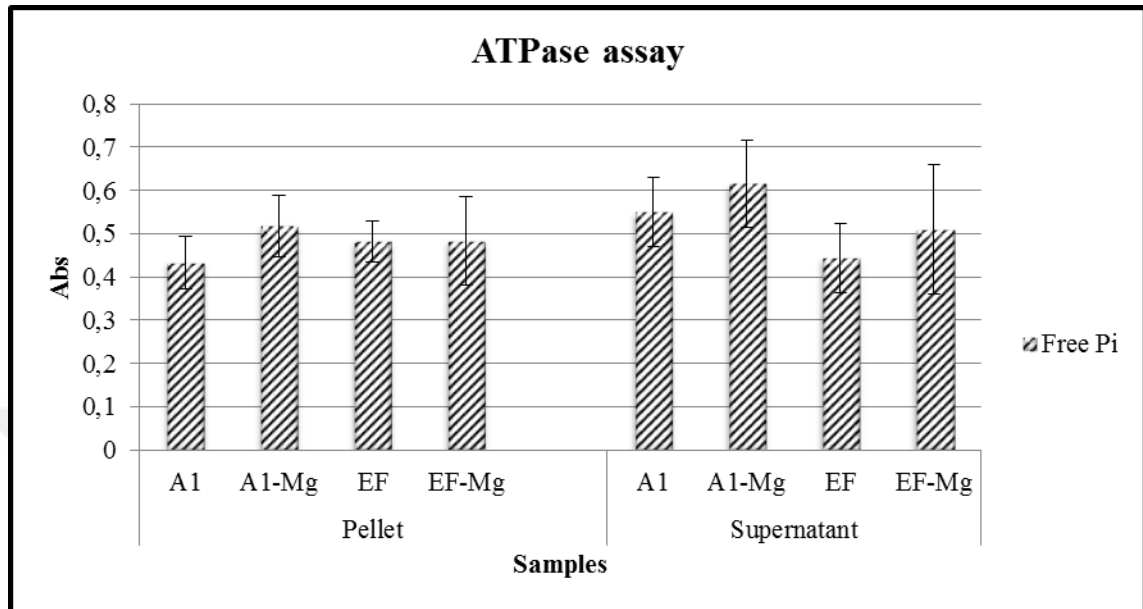
Figure 4.57. ATPase assay results of A1 and EF microorganisms in different media (A1 and EF refers to GY medium, A1-Mg and EF-Mg refers to GYM medium)

The supernatant of A1 that have grown in GYM medium, have ATPase activity about 1,1 times more than the supernatant A1 that have grown in GY medium. And the supernatant of EF that have grown in GYM medium, have ATPase activity about 1,2 times more than the supernatant EF that have grown in GY medium.

4.4.2.3. Carbonic Anhydrase Assay

Carbonic anhydrase activity has detected in all the samples. But, A1 lysate that have grown in GYM medium, have carbonic anhydrase activity about 2,7 times more than A1 lysate that have grown in GY medium and A1 supernatant sample that have grown in GYM medium have carbonic anhydrase activity about 3,5 times more than A1 supernatant sample that have grown in GY medium. And EF lysate that have grown in GYM medium, have carbonic anhydrase activity about 1,3 times more than EF lysate that have grown in GY medium when EF supernatant sample that have grown in GYM medium, have carbonic anhydrase activity

about 4,5 times more than EF supernatant sample that have grown in GY medium. Carbonic anhydrase activity of A1 cell lysate more than A1 supernatant sample while carbonic anhydrase activity of EF cell lysate less than EF supernatant sample (**Figure 4.58**).
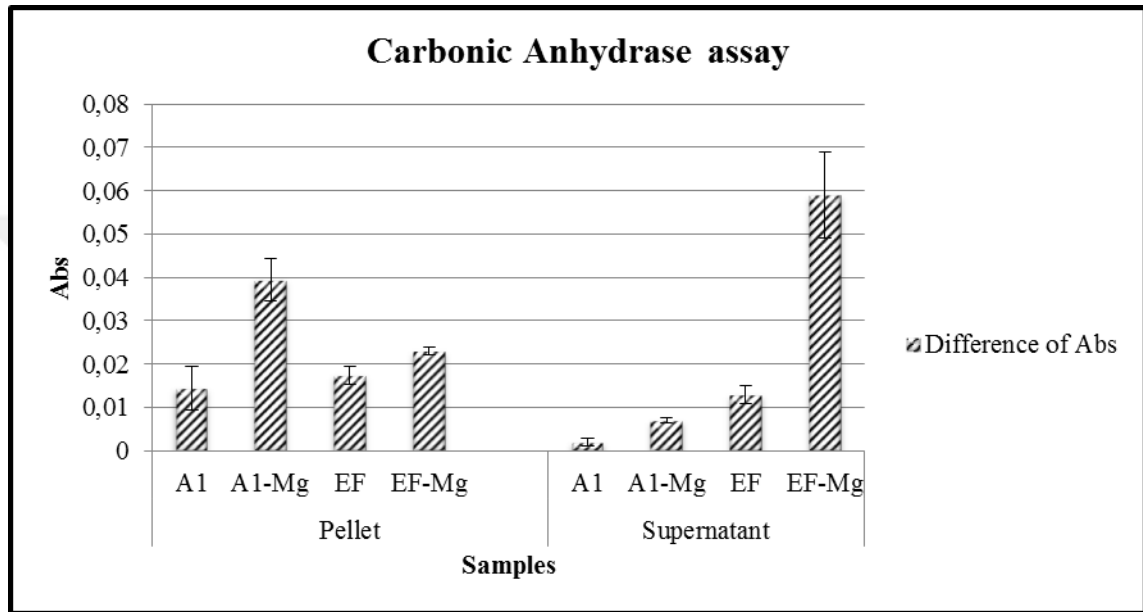
Figure 4.58. Carbonic anhydrase activity graphic of A1 and EF microorganisms in different media (A1 and EF refers to GY medium, A1-Mg and EF-Mg refers to GYM medium)

4.4.2.4. *Whole Genome Sequencing Analysis*

In A1, 18,275,986 reads each 100bp are produced, and total read bases are 1,82G bp. High quality (phred>30) 17,287,054 paired-end reads were assembled into 622 contigs, with a median coverage of 700 fold. This resulted in a genome size of 2,3 Mb with a GC content of 37,8 per cent. The genome of the A1 strain contains 2142 predicted coding sequences (CDSs), and 47 tRNA genes. The RAST annotation covered 750 RAST subsystems (**Figure 4.59**).
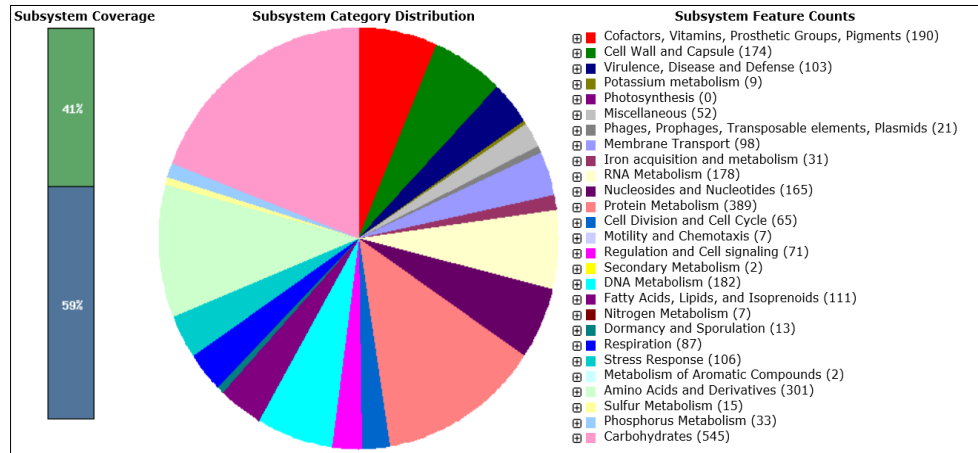
Figure 4.59. Subsystem distribution chart of A1

In EF, 17,935,352 reads are produced, and total read bases are 1,8G bp. A total of 17,501,010 paired-end reads were assembled into 8671 contigs, with a median coverage of approximately 720 fold. This resulted in a genome size of 7 Mb with a GC content of 37,8per cent. 5002 coding sequences (CDS) and 51 tRNA genes were predicted. The RAST annotation covered 686 RAST subsystems with 1,965 CDS (39,3 percent), of which 23 were labeled as hypothetical proteins. On the other hand, 3,037 CDS (60,7 percent), of which 1862 were labeled as hypothetical proteins, were not in any RAST subsystem (**Figure 4.60**).
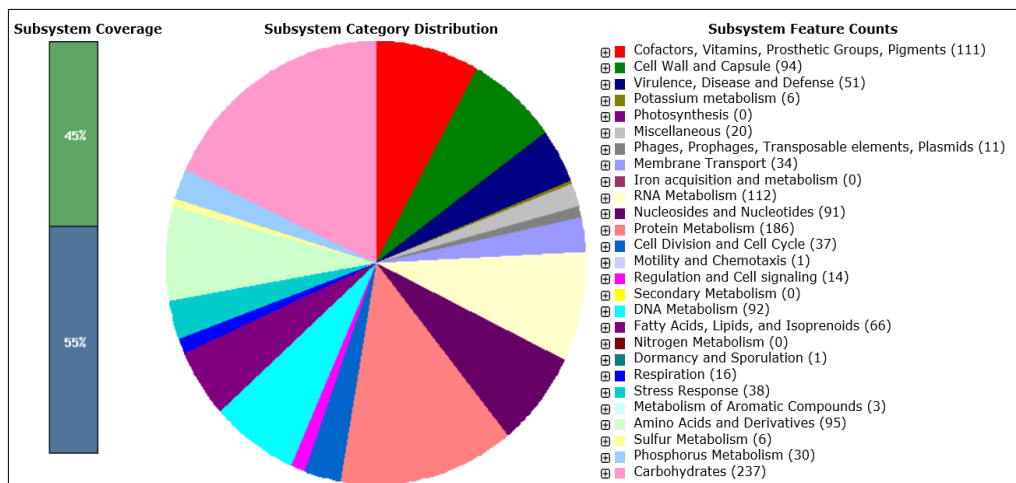
Figure 4.60. Subsystem distribution of EF

4.4.2.5. Transcriptome Analysis

The total number of bases, reads, GC (percent) and Q30 (percent) are calculated for the 12 samples. For example, in EF-Mg-1, 42,000,866 reads are produced, and total read bases are 4,2G bp. The GC content (percent) is 44,05 per cent and Q30 is 88,04 percent (**Table 4.3**).

Table 4.3. Transcriptome Analysis Raw Data Statistics

Sample ID	Total read bases (bp)	Total reads	GC (%)	AT (%)	Q30 (%)
A1-1	3,790,566,966	37,530,366	41,38	58,62	89,67
A1-2	4,217,115,014	41,753,614	41,15	58,85	89,86
A1-3	3,736,391,980	36,993,980	41,24	58,76	89,73
A1-Mg-1	4,455,226,554	44,111,154	48,15	51,85	87,01
A1-Mg-2	4,174,167,794	41,328,394	44,02	55,98	88,77
A1-Mg-3	4,018,447,206	39,786,606	44,63	55,37	88,37
EF-1	3,595,708,878	35,601,078	38,54	61,46	88,87
EF-2	4,326,461,654	42,836,254	38,94	61,06	88,66
EF-3	3,915,362,364	38,765,964	40,07	59,93	89,63
EF-Mg-1	4,242,087,4	42,000,866	44,05	55,95	88,04
EF-Mg-2	3,872,064,068	38,337,268	39,77	60,23	89,69
EF-Mg-3	4,540,006,762	44,950,562	45,23	54,77	87,58

Sample ID: Sample name, Total read bases : Total number of bases sequenced, Total reads : Total number of reads. In illumina paired-end sequencing, read1 and read2 are added, GC (percent): GC content, AT (percent) : AT content, Q30 (percent) : Ratio of reads that have phred quality score of over 30.
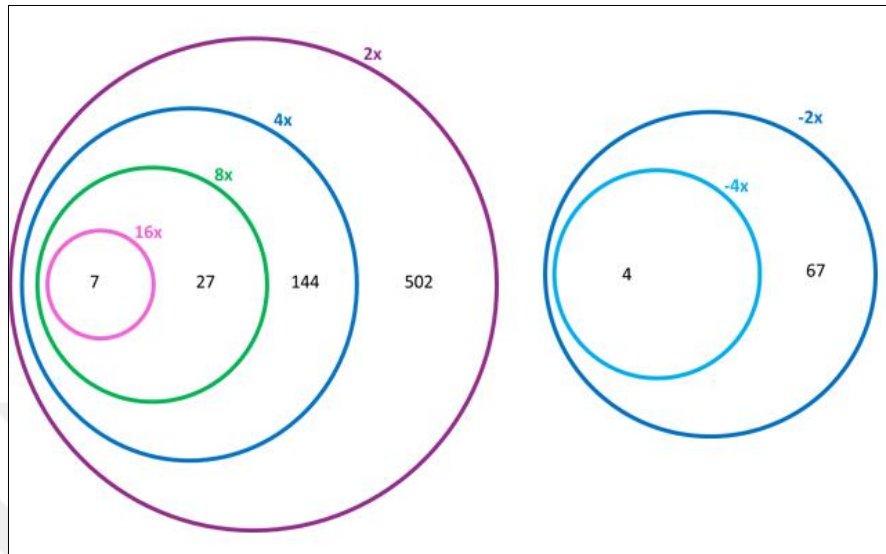
Figure 4.61. Number of A1 genes upregulated and downregulated.
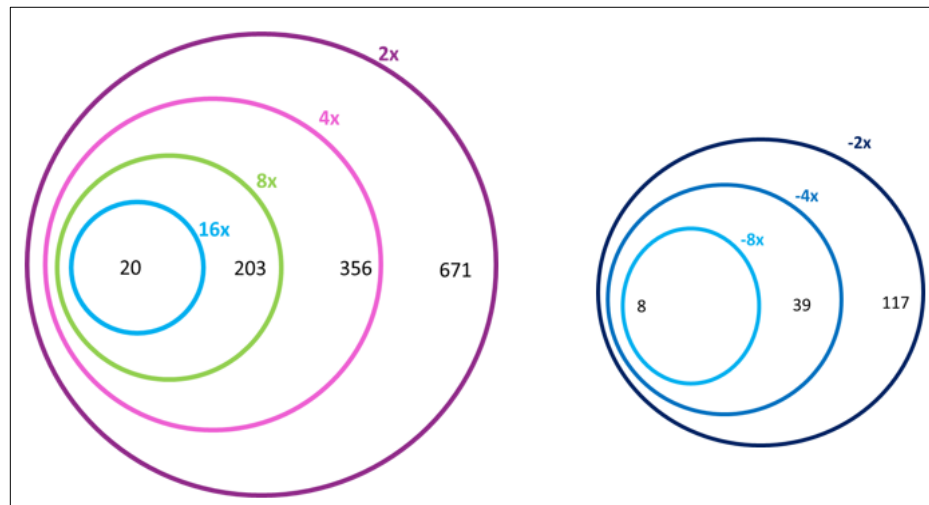
Figure 4.62. Number of EF genes upregulated and downregulated

94
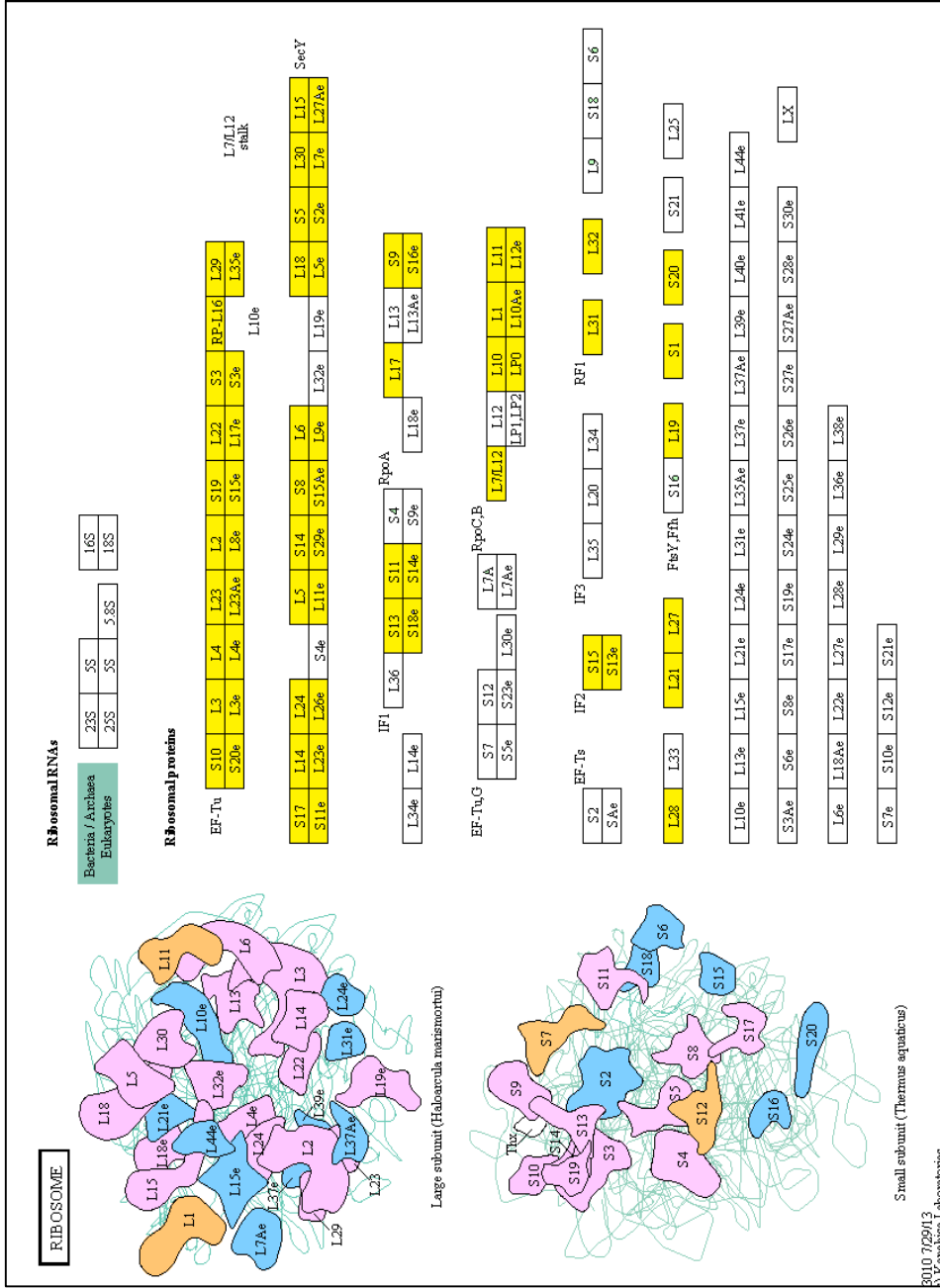
Figure 4.63. Prokaryotic Ribosomal Subunits. Upregulated subunits of A1 are highlighted with yellow [146]
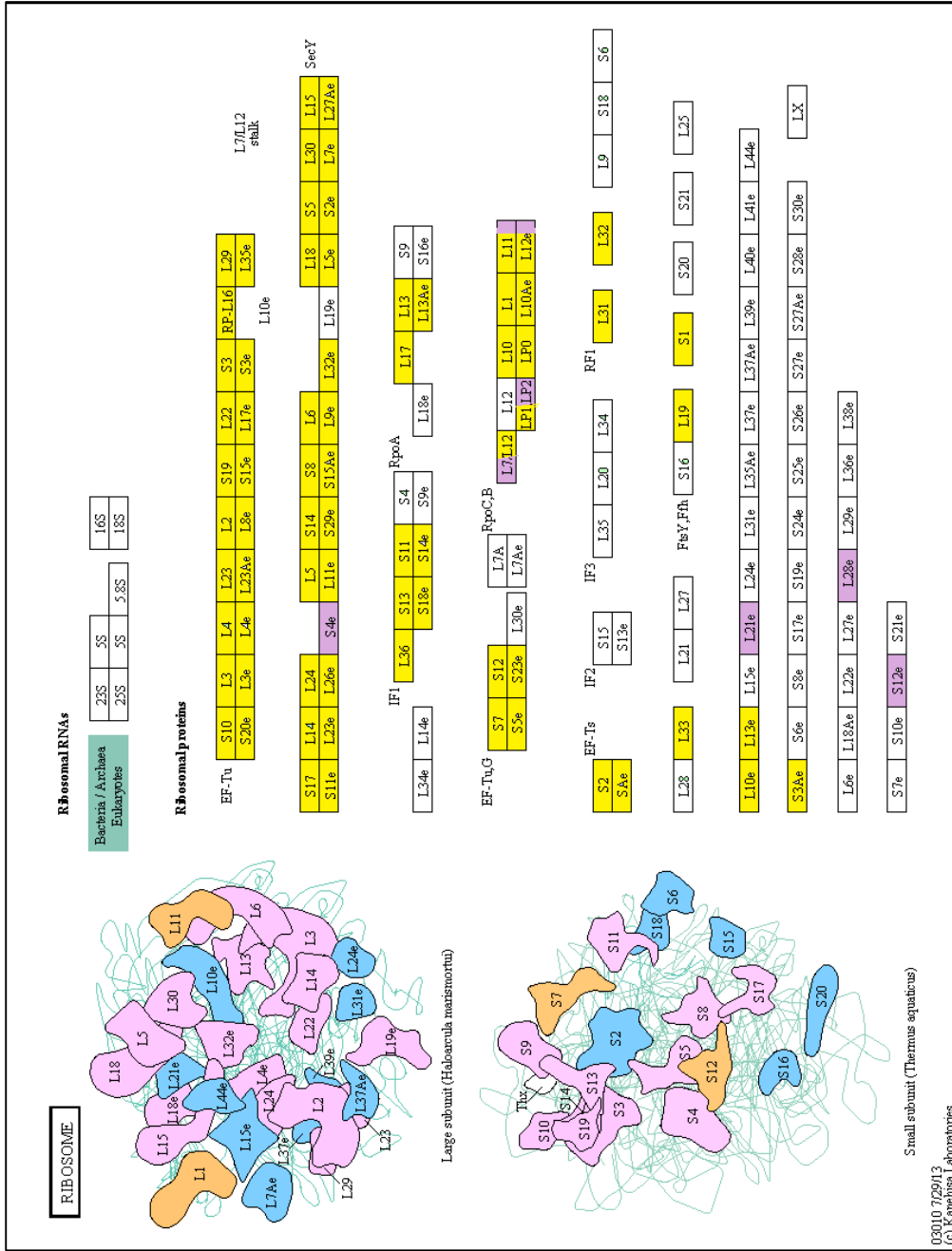
Figure 4.64. Prokaryotic Ribosomal Subunits. Upregulated subunits of EF are highlighted with yellow and downregulated subunits of EF are highlighted with lilac [146]

Table 4.4. List of EF genes that are upregulated at least 16 fold

Name of gene	Fold
Pyrimidine-nucleoside phosphorylase (EC 2.4.2.2)	62,58
Deoxyribose-phosphate aldolase (EC 4.1.2.4)	53,40
Cytidine deaminase (EC 3.5.4.5)	51,67
Predicted nucleoside ABC transporter, substrate-binding component	41,72
Predicted nucleoside ABC transporter, substrate-binding component	32,81
Predicted nucleoside ABC transporter, ATP-binding component	32,78
Putative deoxyribose-specific ABC transporter, permease protein	27,91
Unspecified monosaccharide ABC transport system, permease component 2	26,39
FIG00631857: hypothetical protein	24,30
Phosphopentomutase (EC 5.4.2.7)	23,49
Purine nucleoside phosphorylase (EC 2.4.2.1)	23,38
Purine nucleoside phosphorylase (EC 2.4.2.1)	19,26
Ferrichrome-binding periplasmic protein precursor (TC 3.A.1.14.3)	18,12
Ferrichrome transport ATP-binding protein FhuC (TC 3.A.1.14.3)	17,76
ABC-type Fe3+-siderophore transport system, permease component	17,51
ABC-type Fe3+-siderophore transport system, permease 2 component	17,31
NADH-dependent butanol dehydrogenase A (EC 1.1.1.-)	16,88
Phosphoglycerate mutase (EC 5.4.2.1)	16,87
Phage DNA invertase	16,82
Ribose 5-phosphate isomerase A (EC 5.3.1.6)	16,05

According to the transcriptome analysis, 680 genes of A1 and 1250 genes of EF were upregulated at least 2 fold. 71 genes of A1 and 165 genes of EF were downregulated (**Figure 4.61 and 4.62**). Names of some upregulated genes were listed in **Table 4.4**. and **Table 4.5**. for instance, in the **Figure 4.63** and **Figure 4.64**, upregulated and downregulated ribosomal genes were highlighted.

Table 4.5. List of A1 genes that are upregulated at least 8 fold.

Name of Gene	Fold
ATP synthase epsilon chain (EC 3.6.3.14)	8,02
Manganese ABC transporter, periplasmic-binding protein SitA	8,09
Hypothetical protein	8,26
Hypothetical protein	8,29
Protein probably involved in xylan degradation; possible xylan esterase	8,43
LSU ribosomal protein L16p (L10e)	8,44
Competence factor	8,47
SSU ribosomal protein S17p (S11e)	8,54
Substrate-specific component FolT of folate ECF transporter	8,71
Integrase	8,75
hypothetical protein	8,78
ComF operon protein A, DNA transporter ATPase	8,81
Branched-chain amino acid transport system carrier protein	8,81
Predicted HD superfamily hydrolase	8,97
Glycerophosphoryl diester phosphodiesterase (EC 3.1.4.46)	9,96
ATP synthase F0 sector subunit c	9,96
Hypothetical protein	10,17
Pyruvate-flavodoxin oxidoreductase (EC 1.2.7.-)	10,45
LSU ribosomal protein L14p (L23e)	10,73
Hypothetical protein	11,01
ABC transporter ATP-binding protein	11,94
SSU ribosomal protein S14p (S29e) @ SSU ribosomal protein S14p (S29e), Zinc-dependent	13,21
6-phospho-beta-glucosidase (EC 3.2.1.86)	13,22
Late competence protein ComEC, DNA transport	13,24
Ribonucleotide reductase of class Ib (aerobic), alpha subunit (EC 1.17.4.1)	14,24
Phage-associated HNH homing endonuclease	14,47
Lon-like protease with PDZ domain	14,96
Hypothetical protein	16,02
Phage protein	17,31
Hypothetical protein	20,52
Ribonucleotide reductase of class Ib (aerobic), beta subunit (EC 1.17.4.1)	26,65
Galactosamine-containing minor teichoic acid biosynthesis protein	43,76
Hypothetical protein	53,65
Tagatose-6-phosphate kinase (EC 2.7.1.144)	54,40

$MgCO_3 + H \rightarrow Mg + CO_2 + OH$

Mg^2 Attack

Teichoic acid biosynthesis protein (44 fold)

Glycosyl transferase family

Competence factors ComF, ComEC, ComEA (8-13 fold)

Phenolic acid decarboxylase (4,65 fold)

Magnesite

H+

ATPase

ABC transporters

ATP syntase subunits (5-10 fold)

Lactic acid

Tagatose-6-phosphate kinase (54,4 fold)

SSU

LSU

SecY

SecY
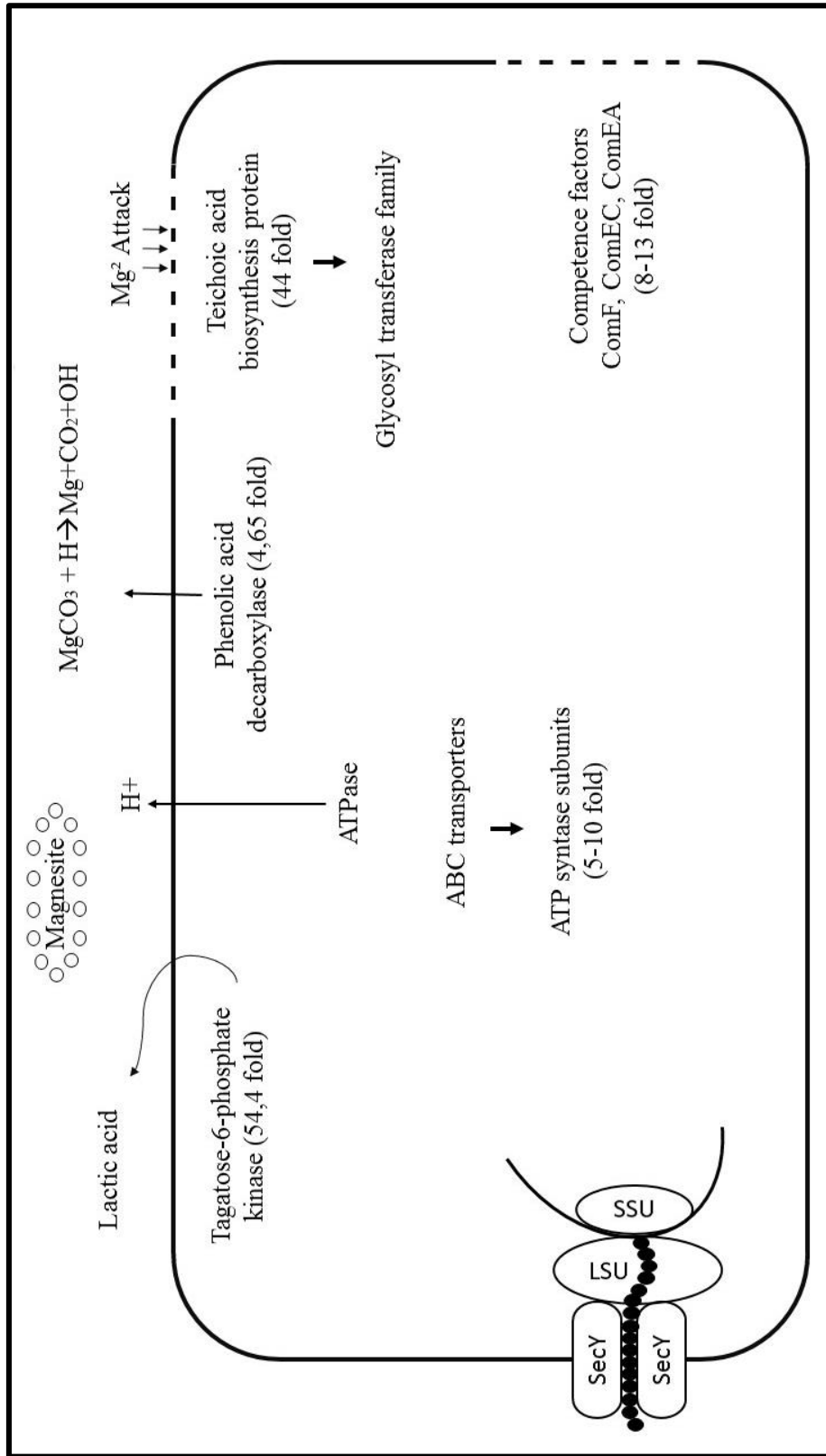
Figure 4.65. Schema of Magnesite bio-solubilization mechanisms of A1
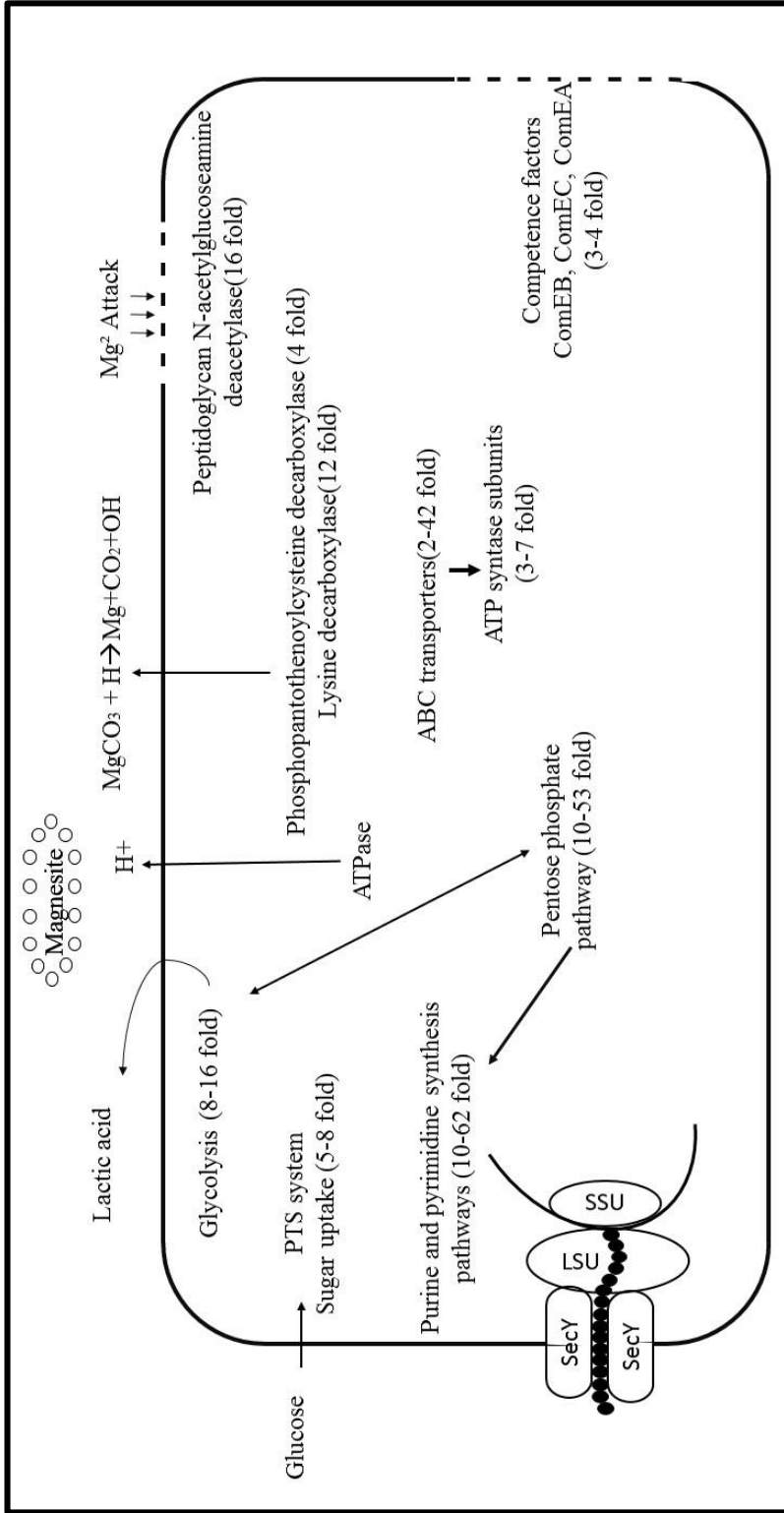
Figure 4.66. Schema of Magnesite bio-solubilization mechanisms of EF

4.4.2.6. SDS-PAGE and Protein Analysis

According to the SDS-PAGE results, protein synthesis differences between A1-GY and A1-GYM; and between EF-GY and EF-GYM were observed. Overexpressed and newly expressed proteins were determined at A1-GYM and EF-GYM samples.
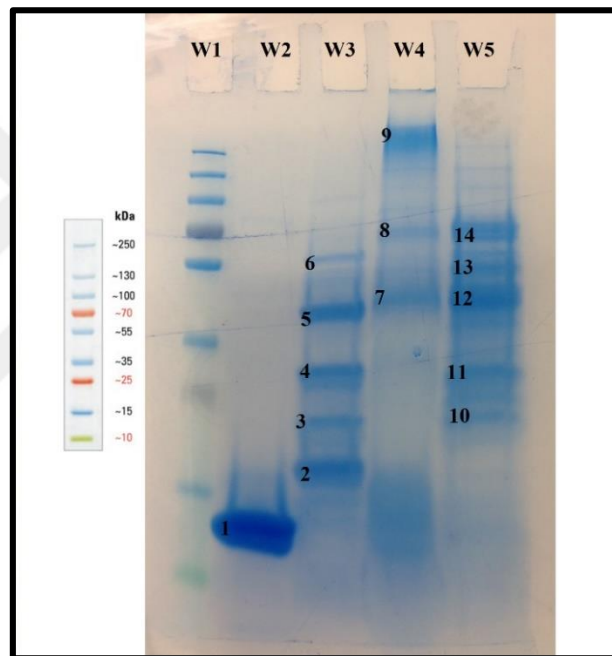
Figure 4.67. SDS-PAGE result of A1 and EF cell lysates. W1: Thermo Scientific page Ruler Plus Prestained Protein Ladder. W2: Total cell protein of A1 (incubated GY medium) W3: Total cell protein of A1 (incubated GYM medium). W4: Total cell protein of EF (incubated GY medium) W5: Total cell protein of EF (incubated GYM medium). Protein Fragments 1: Lysozyme, 2: Superoxide Dismutase, 3: Adenylate Kinase, 4: Triphosphate isomerase, 5: Elongation Factor, 6: Pyruvate Kinase, 7: Tyrosine-tRNA ligase, 8: Chaperonin, 9: 50S Ribosome, 10: Superoxide Dismutase, 11: Carbamate kinase, 12: Phosphoglycerate kinase, 13: Serine tRNA ligase, 14: Chaperonin DNA K

As a result of mass spectrometer protein analysis, protein fragments that were called number 1, 2, 3, 4, 5, 6, 7, 8, 9, 10, 11, 12, 13 and 14 refer to Lysozyme, Superoxide Dismutase,

Adenylate Kinase, Triphosphate isomerase, Elongation Factor, Pyruvate Kinase, Tyrosine-tRNA ligase, Chaperonin, 50S Ribosome, Superoxide Dismutase, Carbamate kinase, Phosphoglycerate kinase, Serine tRNA ligase and Chaperonin DNA K

Table 4.6. Protein analysis results

Number	Description	Da
1	Lyzozyme	16228
	50S Ribozomal protein	12366
2	Superoxide dismutase	23239
3	Superoxide dismutase	23239
	Adenylate kinase	23673
	Deoxyribose-phosphate aldolase	23439
4	Superoxide dismutase	23239
	Deoxyribose-phosphate aldolase	23439
5	Elongation factor	36647
	Phosohoglycerate kinase	42044
	Ornithine carbamoyltransferase	39430
6	Pyruvate kinase	54221
7	Tyrosine tRNA ligase	47231
	Foldase protein	37369
	Elongation factor	32113
	Phosphoglycerate kinase	42371
	Ornithine carbamoyltransferase	38005
8	60 kDa Chaperone protein	57075
	Chaperon protein DnaK	65543
	Phosphoenolpyruvate-protein phosphotransferase	63137
	Chaperon protein DnaK	64947
	60 kDa Chaperone protein	57165
9	DNA directed RNA polymerase subunit beta	136728
	DNA directed RNA polymerase subunit beta	134646
10	Superoxide dismutase	22683
	Deoxyribose-phosphate aldolase	23088
	Pyrrolidone-carboxylate peptidase	22922
	Ribosome recycling factor	20790
	Adenylate kinase	24025

Table (continued)

11	Triosephosphate isomerase	26898
	Carbamate kinase	32906
	2,3-biphosphoglycerate-phosphoglycerate mutase	25991
	Phosphoglycerate kinase	42371
	Superoxide dismutase	22683
	Elongation factor	32113
	Adenylate kinase	24025
12	Phosphoglycerate kinase	42371
	Acetate kinase	43380
	Phosphopentamutase	42772
	Ornithine carbamoyltransferase	38005
	Foldase protein	37369
13	NADH peroxidase	49534
	Phosphoglycerate kinase	42371
	Glucose-6-phosphate isomerase	49703
	NADH oxidase	48883
14	Chaperon protein DnaK	65543
	Phosphoenolpyruvate-protein phosphotransferase	63137
	NADH peroxidase	49534
	Proline tRNA ligase	64226
	60 kDa Chaperone protein	57075

4.5. TOXICOLOGY EXPERIMENTS

According to the test results A1 and EF microorganisms are not pathogenic for human and environment. No mortality, body weight, food consumption or treatment-related findings in clinical observations, macroscopic or microscopic examinations were observed. Differences between treated and control groups in some hematology and clinical chemistry parameters were not considered treatment-related (**Figures 4.66-4.79**).

As a result, A1 and EF could be used at mine scale for biomining of magnesite ore in Turkey.
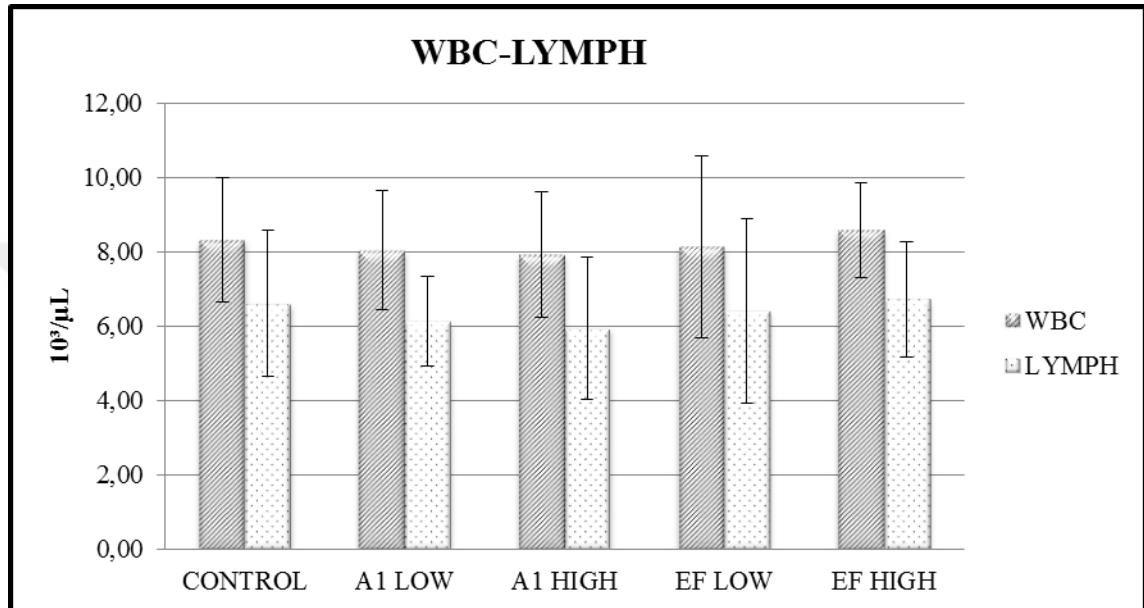
Figure 4.68. White blood cell and lymphocyte results
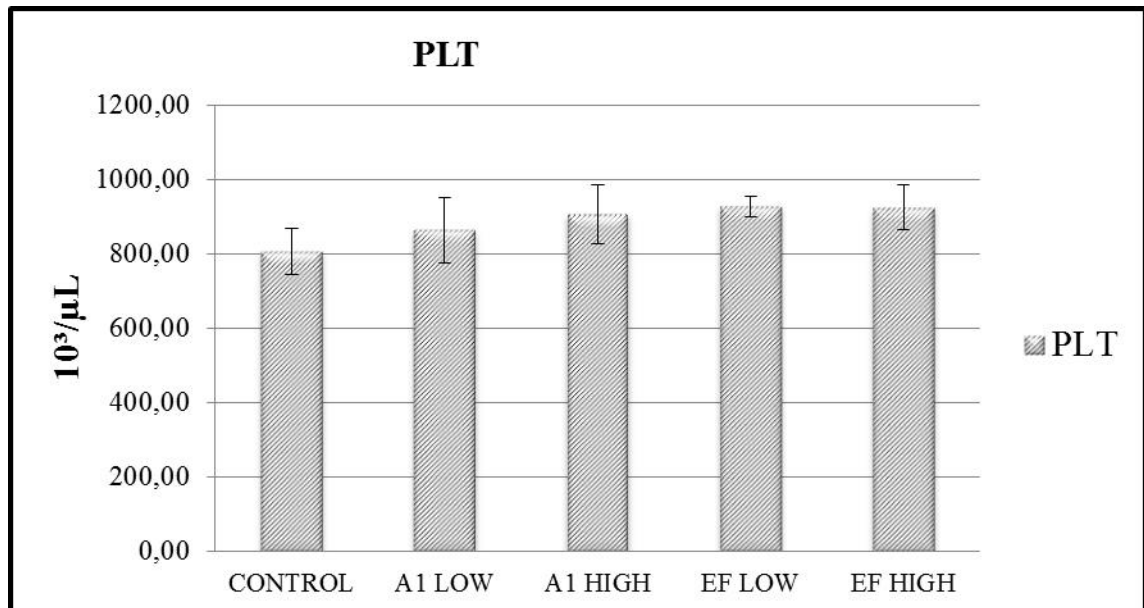
Figure 4.69. Platelet results
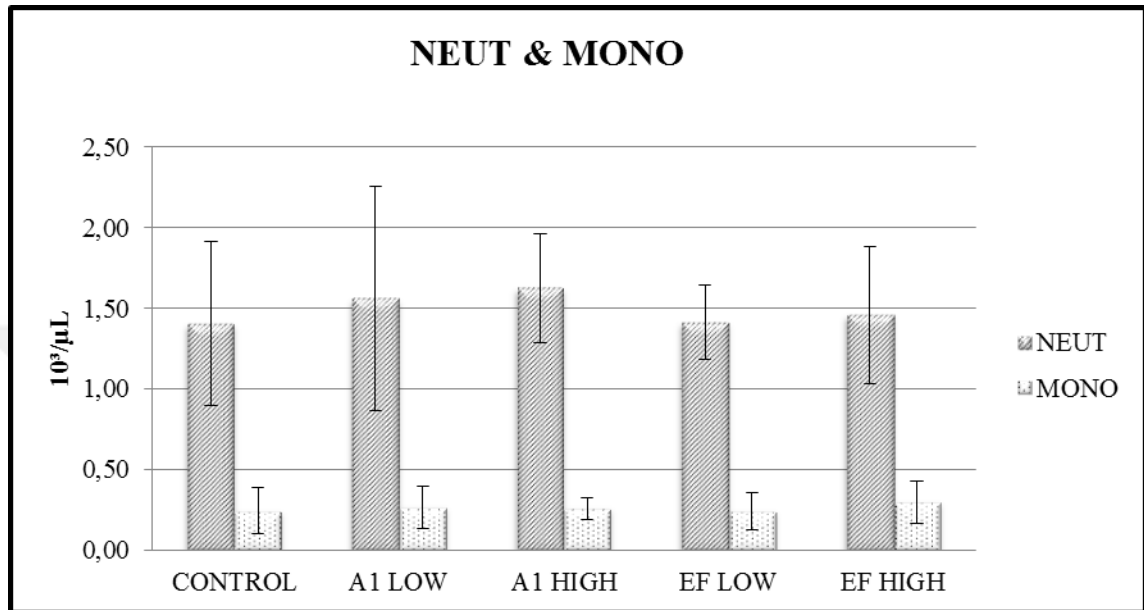
Figure 4.70. Neutrophil and Monocyte results
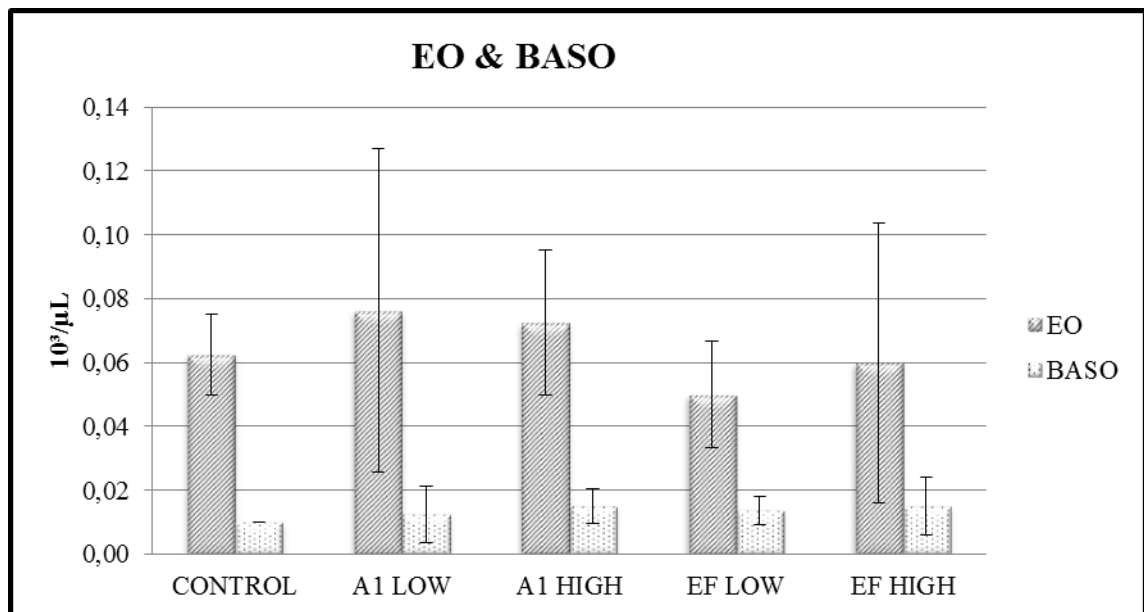
Figure 4.71. Eosinophil and Basophil results
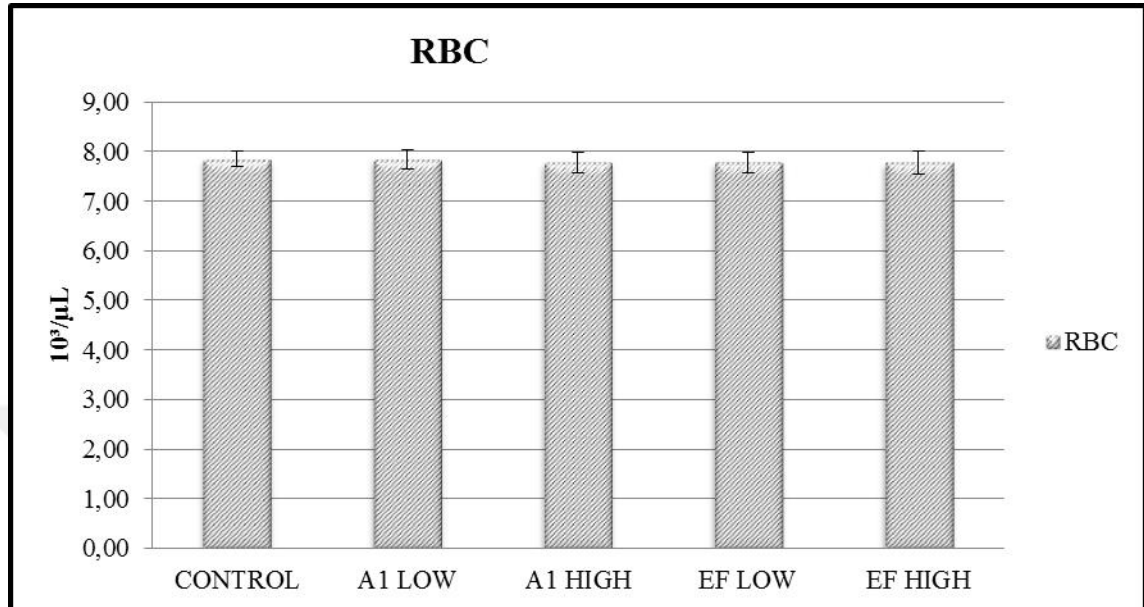
Figure 4.72. Red blood cells result
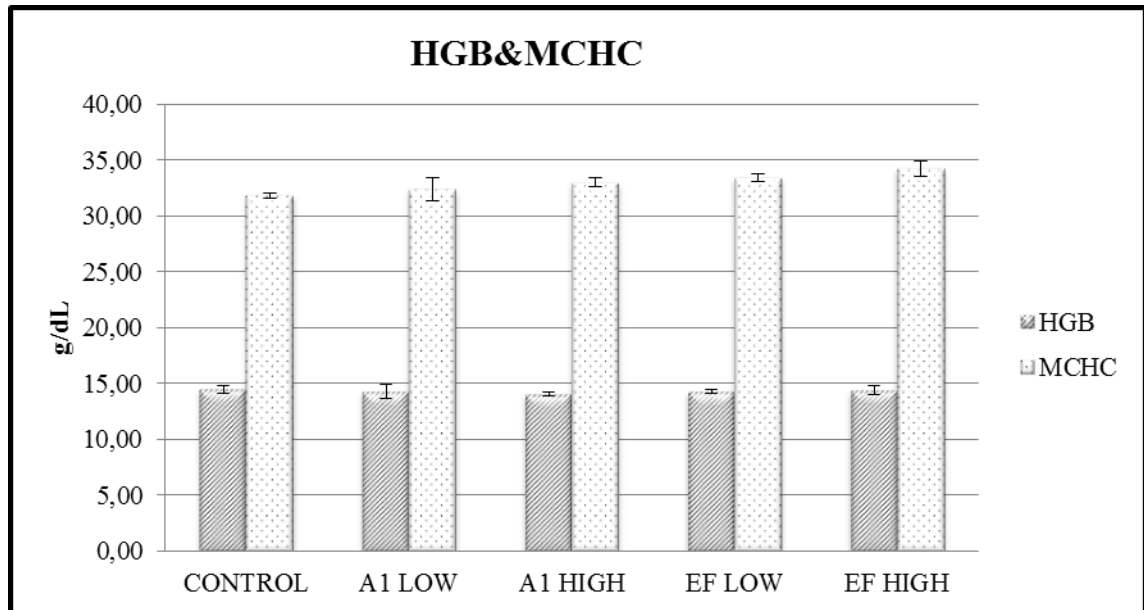
Figure 4.73. Hemoglobin and Mean corpuscular hemoglobin concentration result
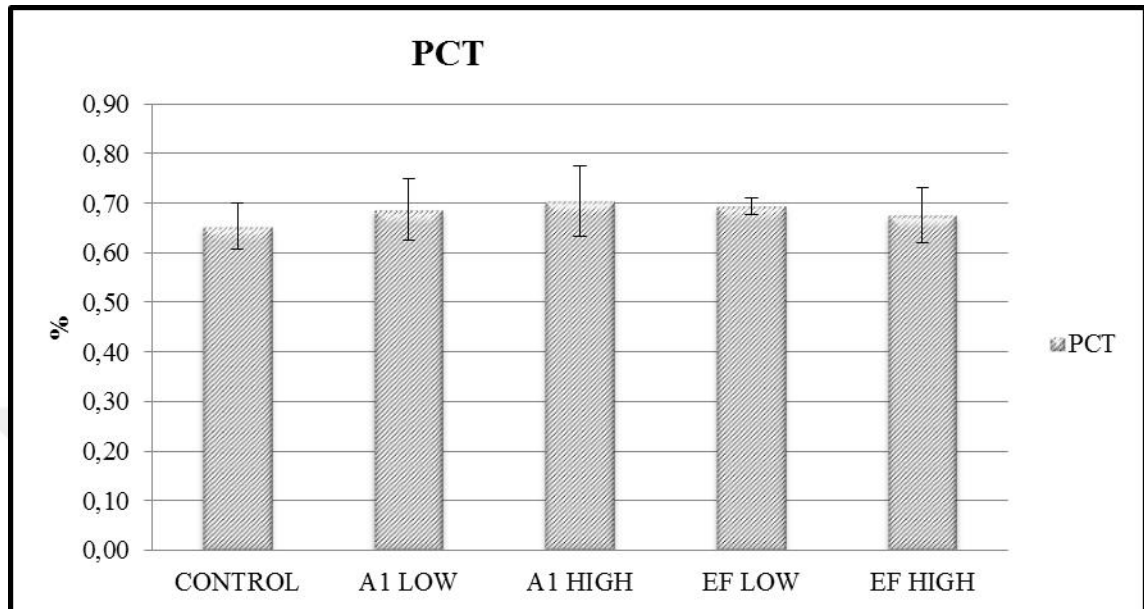
Figure 4.74. Platelet crit results
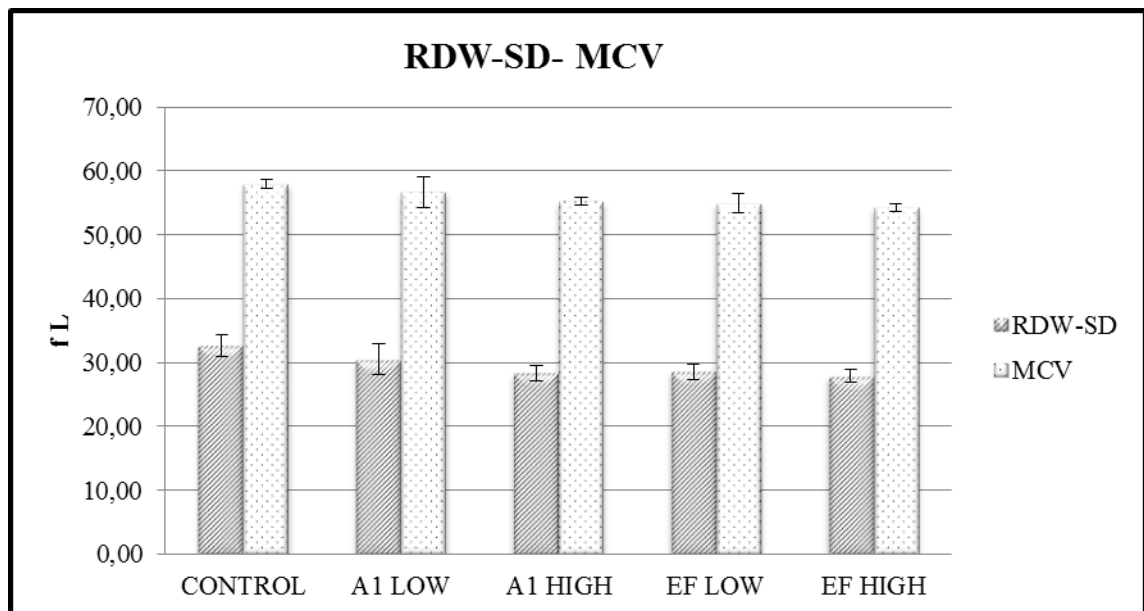
Figure 4.75. Red cell distribution width-Standard Deviation and Mean corpuscular volume results
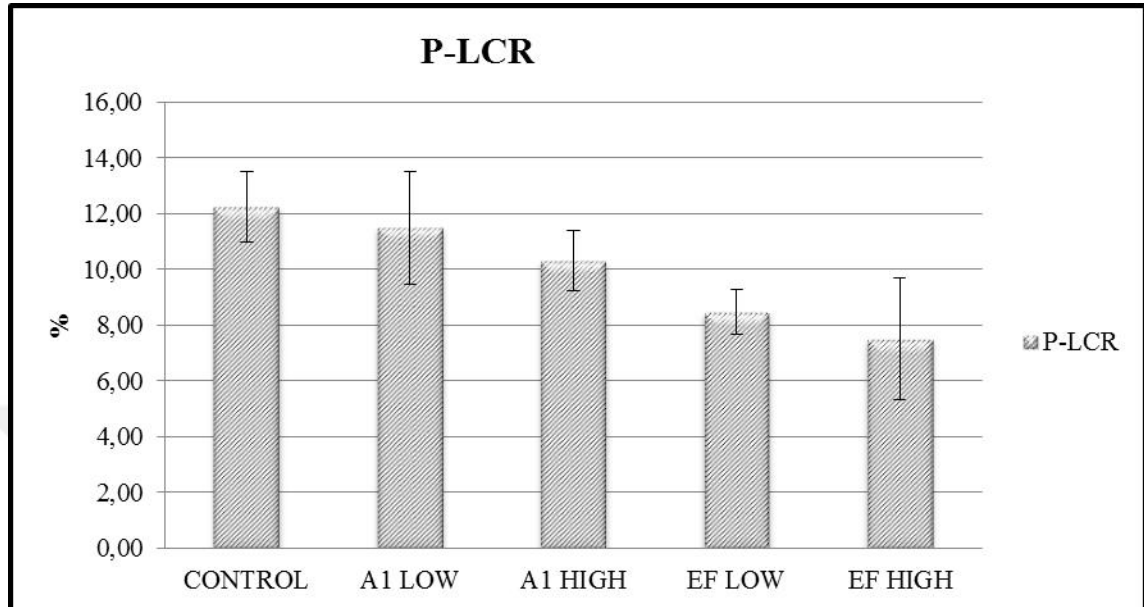
Figure 4.76. Platelet-Large cell ratio result
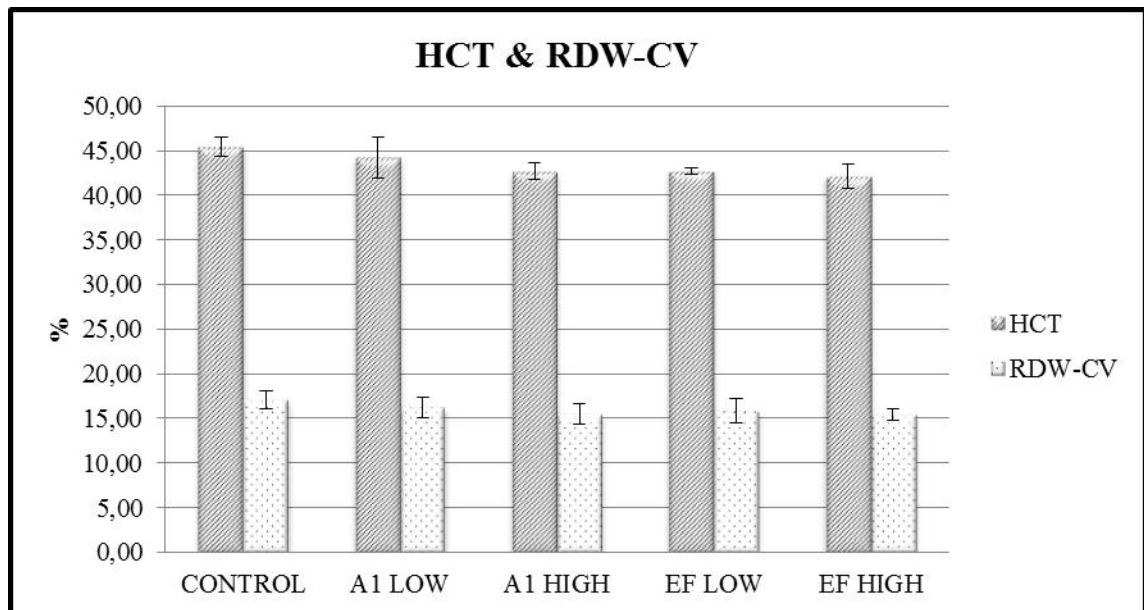
Figure 4.77. Hematocrit and Red cell distribution width results
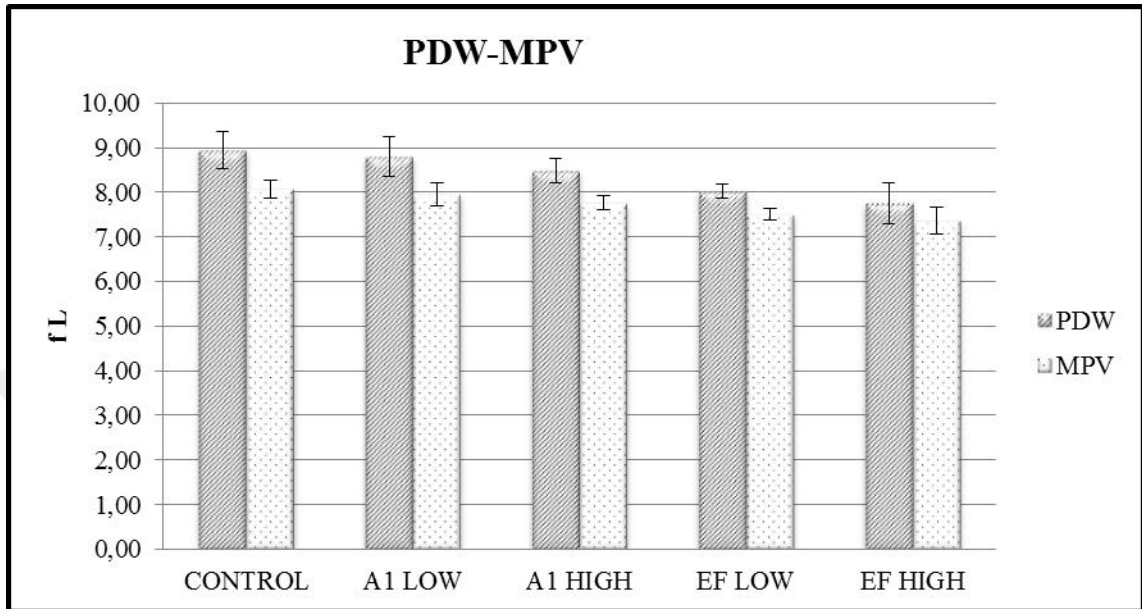
Figure 4.78. Platelet distribution width and Mean platelet volume results
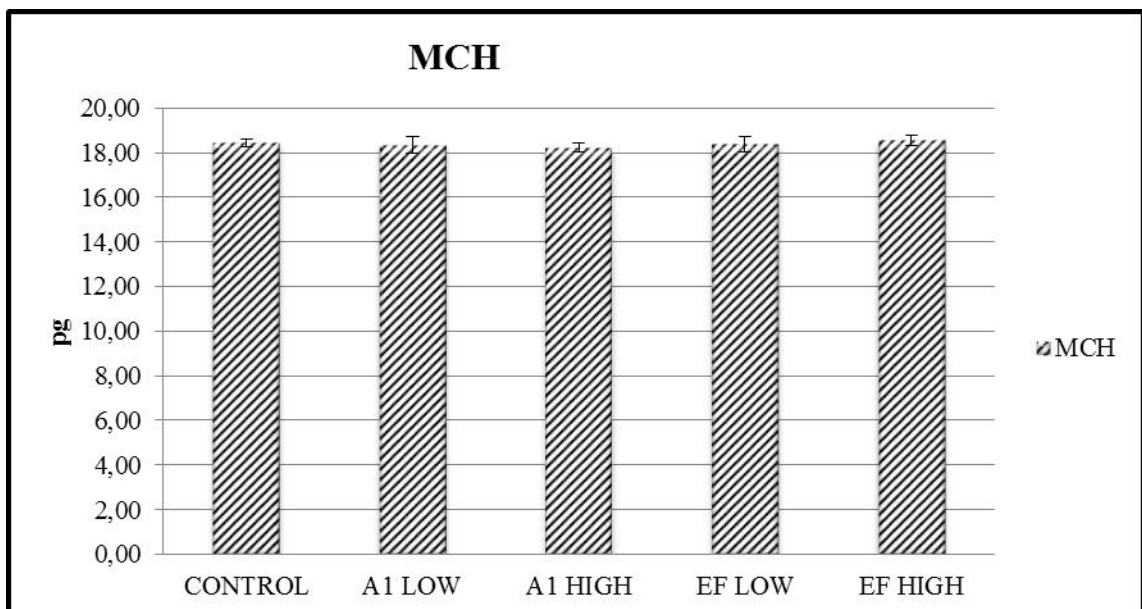
Figure 4.79. Mean corpuscular hemoglobin results
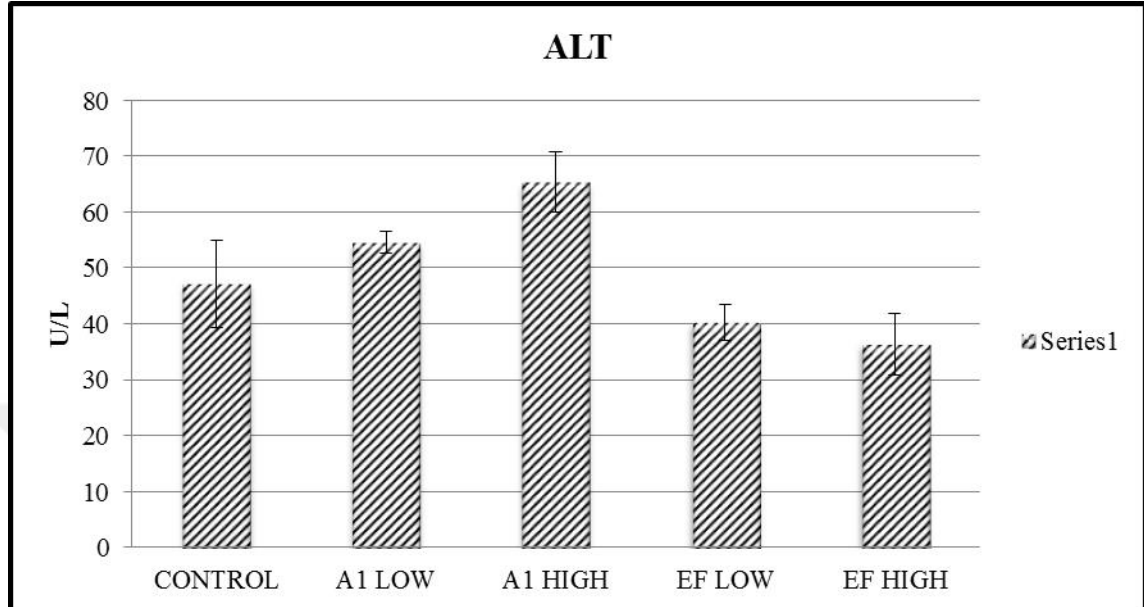
Figure 4.80. Alanine Amino transfer results
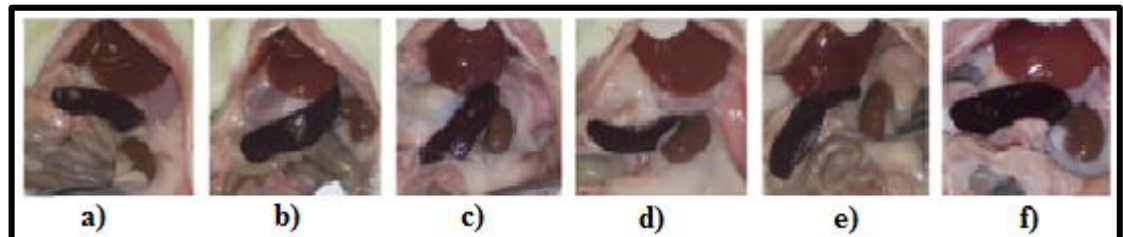
Figure 4.81. Histological results of toxicology experiments, a) and b) control, c) A1 high dose, d) A1 low dose, e) EF high dose, f) EF low dose

5. DISCUSSION

Magnesium is the 6th most common element on the earth and, because of its high reactivity, it does not exist freely in nature. The natural magnesite contains some impurities such as carbonates, silicates and oxides. These can affect the usage of obtained products negatively [2].

Beside the increasing quality of the products of magnesite, enrichment of magnesite is also important to increase its commercial value. As MgO percent of magnesite increases, the unit price increases as well.

In the world market, different forms of magnesite are exhibited as a commercial product such as raw magnesite, sintered magnesite and calcined magnesite. According to the Mining Special Expert Council Report, in Turkey, in the Kütahya 144 000 ton/per annum sintered magnesite, in Eskişehir 90 000 ton/per annum sintered magnesite [66], in Konya 35 000 ton/per annum sintered magnesite and in Tavşanlı (Kütahya) 40 000 ton/per annum calcined magnesite were produced by KÜMAŞ (Kütahya Manyezit Anonim Şirketi), MAŞ (Manyezit Anonim Şirketi), Konya Krom A.Ş. and Comag A.Ş. respectively [67]. Having said that, sintered magnesite is predominantly produced in our country. 90 percent of produced magnesite is used in refractor brick industry and 10 percent of produced magnesite is used as raw magnesite in the drug, magnesium salts, cement, paper and sugar industry [68].

Enrichment of magnesite can be performed by chemical and physical methods, such as the heavy medium separation, hand sorting, magnetic separation and flotation [2] [69]. Some of these methods are not feasible in financial matter. Especially, chemical methods have high costs than physical methods [70]. While chemical methods are harmful for environment, the most used physical method calcination requires high energy consumption. Eventually, these classical methods have many disadvantages such as; low sensitivity, high energy demand, and adverse effects of chemicals on living organisms and the environment. Therefore, it is required to develop more efficient, more economical and safer alternative applications. Biological

approaches are considered to be the best alternative for elimination of the drawbacks of physical and chemical methods used for enrichment of magnesite.

In this study, pre-isolated *Enterococcus feacalis* (EF) and *Lactococcus garvieae* (A1) bacterial strains that patent applications as Ca-dissolver property were completed in 2014, and *Staphylococcus warneri* (K1) bacterial strain and *Neurospora tetrasperma* (NT) fungi isolate which were isolated and identified during the study were used. These microorganisms have not been used as biomining or bioleaching microorganisms previously, up until this study. Only, in 2015 Erzurum research group Yanmış et al. reported that *Lactococcus* spp. could be used as Ca-dissolver on magnesite [71]. In this study, they were used for enrichment of magnesite ore, optimization experiments were performed to obtain the best yield and according to the optimization, scale up study and toxicology experiments were carried out to apply this technology in commercial scale.

Magnesite ore which is main source of magnesium element it is required to be cleared of from its impurities for commercial use of it. In order to trade magnesite, SiO_2 rate needs to be less than 2 percent and $CaCO_3$ rate needs to be less than 1 percent in the raw material. In the present study, following the one week treatment EF bacteria converted the 93 percent of total magnesium to free magnesium, A1 bacteria converted the 95 percent of total magnesium to free magnesium, K1 bacteria converted the 30 percent of total magnesium to free magnesium, NT fungi converted the 40 percent of total magnesium to free magnesium.

- Isolation and Identification

A1 and EF bacterial strains are pre-identified and apart of the Yeditepe University Genetics and Bioengineering Department's culture collection as Ca-dissolver microorganisms. K1 and NT microorganisms are isolated as Ca-dissolver microorganisms during the scanning magnesite ore flora for determining Ca-dissolver microorganisms. K1 and NT microorganisms are isolated from magnesite ores comes from the cities Kütahya and Erzurum, respectively. In order to identify these microorganisms, 16S rRNA and 18S rRNA molecular identification methods were performed for bacteria and fungi, respectively. 16S rRNA is a part of the 30S rRNA. The gene encodes it is referred as 16S rRNA and is used in reconstructing phylogenies, due to the conserved 1500 bp region of the gene. 18S rRNA is a

part of the small eukaryotic RNA 40S rRNA. 18S rRNA is eukaryotic cytoplasmic ribosomes' small structural subunit RNA, and thus one of the basic structure of all eukaryotic cells. Thanks to its 600 bp long conserved region, molecular identification can be carried out. These microorganisms are firstly identified as magnesite biomining microorganisms in this study.

- Optimization

One of the optimization studies to increase the yield is applying different pH experiments. In the previous studies, acid application is used for bioleaching of various ores and it was determined that acidic media facilitate the demineralization [72] [73] [74] [69] [75] [76]. Therefore, microorganisms were grown at different TSB mediums prepared at variable pH values. Then, based on the spectrometer cell density measurement results at OD_{600} optimum pH values were determined as pH 3-9, 3-11 and 5-9 for EF, A1 and K1, respectively. Thus, GYM medium was prepared at pH values between pH 3-9. As reported in the literature, at acidic pH values dissolution of $CaCO_3$ and formation of free Mg were more than basic pH values for each microorganism. Optimum enrichment value was obtained at pH3 for each microorganism. In addition, A1 and EF also have high enrichment values close to optimum values at pH 5 and pH 7. Interestingly, although the optimum enrichment was obtained at pH 3 for K1, K1 could not grow at pH 3. It is possible that carbonate dissolute by the increasing the pH. In summary, starting the biomining at low pH values increases the efficiency.

The effect of the temperature is detected as another optimization parameter. As it is known that there is an optimum temperature value for each microorganism. To detect this temperature values EF, A1 and K1 bacterial strains were inoculated at variable temperatures and then cell densities were measured at spectrometer OD_{600}. Although the microorganisms could live between 15ºC to 45ºC, optimum temperature value was determined as 30ºC. In the literature, it is reported that *Staphylococcus warneri* was incubated at 30ºC for growth [77], and for A1 and EF optimum growth temperature changes between 30ºC-37ºC depend on medium [78] [79]. Results of biomining experiments which were performed with GYM medium at 30ºC, supported this data. Calcination that is a classical method for magnesite enrichment is performed by burning magnesite at different temperatures between 650-2000ºC [7]. But, the

biomining of magnesite occurs at 30ºC. This method requires very low temperature, so it decreases the cost and provides a big energy saving.

Carbon is the source of energy for all organisms. But, all of the organisms prefer/utilize different carbon sources [80]. The carbon source that provides the optimum yield was detected by GYM media that were prepared before with different carbon sources. It is detected that glucose is the optimum carbon source for A1, EF and NT although glucose is the second preferable carbon source for K1 after sucrose. Conversely, sucrose is the worst carbon source for A1 and EF and lactose is the worst carbon source for NT. The worst carbon source for K1 is mannose. Therefore, glucose was accepted optimum carbon source for microorganisms at mixed formulations experiments.

There is not any significant correlation between Mg dissolving capacity and applying different bacterial concentrations. Ineffectiveness of difference of microorganism concentration experiment could be explained as demineralization rate is lower than cell division rate. Moreover, reason of this may be constant nutrient amount. Because, we used batch system. It is not possible to do cell density measurement for fungi as it was easily for bacteria. Because, fungi do not grow homogeneously in the broth medium. Therefore, optimum pH and temperature values determined according to the Mg dissolving results.

After optimum conditions are determined, the difference between the experiments that were performed at optimum and un-optimized conditions showed the importance and profit of optimization. Based on the result, scale-up experiments were performed in the optimum conditions better.

It is expected that mixed formulations of microorganisms would provide the strongest magnesite enrichment by synergic effect. Upon this, microorganism were inoculated to the TSA to detect if there is any competition with each other or not. Based on the absence of the competition, mixed formulations were tested for magnesite enrichment. Unfortunately, the microorganisms had antagonistic effect on each other in magnesite enrichment. Even, the best Mg enrichment microorganisms A1 and EF decreased each other's dissolving capacity. According to the transcriptome analysis, magnesite media causes a stress and microorganisms

give stress response. Metabolites that are resulting of this stress response may affect microorganisms' growth and biomining activity.

- Scale-up

Scale-up is required to apply a laboratory scale study to industrial scale. But, scaling up is a hard process because of decreasing in the yield. Thus, this process is needed to be optimized during the scale-up too. Since mixed formulations could not provide synergic effect, A1 one of the best Ca-dissolver microorganisms was selected for scale-up studies. One of the scale-up methods power per volume (P/V_L) was fitted to our study. In scale up methods, importance ranking from more to less is power per volume (P/V_L), power (P), Tip speed, Rotational speed and Reynold number methods. Fitting the best scale-up method to our study provides more reliability to our scale-up process. pH optimization was not required during the fermenter process optimization. Although, $CaCO_3$ dissolving increased the pH, A1, a member of the lactic acid bacteria compensated the increasing of pH. In fact, A1 held the pH value between pH 4-5 during the study by secreting organic acids. Hereby, acid usage requirement in magnesite enrichment and its cost are removed. Scale up of biomining of magnesite ore was performed successfully from flask to 30 L fermenter. These results provide valuable insight to the potential commercialization of biomining of low grade magnesite ores economic and environmental friendly.

- Lactic acid Production

It's known that acidity is effective on demineralization. Previous studies on the field showed the leaching of magnesite and calcite by organic acids. Firstly, in 2005 Laçin and colleagues worked on dissolution kinetics of magnesite in acetic acid solutions. Their study revealed that the dissolution of natural magnesite was controlled by chemical reaction. Then, Bayrak and colleagues researched on dissolution kinetics of natural magnesite in gluconic acid solutions (2006). In the same year, Bakan et al. studied on dissolution kinetics of natural magnesite in lactic acid solutions. In 2007, Jordon et al. investigated organic and inorganic ligands effects on dissolution of magnesite at $100^{\circ}C$ and pH=5 to 10. pH between 5-7 citrate and EDTA solutions are effective on magnesite demineralization, while oxalate and acetate solutions have no demineralization effect at these conditions. In 2008 Demir et al., worked on optimization of

the dissolution of magnesite in citric acid solutions. In 2009(a) Pokrovsky et al., investigated effect of organic and inorganic ligands on calcite and magnesite dissolution rates at 60 °C and 30 atm pCO_2 and calcite, dolomite and magnesite dissolution kinetics in aqueous solutions at acid to circum neutral pH, 25 to 150 °C and 1 to 55 atm pCO2 (2009b). In 2009(a) Dönmez et al, examined the leaching kinetics of calcined magnesite in acetic acid solutions and magnesium recovery from magnesite tailings by acid leaching and production of magnesium chloride hexahydrate from leaching solution by evaporation. In 2010, Bayrak et al., improved their work which was published in 2006 by performing kinetic study on the leaching of calcined magnesite in gluconic acid solutions. In 2014 Raza et al., investigated utilization of formic acid solutions in leaching reaction kinetics of natural magnesite ores and indicated that formic acid could be promising for the leaching of magnesite.

Thanks to leaching studies on naturally occurring magnesite materials in acetic acid, gluconic acid, citric acid and lactic acid solutions, it was found that leaching kinetics were driven by chemically controlled mechanisms [81] [73] [72] .

Inorganic acids have challenges of selectivity, froth formation and scaling. On the contrary, thanks to the most of the leaching reactions are done in mild acidic conditions (pH 3–5), organic acids could be used as active leaching reagents. In addition, utilization of organic acids for carbonaceous rocks is possible and corrosion risk of organic acids is very low. Another advantage of organic acids as leaching agents is their biodegradability, which generally depends on the carbon chain and other attached groups [76].

In order to investigate magnesite biomining mechanism of A1 and EF microorganisms, lactic acid amounts that they produced were measured. Since they are the members of lactic acid bacteria, they produce organic acids, especially lactic acid. Aerobic heterotrophic bacteria, fermenting, sulphide-oxidizing and nitrifying bacteria, can dissolve acid-labile minerals because of the production of acids as byproducts of metabolism such as; carbonic, organic, sulphuric and nitric acids, respectively [82].

According to the results, lactic acid production and amount of free Mg and Ca released are correlated with each other. Mg and Ca dissolving rates rise with increasing lactic acid production. Moreover, in the studies which we performed with commercial lactic acid,

commercial lactic acid was added to decrease pH of the magnesite samples to pH 5. The last lactic acid density has to be at 0,9 g/ml to reach desired value. After two hours incubation with commercial lactic acid, only 5 percent of total magnesite was converted to free Mg. In order to hold the pH value at pH 5 extra lactic acid addition was required permanently. But, acid usage is unhealthy for human and environment safety as well as causes the high cost. In our study, 90 percent of total Mg was converted to free Mg by biomining while total lactic acid amount had not reached 5 g/ml. Moreover, fermenter study indicated that microorganisms could keep the pH value between 4 and 5 without adding any acid externally, despite carbonate output during the demineralization. Previous studies showed that magnesite and $CaCO_3$ could dissolve with organic acids.

- Enzyme Assays

There is a consensus about enzymes that they have a role in biomineralization/ demineralization/remineralization phenomena. In the literature, carbonic anhydrase, alkaline phosphatase, phosphoprotein phosphatase and vacuolar-type H+-ATPase are the enzymes that are predicted as involved in this phenomena. All of these enzymes generally consist at sites of carbonate and phosphate mineralization, and also at many noncalcifying sites and in noncalcifying organisms [82].

Vacuolar-type proton translocating ATPases (V-ATPases) are large and complex enzymes. They generally consist of two domains; a cytosolic domain, V1, and a transmembrane domain, V0. The V1 domain has 13 subunits; they are three A, three B and two G components, and single C, D, E, F and H components. The V0 domain has five distinct subunits that are called a, c, c', c and d. Multiple genes or alternatively spliced transcript alternatives encode extra isoforms of V1 and V0 subunit proteins. The V-ATPases act as ATP-dependent proton pumps. The V-ATPases pump protons to the other side of membranes coupled to ATP hydrolysis. As a result, endomembrane systems are acidified. This acidic pH is essential for different organelle functions, for instance the zymogen activation, release of ligands from receptors, macromolecules degradation, heap of neurotransmitters in synaptic vesicles and the sorting of newly formed polypeptides, proteolysis in lysosomes. They are included in diverse cellular processes in the majority of eukaryotic cells and also have specialized functions in specific

cell types. In some epithelial cells, V-ATPases are plenty at the plasma membrane, push out protons, and acidify the restricted extracellular space. Extracellular acidification is required of some cellular functions, such as in osteoclast it is required for bone resorption and in the insect midgut it is required for absorption of nutrients [83] [84]. In addition, presence of free Ca increases the ATPase activity in myofibril samples [85].

A1 that have grown in GYM medium has intracellular and extracellular ATPase activity more than A1 that have grown in GY medium. EF that has grown in GYM medium has only extracellular ATPase activity more than EF that has grown in GY medium. Consequently, all samples have ATPase activity. This result was expected as A1 and EF produce lactic acid. Moreover, the GYM medium samples have ATPase activity more than the GY medium samples, indicating that ATPase activity may have additional contribution on biomining of magnesite in addition to the organic acid production.

Carbonic anhydrase (CA) is a metalloenzyme which contains zinc. This enzyme catalyzes the reversible hydration of CO_2 into bicarbonate and a proton. CO_2 hydration can be significantly increased ($\sim 10^7$ times) by CA. CA is immanently distributed in organisms, such as animals, plants, archaebacterial, and eubacteria, and is fundamental to many biological processes such as photosynthesis, respiration, CO_2 and ion transport, mineralization, and acid–base balance. CA has been divided into five divergent families that are called α, β, γ, δ, and ε. These families have no primary sequence homology and evolved separately [86] [87]

Carbonic anhydrase enzyme may exist as intracellular, membrane bounded and extracellular in the organisms. Carbonic anhydrase activity of A1 cell lysate was more than A1 supernatant sample while carbonic anhydrase activity of EF cell lysate was less than EF supernatant sample. Therefore, A1 has intracellular carbonic anhydrase production, while EF has extracellular carbonic anhydrase production. Moreover, carbonic anhydrase activity of microorganisms that have grown in GYM medium was more than microorganisms that have grown in GY medium. In conclusion, carbonic anhydrase activity may have a role in biomining of magnesite ore.

- Omic Studies

The studies to enlighten the mechanism of magnesite biomining is showed that lactic acid probably has role and CA and ATPase enzymes which are in the literature about decalcification may have role in biomining of magnesite. Nevertheless, in 2010 Orrel and his colleagues reported that Cu biomining occurs by response of extremophilic microorganisms against to high concentration of copper. These microorganisms detect the high concentration copper as toxic material and consist the biomining with variable Cu resistance systems, Cu chaperones and an oxidative stress defense system [88]. On this basis, to enlighten the molecular mechanism of magnesite biomining genomic, transcriptomic and proteomic analysis of A1 and EF are performed.

- Genomic Analysis

According to the whole genome sequencing analysis, A1 genome size is 2,3 Mb with a GC content of 37,8 percent. In the literature, different *Lactococcus garvieae* isolates have approximately the same genome size and GC content. In 2011, Aguoda-Urda and his colleagues have reported that their *Lactococcus garvieae* isolate is composed of 2,1 Mb with a GC content of 38 percent [89]. *L. garvieae* UNIUD074 isolate's genome size is reported approximately 2,2 Mb with the GC content of 38 percent [90]. In another work, it was reported that *Lactococcus garvieae* DCC43 is composed of 2,2 Mb genome [91]. In addition, Ricci and his colleagues reported that the *L. garvieae* LG9 isolate genome includes 2,1 Mb, with an average GC content of 38,5 percent and the *L. garvieae* TB25 isolate genome includes 2 Mb, with the GC content of 38,1 percent [92].

Enterococcus feacalis (EF) that is our other biomining microorganism is composed of 7 Mb genome, with a GC content of 37,8 percent. According to the whole genome sequencing results GC content of our isolate is approximately the same with the *Enterococcus feacalis* strains in the literature. Besides this, its genome size is larger than the other *Enterococcus feacalis* strains in the literature. For instance, *Enterococcus feacalis* ATCC 29212 genome contains 3 Mb with the GC content of 37,2 percent [93], while *Enterococcus feacalis* V583

strain has 3,34 Mb genome with the GC content 37,4 percent [94]. A lot of hypothetical protein genes were detected in the EF genome which were not placed in subsystems of the RAST programme.

- Transcriptome Analysis

Total RNA of A1 and EF which were grown in the presence and absence of magnesite, were sequenced to make transcriptome analysis. In the presence of magnesite, down regulated and up regulated genes give ideas about which pathways have a role in biomining or effects of magnesite or Mg^{+2} on A1 and EF metabolism.

According to the A1 transcriptome analysis results, the most upregulated gene belongs to Tagatose-6-phosphate kinase (EC 2.7.1.144) with 54,4 fold increase. Tagatose-6-phosphate kinase (EC 2.7.1.144) is one of the enzymes that participated in galactose metabolism [95] [96]. Moreover, it exists in *Lac* operon. It is also called LacC. It is in phosphotransferase group and uses divalent cation as cofactor. Mg^{+2} is the most effective cofactor for Tagatose-6-phosphate kinase [97] [98]. In our study, we showed that lactic acid production of A1 and EF increases during the biomining of magnesite. Thus, overexpression of one of the Lac operon enzymes is expected result. Furthermore, this enzyme's cofactor is product of magnesite biomining, Mg^{+2}. At the same time, formation of free Mg^{+2} ions make positive feedback to lactic acid production.

The other overexpressed gene belongs to galactosamine-containing minor teichoic acid biosynthesis protein with the 43,76 fold increase. This protein is used in cell wall biosynthesis. In the gram positive bacteria, the cell wall is composed of some molecules, such as glucosamine, muramic acid, lysine, alanine, glutamic acid, aspartic acid, serine, glycine, threonine and teichoic acid, which is rich in galactosamine, phosphate, and choline. 23 percent of the cell wall is three teichoic acid component as weight [99] [100]. Teichoic acids are component of peptidoglycan layer and protect the cell wall against to the cation attacks for instance sodium (Na^{+1}) and magnesium (Mg^{+2}) ions [101] [102]. Formed free Mg^{+2} ions during the magnesite biomining causes the increasing of galactosamine-containing minor teichoic acid biosynthesis protein. Furthermore, overexpression was detected in the genes which are associated with peptidoglycan formation. Glycerol uptake facilitator protein

expression increases 7,88 fold. Cofactor of this enzyme is Mg. It works via binding 2 Mg^{+2} ions. Glycerol is the component of peptidoglycan [103] [104]. Glycosyltransferase gene has 2 copy in the A1 genome and expression of them increased 7,79 and 4,32 fold. Glycosyl transferase family protein and Glycosyl transferase, family 2 proteins' expression increased 4,06 and 3,88, respectively. Acyl-phosphate: glycerol-3-phosphate O-acyltransferase PlsY enzyme gene increased 3,74 fold. Glycosyl transferases and glycerol-phosphate acyltransferases act an important role on regulation of membrane formation [105] [106]. The other enzyme Glycerophosphoryl diester phosphodiesterase (EC 3.1.4.46) involved in glyserophospholipid metabolism, overexpressed 9,96 fold. This enzyme links glycerol phosphate and carbohydrates to each other by phosphodiester bonds to form teichoic acids [107] [108]. Consequently, increasing of free Mg^{+2} ion amount weaken the cell wall, so the genes which are associated in cell wall biogenesis expressed in an increased quantity.

Some bacteria have natural competence. External conditions trigger off natural competence. Attacks of free Mg^{+2} ions to cell wall made the A1 cells more competent. As a result of this competece genes were overexpressed. ComC, ComE, ComF and ComG are different operon which include competence genes. Late competence protein ComEC, which is a channel protein responsible from DNA transport increased 13,24 fold. Late competence protein ComEA, which is responsible for DNA reception increased 6,92 fold. [109] [110]. ComF operon protein A, which is a DNA transporter ATPase increased 8,81 fold in one copy, expression of the other copy of this gene increased 3,90 fold [111]. Competence factor which is a surface protein. It provides transformation via binding to extracellular DNA. It's expression increased 8,7 fold [112]. Late competence protein ComGB and Late competence protein ComGA that genes exist in the same operon, expressions increased 7,51 fold and 3,64 fold, respectively. Both of them are responsible for access of DNA to ComEA [113].

According to the transcriptome analysis, expression of large subunit (LSU) and small subunit (SSU) ribosomal proteins increased. LSU ribosomal protein L27p (2,01 fold), LSU ribosomal protein L19p (2,08 fold), LSU ribosomal protein L7/L12 (P1/P2) (4,78 fold), LSU ribosomal protein L4p (L1e) (5,02 fold), LSU ribosomal protein L31p (6,86), LSU ribosomal protein L32p (7,81 fold), LSU ribosomal protein L16p (L10e) (8,44 fold), LSU ribosomal protein L14p (L23e) (10,73 fold), SSU ribosomal protein S17p (S11e) (8,54 fold), SSU ribosomal

protein S9p (S16e) (2,02 fold), SSU ribosomal protein S19p (S15e) (4,51 fold), SSU ribosomal protein S13p (S18e) (2,25 fold), SSU ribosomal protein S20p (5,33 fold), SSU ribosomal protein S3p (S3e) (7,88 fold), SSU ribosomal protein S17p (S11e) (8,54 fold), SSU ribosomal protein S14p (S29e) (13,21 fold) are some of them. Besides this, expression of transcription regulator and activator proteins increased. Such as, Transcriptional regulator, AraC family (4,04 fold), Transcriptional regulator, TetR family (4,27 fold), Transcriptional activator tipA (2,34 fold), Transcriptional regulator, MarR family (5,5 fold), Transcriptional regulator SpxA1 (2,91 fold), Transcriptional regulator, XRE family (2,92 fold). LSU ribosomal protein L31p, LSU ribosomal protein L32p and LSU ribosomal protein L16p (L10e) parts of peptidyl-tRNA or aminoacyl-tRNA binding sites which is important in protein synthesis [114] [115]. LSU ribosomal protein L7/L12 (P1/P2) stalk is assigned in touch with translational factors [116]. There is no information about relation between increasing ribosome formation and biomining. Overexpression of these genes may be related stress response. Further studies could explain this relation.

The other overexpressed genes are belong to the ABC transporters. These transporters provides the transfers of some molecules out of the cell. These molecules could be cell surface proteins and lipoproteins, antibiotics, toxins, pathogenic proteins, drugs, competence factors [117]. As we said before, a lot of gene which involve in cell wall biogenesis overexpressed in A1. Therefore, to export these molecules expression of ABC transporters increased. For instance, Teichoic acid translocation permease protein TagG expression increased 3,63 fold, while Teichoic acid export ATP-binding protein TagH (EC 3.6.3.40) expression increased 3,32 fold. These transfers require energy. Already, ABC transporters are ATP dependent. Moreover, the lot of anabolic activities increased in the cell and ATP requirement for these activities increased, too. All subunits of ATP synthase genes expressions increased. They are ATP synthase F0 sector subunit c (9,96 fold increase), ATP synthase epsilon chain (EC 3.6.3.14) (8,03 fold increase), ATP synthase epsilon chain (EC 3.6.3.14) (5,95 fold increase), ATP synthase gamma chain (EC 3.6.3.14) (5,37 fold increase), ATP synthase alpha chain (EC 3.6.3.14) (5,06 fold increase), ATP synthase F0 sector subunit b 5,02 fold ATP synthase beta chain (EC 3.6.3.14) (4,84 fold increase), ATP synthase F0 sector subunit a (4,47 fold increase).

Although A1 cells incubated at 30˚C, its cold shock proteins overexpressed. Three different gene copies of cold shock protein expressions increased 5,85, 6,42 and 7,66 fold. Instead of adaptation to cold conditions, cold shock protein is expressed for 50S rRNA biogenesis [118].

According to the result of the EF transcriptome analysis more genes were upregulated or downregulated than A1 transcriptome analysis results. 1250 genes upregulated 2 times or more. 20 of them upregulated 16 times or more. Although, increasing amount is not exactly the same for each A1 gene, upregulated genes' profiles are similar to the A1 upregulated genes.

At first sight, the most upregulated gene belongs to pyrimidine metabolism. It is Pyrimidine-nucleoside phosphorylase (EC 2.4.2.2) with 62,58 fold increase. The other pyrimidine and purine genes followed it such as, Cytidine deaminase (EC 3.5.4.5) with 51,67 fold increase, Purine nucleoside phosphorylase (EC 2.4.2.1) with 42,5 fold increase and Guanylate kinase (EC 2.7.4.8) with 10,69 fold increase. Synthesis of purine and pyrimidine nucleotides are important pathways for amino acids. There are some reasons for their importance. For instance, ATP and GTP are used as energy source for cells. Although GTP is not used commonly as ATP, it is important because for using in protein synthesis. On the other hand, glucose and galactose activating is performed by using UTP as an energy source and lipid metabolism's energy source is CTP. In addition, AMP also has a role with being structural subunit of some coenzymes as Coenzyme A and NAD. Moreover, the main consumption area of nucleotides are DNA and RNA synthesis [119] [120]. During the biomining, energy consumption, growth rate, protein and enzyme synthesis, DNA and RNA synthesis, and lipoprotein synthesis for cell wall are increased, as we said for A1. That's why, this is the significant result for biomining.

The second overexpressed gene belongs to Deoxyribose-phosphate aldolase (EC 4.1.2.4) enzyme with 53,39 fold increase. This enzyme is one of the enzymes in the Pentose phosphate pathway. There were another enzymes which belong to Pentose phosphate pathway. For instance, Phosphopentomutase (EC 5.4.2.7) with 23,48 fold increase, Ribose 5-phosphate isomerase A (EC 5.3.1.6) with 16 fold increase, Gluconate dehydratase (EC 4.2.1.39) with 5,73 increase, and NAD-dependent protein deacetylase of SIR2 family with 11,39 fold

increase which stimulates the pentose phosphate pathway [121]. Pentose phosphate pathway is an anabolic pathway which is parallel to glycolysis. This pathway oxidizes the glucose and generates pentoses and NADPH. Pentose phosphate pathway mainly has three functions. First of them is generating ribose-5-phosphate (R5P) which is used as precursor for nucleotide synthesis. The second is generating NADPH as reducing power for biosynthesis reactions. Parallel to this function some genes belong to nicotinate and nicotinamide metabolism are overexpressed. For instance, Nicotinamide N-methyltransferase (EC 2.1.1.1) with 6,8 fold increase and Nicotinate phosphoribosyltransferase (EC 2.4.2.11) with 6,36 fold increase. NADPH prevents the oxidative stress in the cell. The third function of Pentose phosphate pathway is metabolizing pentose sugars and rearranging the carbon skeletons of carbohydrates for converting them to glycolytic/gluconeogenic intermediates. As we said before, glycolysis and Pentose phosphate pathway parallel pathways. During the biomining glycolysis pathway is induced, too. Some of overexpressed glycolysis pathway enzymes are Phosphoglycerate mutase (EC 5.4.2.1) with 16,8 fold increase, L-lactate dehydrogenase (EC 1.1.1.27) with 11,12 fold increase, 6-phosphofructokinase (EC 2.7.1.11) with 16,2 fold increase and, Glucose-6-phosphate isomerase (EC 5.3.1.9) with 7,58 fold increase. L-lactate dehydrogenase (EC 1.1.1.27) is involved in lactic acid fermentation. In addition, NADH-dependent butanol dehydrogenase A (EC 1.1.1.-) which is involved in fermentation was overexpressed 16,87 fold. This result confirms the HPLC results. Because, according to the HPLC measurement results lactic acid production increased during the biomining. This is expected result, because of increasing growth rate causes energy demand, and lactic acid production increases during the energy production.

The other induced system is Phosphotransferase System (PTS). Some overexpressed genes belong to PTS system, IIA component (9,66 fold increase), PTS system, trehalose-specific IIB component (EC 2.7.1.69) / PTS system, trehalose-specific IIC component (EC 2.7.1.69) (7,5 fold increase), putative PTS system, IIb component (5,86 increase), PTS system, galactitol-specific IIB component (EC 2.7.1.69) (5,72 increase) and PTS system, galactitol-specific IIA component (5,7 increase). This system involves in sugar transport. It provides to uptake of sugar inside the cell by phosphorilation [122]. It is a coherent result with our study. Because, sugar is necessary for energy and lactic acid production.

According to the EF transcriptome analysis, expression of large subunit (LSU) and small subunit (SSU) ribosomal proteins increased at EF in the presence of magnesite. In the ribosomal large and small subunits, Ef-Tu binding parts proteins' expressions increased between 14,89 and 13 fold. This part of ribosome interacts with elongation factors [123]. Proteins of the other elongation factors interacting domain Ef-G increased 15 fold. Increase of this part shows the increase at protein synthesis [124] [125]. Other increased part of ribosome is SecY binding domain. The proteins which belong to SecY binding domain increased between 13-14 fold. SecY is a membrane protein that involves in protein secretion [126]. The increase of this part is a sign of the increase in the extracellular protein or enzyme secretion. Proteins of IF1 binding domain of ribosome increased 12 fold. IF1 is initiation factor for translation [127] [128]. Large subunits proteins' of RF1 domain of ribosome expressions increased 10 fold. RF1 is the releasing factor that mediates stopping the translation and releasing the nascent protein [129]. Genes expression of RpoC and RpoB proteins increased between 4,5 and 14 fold. These proteins generate RNA polymerase [130].

Another the most overexpressed genes are belong to the ABC transporters, as A1. More than 50 the ATP-binding cassette (ABC) transporter genes were upregulated between 2 to 41,7 fold. These transporters are the largest transmembrane protein family and bind to ATP to provide the active transport. ABC transporters export some molecules out of the cell such as, cell surface proteins and lipoproteins, antibiotics, toxins, vitamins, pathogenic proteins, drugs, competence factors, metal ions [131]. As I said for A1, a lot of gene which involve in cell wall biogenesis overexpressed in EF, too. Therefore, to throw out these molecules expression of ABC transporters increased. For instance, Teichoic acid translocation permease protein TagG expression and Teichoic acid export ATP-binding protein TagH (EC 3.6.3.40) expressions increased 6,11 fold. These transfers require energy. Already, ABC transporters are ATP dependent. Moreover, a lot of anabolic activities increased in the cell and ATP requirement for these activities increased, too. All subunits of ATP synthase genes expressions increased. They are ATP synthase F0 sector subunit a (3,84 fold increase), ATP synthase F0 sector subunit b (3,83 fold increase), ATP synthase F0 sector subunit c (6,14 fold increase), ATP synthase epsilon chain (EC 3.6.3.14) (3,81 fold increase), ATP synthase gamma chain (EC 3.6.3.14) (3,82 fold increase), ATP synthase alpha chain (EC 3.6.3.14) (6,25 fold increase),

ATP synthase beta chain (EC 3.6.3.14) (4,84 fold increase), ATP synthase delta chain (6,34 fold increase).

Some bacteria have natural competence. External conditions trigger off natural competence. Attacks of free Mg^{+2} ions to cell wall made the EF cells more competent as A1. As a result of this competece genes were overexpressed. Late competence protein ComEA (DNA receptor), Late competence protein ComEB, Late competence protein ComEC (DNA transport) were overexpressed in EF as A1, respectively 3,32-3,35-3,31 fold. Unlike A1, Competence protein CoiA which induces the transformability was overexpressed 4,25 fold and ComK regulator was overexpressed 3,35 fold [132].

Another overexpressed genes are belong to the heat shock proteins, chaperone proteins, antitoxin proteins and some resistance proteins. For instance, Ribosome-associated heat shock protein which is implicated in the recycling of the 50S subunit (S4 paralog) is overexpressed 11 fold. Heat shock protein 60 family co-chaperone GroES and Heat shock protein 60 family chaperone GroEL expressions increased 6,04 and 8,97 fold, respectively. Chaperone protein DnaJ which is also known Hsp40 (Heat shock protein 40) is expressed 5,4 fold more. Heat shock proteins are not produced in only heat shock, they are induced in stress conditions [133]. The other is an antitoxin protein HigA protein. This proteins' gene has two copies and each copy expressed 8,11 and 2,24 fold. It is produced for response to stress [134]. Tellurium resistance protein TerD genes' expression increased 11,64 fold. This protein involved in tellurium transport but it is also produced for metal stress [135]. The other increased resistance protein is cobalt-zinc-cadmium resistance protein with 2,6 fold increase. It is produced due to heavy metal poisoning [136]. As a result, all of these proteins were synthesized for responding to increased free metal concentration in the medium.

In A1 galactosamine-containing minor teichoic acid biosynthesis protein which is involved in cell wall synthesis, increased 43,76 fold because of Mg^{+2} attacks. In EF galactosamine-containing minor teichoic acid biosynthesis protein gene did not have distinct increase as A1, but many genes which are involved in cell wall and peptidoglycan synthesis are increased, similarly. Some of these are Peptidoglycan N-acetylglucosamine deacetylase (EC 3.5.1.-) (15,7 fold increase), Cell wall-binding protein (6,76 fold increase), membrane bound

lipoprotein (5,2 fold increase), cell wall surface anchor family protein (6,9 fold increase), cell surface protein precursor (7 fold increase), N-acetylmuramoyl-L-alanine amidase, family 4 (3,89 fold increase), Teichoic acid glycosylation protein (3,88 fold increase), N-acetylmuramic acid 6-phosphate etherase (3,25 fold increase), putative secreted cell wall protein (5,83 fold increase), N-acetylmuramoyl-L-alanine amidase (EC 3.5.1.28) (2,9 fold increase).

Gene expression of Phenolic acid decarboxylase (EC 4.1.1.-) enzyme in A1, and Phosphopantothenoylcysteine decarboxylase (EC 4.1.1.36) and Lysine decarboxylase enzyme in EF were increased 4,65 fold , 4,06 fold and 11,7 fold, respectively. These enzymes catalyzes the decarboxylation reactions and CO_2 releases at the end of the reaction. These enzymes may have a role in biomining mechanism. Carbonate in calcium carbonate and magnesite may be dissolved as bicarbonate. The, bicarbonate may be used as substrate by decarboxylases and CO_2 releases.

- Proteomics

Proteins of A1 and EF which were grown in the presence and absence of magnesite, were detected. As a result of SDS PAGE screening, in the presence of magnesite more protein expression and overexpression in some proteins were determined for A1 and EF. After protein analysis with Mass Spectroscopy, it was indicated that these proteins were belongs to lactic acid production pathway proteins, ATP production pathway proteins and enzymes of toxicity resistance. Of course, protein results were not neat and detailed as transcriptome results. But, protein results corresponded with transcriptome analysis result.

- Toxicology

Microorganisms that are used for any processes and released to environment must be non-pathogenic. Since, biomining is a biotechnological method that is applied to mines, biomining microorganisms must be safe organisms, too. Firstly, the literature research was made for the microorganisms that were used in this study. According to the newly published literature, K1 is not pathogenic organism [137] [138]. Perkins and Davis, 2000 mentioned that Neurospora species are not pathogenic and have been used for nearly ninety years at laboratories [139]. Alomar et al., showed that *Lactococcus garvieae* and *Enterococcus feacalis* strains inhibit the

pathogen *Staphylococcus aureus* strains' proliferation in the milk [28]. Another study, reported that *Enterecoccus feacalis* strain could be used as food additive because of its bacteriocins which are called enterocin [26]. Cross and colleagues (2001) reported that LAB prevent the development of allergic reactions by regulating the immune system [140]. *Lactococcus* genus members are most commonly classed as Generally Recognized as Safe (GRAS) [25]. In 2015, it is reported that lactic acid could be used as antimicrobial agent on *Salmonella enterididis, Escherichia coli* and *Listeria monocytogenes* [141]. Already, A1 and EF belong to the LAB they are the strains mostly probiotic than pathogenic.

Since, A1 and EF microorganisms are suitable to apply in large scale, subchronic toxicology tests were performed. After the 15 days high and low doses treatments, no pathogenic effect was detected. Therefore, there is no drawback to use A1 and EF in the biomining studies.

6. CONCLUSION

Bioleaching technologies have been applied commercially in the mining industry for many years. The future of biomining is challenging, as it offers advantages of operational simplicity, low capital and operating cost and shorter construction times that no other alternative process can provide. In addition, minimum environmental impact and the use of this technology in the mining industry is set to increase [14]. Our process and our microorganisms' demineralization mechanism are not the same with previous bioleaching processes. That's why, we called this process as "Bio-solubilization". Bio-solubilization and biomining offers enormous potential as a technology to mine or to pre-concentrate valuable metals and needs to be fully exploited in a mineral-rich country like Turkey. In this project, successful scale-up studies show that Bio-solubilization technology could be feasible in low grade magnesite ores.

In addition, we gained insight into demineralization mechanism of magnesite by magnesite biomining mechanism studies. Production of lactic acid initiates free Mg^{+2} ions formation from magnesite. Solved carbonate and free Mg^{+2} ions provide positive feedback to lactic acid production by increasing pH and being cofactor for *Lac* operon enzymes, respectively. Moreover, increasing free Mg^{+2} ion concentration in the medium was perceived as attack to cell wall. While cell wall material production is increasing, cell wall weakens and free Mg^{+2} ions enter the inside of cell. Because of Mg^{+2} ion is cofactor of many enzymes, enzyme production and efflux to outside of the cell increase. Probably, many or some of these enzymes have a role in magnesite biomining with lactic acid. Further detailed proteomic and enzymatic studies could provide to detect this enzyme or enzymes. It could be produced at high amounts by cloning and used in industrial and medical area which is needed to solve calcium carbonate and magnesium carbonate compounds.

Based on the results of this thesis, new magnesite biomining microorganisms could be isolated and biomining mechanisms of them could be determined for further studies. According to the comparison and compound of these new result and our results, new formulation could be produced for industrial scale processes.

REFERENCES

1.   T.C. Ekonomi Bakanlığı Sektör Raporları, Madencilik Sektörü, 2012. http://www.ibp.gov.tr/pg/sektorpdf/sanayi/madencilik_2012.pdf. [retrieved 12 March 2013].

2.   N. Gence, Enrichment of Magnesite Ore. *Osmangazi Üniversitesi Mühendislik ve Mimarlık Fakülte Dergisi,* 14:2-11, 2001.

3.   M. Özdemir, D. Çakır and İ. Kıpçak. Magnesium Recovery From Magnesite Tailings by Acid Leaching and Production of Magnesium Chloride Hexahydrate From Leaching Solution by Evaporation. *International Journal of Mineral Processing,* 93:209-212, 2009.

4.   F. Sha-Sha, L. Pei-Jun, F. Qian, L. Xiao-Jun, L. Peng, S. Yue-Bing and C. Yang. Soil Quality Degradation in a Magnesite Mining Area. *Pedosphere,* 21:98-106, 2011.

5.   Maden Tetkik Arama, Türkiye Maden Yatakları Haritaları, http://www.mta.gov.tr/v2.0/default.php?id=maden_yataklari [retrieved 30 March 2016].

6.   H. Gürcan, A. Sesver, N. Özdemir and B. Özdemir, Cryptocrystalline and Macrocrystalline Magnesite Ores: Comparing Microstructures and Thermal Behaviour,2012. http://www.arber.com.tr/imps2012.org/proceedingsebook/Abstract/absfilAbstractSub mi [retrieved 30 March 2016].

7.   G. Chen and D. Tao. Effect of Solution Chemistry on Flotability of Magnesite and Dolomite. *International Journal of Mineral. Processing,* 74:343-357, 2004.

8.   I. Bentli, N. Erdoğan, B. Birici, U. Topal and O. Şahbaz, Manyezit Ara Ürünün Kalsinasyon-Manyetik Ayırma Yöntemleriyle Zenginleştirilmesi, *Endüstriyel*

Hammaddeler Sempozyumu, İzmir, 2004.

9. C. Aksela, F. Kasap and A. Sesver. Investigation of Parameters Affecting Grain Growth of sintered Magnesite Refactories. *Ceramics International,* 31:121-127, 2005.

10. F. Demir and B. Dönmez. Optimization of the Dissolution of Magnesite in Citric Acid Solutions. *International Journal of Mineral Processing,* 87:60-64, 2003.

11. E. Hoque and O. J. Philip. Biotechnological Recovery of Heavy Metals From Secondary Sources—An overview. *Materials Science and Engineering C,* 5:57-66, 2011.

12. D. E. Rawlings and D. B. Johnson. The Microbiology of Biomining: Development and Optimization of Mineral-Oxidizing Microbial Consortia. *Microbiology,* 153:315-324, 2007.

13. V. Appanna, J. Lemire and R. Hnatiuk, Biomining: A Green Technology to Mine, 2011.
    http://oldwebsite.laurentian.ca/chem/vappanna/biotechnologiepercent20information/Biomining [retrieved 30 March 2016].

14. M. H. Siddiqui, A. Kumar, K. K. Kesari and J. M. Arif. Biomining - A Useful Approach Toward Metal Extraction. *American-Eurasian Journal of Agronomy,* 2:84-88, 2009.

15. D. Rawlings. Heavy Metal Mining Using Microbes. *Annual Reviev of Microbiology,* 56:65-91, 2002.

16. C. L. Brierley. How Will Biomining Be Applied in Future? *Transactions of Nonferrous Metals Society of Chin*a*,* 10:1302-1310, 2008.

17. L. Valenzuelaa, A. Chib, S. Bearda, A. Orella, N. Guiliania, J. Shabanowitzb, D. Huntb and C. Jereza. Genomics, Metagenomics and Proteomics in Biomining

Microorganisms. *Biotechnology Advences,* 3:197-211, 2006.

18. H. Brandl and M. A. Faramarzi. Microbe-Metal-Interactions for the Biotechnological Treatment of Metal-Containing Solid Waste. *China Particuology,* 5:93-97, 2006.

19. A. Schippers and W. Sand. Bacterial Leaching of Metal Sulfides Proceeds By Two Indirect Mechanisms Via Thiosulfate or Via Polysulfides And Sulfur. *Applied Environment Microbiology,* 65:319-321, 1999.

20. H. R. Watling. The Bioleaching of Sulphide Minerals With Emphasis on Copper Sulphides-A Review. *Hydrometallurgy,* 84:81-108, 2006.

21. J. Barrett, M. N. Hughes, G. I. Karavaiko and P. A. Spencer. Metal Extraction by, Ellis Horwood Limited, 1993

22. D. Cavanagh, G. F. Fitzgerald and O. McAuliffe. From Field to Fermentation: The Origins of *Lactococcus lactis* and Its Domestication to the Dairy Environment. *Food Microbiology,* 47:45-62, 2015.

23. B. Haghshenas, N. Abdullah, Y. Nani, D. Radiah, R. Rosli and A. Y. Khosroushahi. Different Effects of Two Newly-Isolated Probiotics *Lactobacillus plantaru*m 15HN and *Lactococcus lactis* subsp. *Lactis 44Lac* Strains From Traditional Dairy Products on Cancer Cell Lines. *Clinical Microbiology,* 30:51-59, 2014.

24. B. Pot, L. A. Devriese, D. Ursi, P. Vandamme, F. Haesebrouck and K. Kerstersi. Phenotypic Identification and Differentiation of *Lactococcus* Strains Isolated From Animals. *Systems Appied Microbiology,* 19:213-222, 1996.

25. E. Casalta and M. Montel. Safety Assessment of Diary Microorganisms: The *Lactococcus* Genus. *International Journal of Food Microbiology,* 126:271-273, 2008.

26. Y. Gao, D. Li, S. Liu and L. Zhang. Garviecin LG34, A Novel Bacteriocin Produced by *Lactococcus garvieae* Isolated From Traditional Chinese Fermented Cucumber.

Food Control, 50:896-900, 2015.

27. V. Strompfová, A. Lauková and A. C. Ouwehand. Selection of *Enterococci* for Potential Canine Probiotic Additives. *Veterinary Microbiology,* 100:107-114, 2004.

28. J. Alomar, P. Loubiere, C. Delbes, S. Nouaille and M. Montel. Effect of *Lactococcus garviaea, Lactococcus lactis* and *Enterococcus feacalis* on the Behaviour of *Staphylococcus aereus* in Microfiltered Milk. *Food Microbiology,* 25:502-508, 2008.

29. C. Reyes, C. Pena and E. Galindo. Reproducing Shake Flasks Performance In Stirred Fermentors: Production of Alginates by *Azotobacter vinelandii*. *Journal of Biotechnology,* 105:189-198, 2003.

30. D. K. Kundiyana, R. I. Huhnke and M. R. Wilkins. Syngas Fermentation in a 100-L Pilot Scale Fermentor: Design and Process Considerations. *Journal of Bioscience and Bioengineering,* 109:492-498, 2010.

31. C. Pena, M. Millan and E. Galindo. Production of Alginate by *Azotobacter vinelandii* in a Stirrer Fermentor Simulating the Evolution Of Power Input Observed In Shake Flasks. *Process Biochemistry,* 43:775-778, 2008.

32. F. H. El-Sedawy, M. M. M. Hussein, T. Essam, M. O. El-Tayeb and H. A. F. Mohammad. Scaling Up For The Industrial Production of Rifamycin B; Optimization of The Process Conditions In Bench-Scale Fermentor. *Bulletin of Faculty of Pharmacy,* 51:43-48, 2013.

33. J. A. Rocha-Valadez, E. M., E. Galindo and L. Serrano-Carreon. From Shake Flasks To Stirred Fermenters: Scale-Up of An Extractive Fermentation Process For 6-Pentyl-A-Pyrone Production By Trichoderma Harzianum Using Volumetric Power Input. *Process Biochemistry,* 41:1347-1352, 2006.

34. S. G. Cull, J. W. Lovick, G. J. Lye and P. Angeli. Scale-Down Studies On The Hydrodynamics Of Two-Liquid Phase Biocatalytic Reactors. *Bioprocess Biosystem*

Engineering, 25:143-153, 2002.

35.   O. Morozova and M. A. Marra. Applications of Next-Generation Sequencing. *Genomics,* 92:255-264, 2008.

36.   The Sanger method: How it, works? http://explorecuriocity.org/Explore/ArticleId/2027/sanger-sequencing-2027.aspx. [retrieved 28 February 2016].

37.   M. Pop and S. L. Salzberg. Bioinformatics Challenges of New Sequencing Technology. *Cell: Trends in Genetics,* 24:142-149, 2007.

38.   W. J. Ansorge. Next-Generation DNA Sequencing Techniques. *New Biotechnology,* 25:195-203, 2009.

39.   S. C. Schuster. Next-Generation Sequencing Transforms Today's Biology. *Nature Methods,* 5:16-18, 2008.

40.   Illumina Inc., *An Introduction to Next-Generation Sequencing Technology,* 2016.

41.   E. R. Mardis. The Impact of Next-Generation Sequencing Technology on Genetics. *Cell: Trends in Genetics,* 24:133-141, 2008.

42.   J. Shendure and H. Ji. Next-Generation DNA Sequencing. *Nature Biotechnology,* 26:1135-1145, 2008.

43.   J. S. Reis-Filho. Next-Generation Sequencing. *Breast Cancer Research,* 11:1-7, 2009.

44.   H. Kuyama , C. Nakajima, K. Kaneshiro, C. Hamana, K. Terasawa and K. Tanaka. Characterization of N- and C-termini of HER2 Protein By Mass Spectrometry-Based Sequencing: Observation of Two Types Of N-Terminal Sequence. *International Journal of Mass Spectrometry,* 373:81-87, 2014.

45.   A. Scherl. Clinical Protein Mass Spectrometry, *Methods,* 15:3-14, 2015.

46. S. A. Traguer, W. Webb and G. Suizdak. Peptide and Protein Analysis With Mass Spectrometry. *Spectroscopy,* 16:15-28, 2002.

47. L. A. McDonnell, G. L. Corthals, S. M. Willems, A. van Remoortere, R. J. van Zeijl and A. M. Deelder. Peptide and Protein Imaging Mass Spectrometry In Cancer Research. *Journal of Proteomics,* 73:1921-1944, 2010.

48. G. Zhang, R. Annan, S. Carr and T. Neubert. Overview of Peptide And Protein Analysis By Mass Spectrometry. *Current Protocols in Protein Science,* 16:1601-1662, 2010.

49. J. Kooken, K. Fox, A. Fox, D. Altomare, K. Creek, D. Wunsche, S. Pajares-Merino, I. M. Ballesteros, J. Garaizar, O. Oyarzabal and M. Samadpour. Reprint of Identification of Staphylococcal Species Based on Variations. *Molecular and Cellular Probes,* 28:73-82, 2008.

50. H. W. Lee, S. W. Roh, K. Cho, K. N. Kim, I. T. Cha, K. J. Yim, H. S. Song, Y. D. Namd, T. Oda, Y. H. Chung, S. J. Kim, J. S. Choi and D. Kim. Phylogenetic Analysis of Microalgae Based On Highly Abundant Proteins Using Massspectrometry. *Talanta,* 132:630-634, 2015.

51. U. Leurs, U. H. Mistarz and K. D. Rand. Getting to the Core of Protein Pharmaceuticals–Comprehensive. *European Journal of Pharmaceutics and Biopharmaceutics,* 93:95-109, 2015.

52. S. Sharafi, I. Rasooli and K. Beheshti-Maal. Isolation, Characterization and Optimization of Indigenous Aceticacid Bacteria and Evaluation of Their Preservation Method. *Iranian Journal of Microbiology,* 2:41-48, 2010.

53. K. S. Danadurai, S. Chellam, C. Lee and M. P. Fraser. Trace Elemental Analysis of Airborne Particulate Matter Using Dynamic Reaction Cell Inductively Coupled Plasma – Mass Spectrometry: Application to Monitoring Episodic Industrial Emission

Events. *Analytica Chimica Acta,* 686:40-49, 2011.

54. S. Demirci, Z. Ustaoğlu, G. Altın Yılmazer, F. Şahin and N. Baç. Antimicrobial Properties of Zeolite-X and Zeolite-A Ion-Exchanged with Silver, Copper and Zinc Against a Broad Range of Microorganisms. *Applied Biochemistry and Biotechnology,* 2013.

55. V. I. Siarkou, M. E. Mylonakis, E. Bourtzi-Hatzopoulou and A. F. Koutinas. Sequence and Phylogenetic Analysis of the 16S rRNAgene of *Ehrlichia canis* Strains in Dogs with Clinical Monocytic Ehrlichiosis. *Veterinary Microbiology,* 125:304-312, 2007.

56. F. Cappa and P. S. Cocconcelli. Identification of Fungi From Dairy Products by Means of 18S rRNA Analysis. *International Journal of Food Microbiology,* 69:157-160, 2001.

57. Center for Integrated Fungal Research, CTAB Method for Fungal DNA Isolation of *A. flavus,* 2005. http://www.aspergillusflavus.org/pdfs/CTAB%20Method.pdf [retrieved 30 November 2015].

58. W. McCabe, J. Smith and P. Harriot, Unit Operations of Chemical Engineering, Fourth Edition ed., New York: McGraw-Hill, 1985.

59. B. N. Ames. Assay of Inorganic Phosphate, Total Phosphate and Phosphotases, *in Methods in Enzymology*, 8: 115-118, 1966.

60. C. Caspaso, V. De Luca, V. Carginale, P. Caramuscio, C. F. Cavalheiro, R. Cannio and M. Rossi. Characterization and Properties of a New Thermoactive and Thermostable Carbonic Anhydrase. *Chemical Engineering Transactions,* 27: 271-276, 2012.

61 G. Altın, *Purification and Characterization of Recombinant Geobacillus kaustophilus Protein HslV and HslU from Escherichia coli,* Kocaeli: Gebze Yüksek Teknoloji

Enstitüsü, 2009.

62.   M. Kinter and N. E. Sherman, The Preparation of Protein Digests for Mass Spectrometric Sequencing Experiments, *in Protein Sequuencing and Indetification Using Tandem Mass Spectrpmetry*, 153-159, Canada, John Wiley and Sons, Incorporation All rights reserved, 2000.

63.   D. Prieur, D. Young, R. Davis, D. Cooney, E. Homan and R. Dixon. Procedures for Preclinical Toxicologic Evaluation of Cancer Chemotherapeutic Agents, Protocols of the Laboratory of Toxicology. *Cancer Chemotheraphy Report,* 4:1-28, 1973.

64.   M. N. Ghosh, Toxicity Studies, *in Fundamentals of Experimental Pharmacology*, Calcutta, India: Scientific Book Agency, 1984, 153-158.

65.   X. Jia, W. Wang, Y. Song and N. Li. A 90-day Oral Toxicity Study on a New Strain of *Lactabacillus paracasei* in Rats. *Food and Chemical Toxicology,* 49:1148-1151, 2011.

66.   Manyezit Anonim Şirketi, "Manyezit AŞ Hakkında" 2014. http://www.mas.com.tr/internet_tr/Hakkimizda/MAS/;jsessionid=763BA53B43588D B529F8DD70100D86B2) [retrieved 30 March 2016].

67.   Devlet Planlama Teşkilatı, Madenciliik Özel İhtisas Komisyonu Raporu, 2001.

68.   A. Yılmaz ve M. Kuşcu. Manyezit Yataklarının Oluşumu, Sınıflandırılması, Kullanım Alanları ve Kalite Sınıflandırması. *Erciyes Üniversitesi Fen Bilimleri Enstitüsü Dergisi,* 2012.

69.   F. Demir and B. Dönmez. Optimization of the Dissolution of Magnesite in Citric Acid Solutions, *International Journal of Mineral Processing,* 87:60-64, 2008.

70.   S. Sözal, *Göcekler (Mut-Mersin) Manyezitlerinin Meram (Konya) Manyezitleri ile Karşılaştırılması,* Selçuk Üniversitesi Fen Bilimleri Enstitüsü, 2011.

71. D. Yanmış, F. Orhan, M. Güllüce and F. Şahin, Biotechnological Magnesite Enrichment Using a Carbonate Dissolving Microorganism. *International Journal of Mineral Processing,* 15:30031-30034, 2015.

72. O. Laçin, B. Dönmez and F. Demir. Dissolution Kinetics of Natural Magnesite in Acetic Acid Soluitons. *International Journal of Mineral Processing,* 75:91-99, 2005.

73. B. Bayrak, O. Laçin, F. Bakan and H. Saraç. Investigation of Dissolution Kinetics of Natural Magnesite in Gluconic Acid, *Chemical Engineering,* 117: 109-115, 2006.

74. G. Jordan, O. S. Pokrovsky, X. Guichet and W. W. Schmahl. Organic and inorganic Ligand Effects on Magnesite Dissolution at 100°C and pH=5 to 10. *Chemical Geology,* 242:484-496, 2007.

75. B. Dönmez, F. Demir and O. Laçin. Leaching Kinetics of Calcined Magnesite in Citric Acid Solutions. *Journal of Industrial Engineering Chemistry,* 15:865-869, 2009.

76. N. Raza, Z. I. Zafar and M. Najam-ul-Haq. Utilization of Formic Acid Solutions in Leaching Reaction Kinetics of Natural Magnesite Ores. *Hydrometallurgy,* 149:183-188, 2014.

77. R. Talon, N. Duplet, M. Montel and M. Cantonnet. Purification and Characterization of Extracellular *Staphylococcus warneri* Lipase, *Current Microbiology,* 30:11-16, 1995.

78. D. Vendrell, J. Balcasar, I. Zarzuela, I. Blas, O. Girones and J. Muzquiz. *Lactococcus garvieae* in Fish: A Review, *Comparative Immunology, Microbiology and Infectious Diseases,* 29:177-198, 2006.

79. M. Lleo, M. Tafi and P. Canepari. Nonculturable *Enterococcus faecalis* Cells Are Metabolically Active and Capable of Resuming Active Growth, *Systematic and Applied Microbiology,* 21:333-339, 1998.

80. H. Deng, L. Ge, T. Zu, M. Zhang, X. Wang, Y. Zhang ve H. Peng. Analysis of the Metabolic Utilization of Carbon Sources and Potential Functional Diversity of the Bacterial Community in Lab-Scale Horizontal Subsurface-Flow Constructed Wetlands, *Journal of Environmental Quality,* 40:1730-1736, 2011.

81. B. Bayrak, O. Laçin and H. Saraç. Kinetic Study on The Leaching of Calcined Magnesite in Gluconic Acid Solutions. *Journal of Industrial Engineering Chemistry,* 16:479-484, 2010

82. H. Ehrlich, P. G. Koutsoukos, K. D. Demadis and O. S. Pokrovsky. Principles of Demineralization: Modern Strategies for the Isolation of Organic Frameworks Part II Decalcification. *Micron,* 40:169-193, 2009.

83. K. Tomochikaa, S. Shinodaa, H. Kumonb, M. Moric, Y. Moriyamad and M. Futaid. Vacuolar-Type H+-ATPase in Mouse Bladder Epithelium is Responsible for Urinary Acidification. *Febs Letters,* 404: 61-64, 1997.

84. S.Gluck. V-ATPases of the Plasma Membrane. *Journal of Experimental Biology,* 172:29-37, 1992.

85. P. Held and J. Hurley, *Determination of ATPase Activity Using BioTek's ELx808 Micrplate Reader,* Vermont: BioTek Instruments Incorporation, 2006.

86. I. G. Kim, B. H. Jo, D. G. Kang, C. S. Kim and Y. S. Choi. Biomineralization-Based Conversion of Carbon Dioxide to Calcium Carbonate Using Recombinant Carbonic Anhydrase. *Chemosphere,* 887:1096-1096, 2012.

87. W. Li, L. Liu, W. Chen, L. Yu, W. Li and H. Yu. Calcium Carbonate Precipitation and Crystal Morphology Induced By Microbial Carbonic Anhydrase and Other Biological Factors. *Process Biochemisstry,* 45:1017-1021, 2010.

88. A. Orell, C. A. Navarro, R. Arancibia, J. C. Mobarec and C. A. Jerez. Life in Blue: Copper Resistance Mechanisms of Bacteria and Archaea Used in Industrial.

Biotechnology Advances, 28: 839–848, 2010.

89.   A. U. Mónica, G. H. López-Campos, G. Alicia, L. A. Victoria, J. F. Fernández-Garayzábal and M. M. Blanco. Genome Sequence of *Lactococcus garvieae* 8831, Isolated from Rainbow Trout Lactococcosis Outbreaks in Spain. *Journal of Bacteriology,* 193:4263–4264, 2011.

90.   P. Reimundo, M. Pignatelli, D. L. Alcaraz, G. D'Auria, A. Moya and J. A. Guijarro. Genome Sequence of *Lactococcus garvieae* UNIUD074, Isolated in Italy from a Lactococcosis Outbreak. *Journal of Bacteriology,* 193:3684–3685, 2011.

91.   C. Gabrielsen, D. A. Brede , P. E. Hernández, I. F. Nes and D. B. Die. Genome Sequence of the Bacteriocin-Producing Strain *Lactococcus garvieae DCC43. Journal of Bacteriology,* 194:6976-6977, 2012.

92.   G. Ricci, C. Ferrario, F. Borgo, A. Rollando and M. G. Fortina. Genome Sequences of *Lactococcus garvieae* TB25, Isolated from Italian Cheese, and *Lactococcus garvieae* LG9, Isolated from Italian Rainbow Trout. *Journal of Bacteriology,* 194:1249-1250, 2012.

93.   E. Bae Kim, L. M. Kopit, L. J. Harris and M. L. Marco. Draft Genome Sequence of the Quality Control Strain *Enterococcus faecalis* ATCC 29212. *Journal of Bacteriology,* 194:6006-6007, 2012.

94.   I. T. Paulsen, L. Banerjei, G. S. Myers, K. E. Nelson, R. Seshadri , T. Read, D. Fouts, J. Eisen, S. R. Gill, J. Heidelberg, H. Tettelin, R. Dodson, L. Umayam, L. Brinkac, M. Beanan , S. Daugherty, R. DeBoy, S. Durkin, J. Kolonay, R. Madupu, W. Nelson, J. Vametyan, B. Tran, J. Upton and T. Hansen. Role of Mobile DNA in the Evolution of Vancomycin-Resistant *Enterococcus faecali*s. *Science,* 5615:2071-2074, 2003.

95.   Tagatose-6-Phosphate Kinase (IPR005926),
        http://www.ebi.ac.uk/interpro/entry/IPR005926 [retrieved 30 March 2016].

96.   L. Miallau, W. Hunter, S. McSweeney and G. Leonard. Structures of *Staphylococcus aureus* D-Tagatose-6-Phosphate Kinase Implicate Domain Motions in Specificity and Mechanism. *The Journal of Biological Chemistry,* 282:19948-19957, 2007.

97.   R. J. van Rooijen, S. van Schalkwijk and W. M. de Vos. Molecular Cloning, Characterization, and Nucleotide Sequence of the Tagatose 6-Phosphate Pathway Gene Cluster of the Lactose Operon of *Lactococcus lacti*s. *The Journal Of Biological Chemistry,* 266:7176-7181, 1991.

98.   P. Bork, C. Sander and A. Valencia. Convergent Evolution of Similar Enzymatic Function on Different Protein Folds: The Hexokinase, Ribokinase, and Galactokinase Families of Sugar Kinases. *Protein science,* 2:31-40, 1993.

99.   J. L. Mosser and A. Tomasz. Choline-Containing Teichoic Acid As a Structural Component of Pneumococcal Cell Wall and Its Role in Sensitivity to Lysis by an Autolytic Enzyme. *The Journal of Biological Chemistry,* 24, 1970.

100.   H. Yamamoto, Y. Miyake, M. Hisaoka and S. Kurosawa. The Major and Minor Wall Teichoic Acids Prevent the Sidewall Localization of Vegetative Dl-Endopeptidase LytF in *Bacillus subtilis*. *Molecular Microbiology,* 70:297-310, 2008.

101.   J. B. Ward. Teichoic and Teichuronic Acids: Biosynthesis, Assembly, and Location. *Microbiological Reviews,* 45:211-243, 1981.

102   R. Garimella, W. Halye, P. Klebba and C. Rice. Conformation of the Phosphate D-Alanine Zwitterion in Bacterial Teichoic Acid From Nuclear Magnetic Resonance Spectroscopy. *Biochemistry,* 48: 9242–9249, 2009.

103.   Glycerol Uptake Facilitator Protein, http://www.uniprot.org/uniprot/P0AER0 [retrieved 30 March 2016].

104.   J. Wicken. The Glycerol Teichoic Acid From the Cell Wall of *Bacillus stearothermophilus* B65. *Biochem Journal,* 99:108-116, 1966.

105. Y. Zhang and C. O. Rock. Thematic Review Series: Glycerolipids. Acyltransferases in Bacterial Glycerophospholipid Synthesis. *Journal of Lipid Research,* 49:1867-1874, 2008.

106. Y. Hara, M. Seki, S. Matsuoka, H. Hara, A. Yamashita and K. Matsumota. Involvement of PlsX and the Acyl-Phosphate Dependent and-Glycerol-3-Phosphate Acyltransferase PlsY in the Initial Stage of Glycerolipid Synthesis in *Bacillus subtili*s. *Genes Genetics Systems,* 83:433-442, 2008.

107. M. M. Burger and L. Glaser. The Synthesis of Teichoic Acids:I. Polyglycerophosphate. *The Journal of Biological Chemistry,* 239:10, 1964.

108. H. Pooley, F. Abellan and D. Karamata. CDP-Glycerol:Poly(Glycerophosphate) Glycerophosphotransferase, Which Is Involved In The Synthesis of The Major Wall Teichoic Acid in *Bacillus subtilis* 168, is Encoded by tagF (rodC). *Journal of Bacteriology,* 174:646-649, 1992.

109. I. Draskovic and D. Dubnau. Biogenesis of a Putative Channel Protein, ComEC, Required for DNA Uptake: Membrane Topology, Oligomerization and Formation of Disulphide Bonds. *Molecular Biology,* 55:881–896, 2005.

110. G. S. Inamine and D. Dubnau. ComEA, A *Bacillus subtili*s Integral Membrane Protein Required for Genetic Transformation, is Needed for Both DNA Binding and Transport. *Journal of Bacteriology,* 177:3045-3051, 1995.

111. D. Dubnau. Binding and Transport of Transforming DNA by *Bacillus subtili*s: the Role of Type-IV Pilin-Like Proteins – A Review. *Gene,* 192:191–198, 1997.

112. Competence Factor, http://www.genscript.com/molecular-biology-glossary/9152/competence-factor [retrieved 30 March 2016].

113. I. Chen and D. Dubnau. DNA Uptake During Bacterial Transformation. *Nature Reviews Microbiology,* 2:241–249, 2004.

114. J. Hansen, P. Moore and T. Steitz. Structures of Five Antibiotics Bound at the Peptidyl Transferase Center of the Large Ribosomal Subunit. *Journal of Bacteriology,* 330:1061-1075, 2003.

115. M. Nishimura, T. Yoshida, M. Shirouzu, T. Terada, S. Kuramitsu, S. Yokoyama, T. Ohkubo and Y. Kobayashi. Structure of Ribosomal Protein L16 from *Thermus thermophilus* HB8. *Journal of Bacteriology,* 344:1369-1383, 2004.

116. J. Harms, F. Schluenzen, R. Zarivach, A. Bashan, S. Gat, I. Agmon, H. Bartels, F. Franceschi and A. Yonath. High Resolution Structure of the Large Ribosomal Subunit from a Mesophilic Eubacterium. *Cell,* 107: 679–688, 2001.

117. R. Poole, F. Gibson and G. Wu. The cydD Gene Product, Component of a Heterodimeric ABC Transporter, is Required for Assembly of Periplasmic Cytochrome c and of Cytochrome Bd in *Escherichia coli. Fems Microbiology Letters,* 117:217–223, 1994.

118. D. Ermolenko and G. Makhatadze. Bacterial Cold-Shock Proteins. *Cell Molecular Life Science,* 9:1902-1913, 2002.

119. F. Ling, Y. Inoue and A. Kimura. Purification and Characterization of a Novel Nucleoside Phosphorylase From a *Klebsiella* sp. and Its Use in the Enzymatic Production of Adenine Arabinoside. *Appllied Environmental Microbiology,* 56:3830-3834, 1990.

120. C. Angstadt. Purine and Pyrimidine Metabolism. 12 4 1997. http://library.med.utah.edu/NetBiochem/pupyr/ htm. [retrieved 30 March 2016].

121. Y. P. Wang, L. S. Zhou, Y. Zhao, S. W. Wang, L. L. Chen, L. X. Liu, Z. Q. Ling, F. J. Hu, J. Sun, J. Zhang, C. Yang, Y. Yang, Y. Xiong, K. Guan and D. Ye. Regulation of G6PD Acetylation by SIRT2 and KAT9 Modulates NADPH Homeostasis and Cell Survival During Oxidative Stress. *EMBO Journal,* 33:1304–1320, 2014.

122.　M. Dworkin, S. Falkow and E. Rosenberg, *The Prokaryotes: A Handbook on the Biology of Bacteria,* pages 19-20, Singapore: Springer Science and Business Media, 2006.

123.　E. Villa, L. Trabuco and B. Liu, Mechanisms of Protein Synthesis by the Ribosome, http://www.ks.uiuc.edu/Research/ribosome/. [retrieved 30 March 2016].

124.　W. Holtkamp, C. Cunha, F. Peske, A. Konevega, W. Wintermeyer and M. Rodnina. GTP Hydrolysis by EF-G Synchronizes tRNA Movement on Small and Large Ribosomal Subunits. *EMBO Journal,* 33:1073-1085, 2014.

125.　Y. Chen, S. Feng, V. Kumar, R. Ero and Y. Gao. Structure of EF-G–Ribosome Complex in a Pretranslocation State. *Nature Structural and Molecular Biology,* 20:1077–1084, 2013.

126.　F. Menetret, J. Schaletzky, W. Clemons, A. Osborne, S. Ska, C. Denison, T. Rapoport and C. Akey. Ribosome Binding of a Single Copy of the SecY Complex: Implications for Protein Translocation. *Molecular Cell,* 28:1083-1092, 2007.

127.　Marazova, M. Initiation of Protein Synthesis in Bacteria. *Microbiology and Molecular Biology Reviews,* 69:101–123, 2005.

128.　S. Langberg, L. Kahan, R. Traut and J. Hershey. Binding of Protein Synthesis Initiation Factor IF1 to 30 S Ribosomal Subunits: Effects of Other Initiation Factors and Identification of Proteins Near the Binding Site. *Journal of Molecular Biology,* 17:307-319, 1977.

129.　K. S. Wilson, K. Ito, H. Noller and Y. Nakamura. Functional Sites of Interaction Between Release Factor RF1 and the Ribosome. *Nature Structural Biology,* 7:866-870, 2000.

130.　L. Post, G. Styrscarz, M. Nomura, H. Lewis and P. Dennis. Nucleotide Sequence of the Ribosomal Protein Gene Cluster Adjacent to the Gene for RNA Polymerase

Subunit :in *Escherichia coli* (Protein Sequence/Transcription Initiation/Transcription Termination/Codon Usage/Isoaccepting tRNAs). *Proceeding of National Academy of Science,* 76:1697-1701, 1979.

131. M. Dean, The Human ATP-Binding Cassette (ABC) Transporter Superfamily, Bethesda: National Center for Biotechnology Information, 2002.

132. B. Desai and D. Morrison. An Unstable Competence-Induced Protein, CoiA, Promotes Processing of Donor DNA after Uptake during Genetic Transformation in *Streptococcus pneumoniae. Bacteriology,* 188:5177–5186, 2006.

133. M. G. Santoro. Heat Shock Factors and the Control of the Stress Response. *Biochemical Pharmacology,* 59:55–63, 2000.

134. A. S. Fivian-Hughes and E. O. Davis. Analyzing the Regulatory Role of the HigA Antitoxin within *Mycobacterium tuberculosis*. *Journal of Bacteriology,* 192:4348–4356, 2010.

135. V. Anantharaman, L. Iyer and L. Aravind. Ter-Dependent Stress Response Systems: Novel Pathways Related to Metal Sensing, Production of a Nucleoside-Like Metabolite, and DNA-Processing. *Molecular BioSystems,* 8:3142–3165, 2012.

136. Cobalt/zinc/cadmium resistance protein CzcB (IPR005695), https://www.ebi.ac.uk/interpro/entry/IPR005695. [retrieved 30 March 2016].

137. M. Bronowska, R. Steborowski and G. Bystrzejewska-Piotrowska. Estimation of the Acute Cesium Toxicity by the Microbial Assay for Risk Assessment (MARA) Test. *Nukleonika,* 58:481-485, 2013.

138. R. Musharrafieh, L. Tacchi, J. Trujeque and S. LaPatra. *Staphylococcus warnerii* a Resident Skin Commensal of Rainbox Trout (*Oncorhynchus mykis*s) with Pathobiont Characteristics. *Veterinary Microbiology,* 169:80-88, 2014.

139. D. D. Perkins and R. H. Davis. Evidence for Safety of Neurospora Species for Academic and Commercial Uses. *Applied and Environmental Microbiolgy,* 66:5107-5109, 2000.

140. M. L. Cross, L. M. Stevenson and H. S. Hill. Anti-Allergy Properties of Fermented Foods: An Important Immunoregulatory Mechanism of Lactic Acid Bacteria. *International Immunopharmacology,* 1:891–901, 2001.

141. C. Wang, T. Chang, H. Yang and M. Cui. Antibacterial Mechanism of Lactic Acid on Physiological and Morphological Properties of *Salmonella enteritidis*, *Escherichia coli* and *Listeria monocytogenes*. *Food Control,* 47:231-236, 2015.

142. M. Özdemir, D. Çakır and I. Kıpçak. Magnesium Recovery From Magnesite Tailings by Acid Leaching and Production of Magnesium Chloride Hexahydrate From Leaching Solution by Evaporation. *Internaitonal Journal of Mineral Process,* 93:209-212, 2009.

143. O. S. Pokrovskyi, S. V. Golubev, J. Schott and A. Castillo. Calcite, Dolomite and Magnesite Dissolution Kinetics in Aqueous Solutions at Acid to Circumneutrl pH, 25 to 150°C and 1 to 55 atm pCO_2: New Constrains on CO_2 Sequestration in Sedimentary Basins. *Chemical Geology,* 265:20-32, 2009.

144. O. S. Pokrovskyi, S. V. Golubev and G. Jordan. Effect of Organic and Inorganic Ligands on Calcite and Magnesite Dissolution Rates at 60 °C and 30 atm pCO_2. *Chemical Geology,* 265:33-433, 2009.

145. L. Green, B. Houck-Loomis, A. Yueh ve S. P. Goff. Large Ribosomal Protein 4 Increases Efficiency of Viral Recoding Sequences, *Journal of Virology,* 86:8949–8958, 2012.

146. Kyoto Encyclopedia of Genes and Genomes, Ribosome, http://www.genome.jp/kegg-bin/show_pathway?ko03010 [retrieved 30 January 2016].

147.	E. Villa, L. Trabuco and B. Liu, Mechanisms of Protein Synthesis by the Ribosome, http://www.ks.uiuc.edu/Research/ribosome. [retrieved 30 March 2016].